National Library of Canada
Acquisitions and Bibliographic Services Branch
395 Wellington Street
Ottawa, Ontario
K1A 0N4

Bibliothèque nationale du Canada
Direction des acquisitions et des services bibliographiques
395, rue Wellington
Ottawa (Ontario)
K1A 0N4

Your file *Votre référence*

Our file *Notre référence*

NOTICE

The quality of this microform is heavily dependent upon the quality of the original thesis submitted for microfilming. Every effort has been made to ensure the highest quality of reproduction possible.

If pages are missing, contact the university which granted the degree.

Some pages may have indistinct print especially if the original pages were typed with a poor typewriter ribbon or if the university sent us an inferior photocopy.

Reproduction in full or in part of this microform is governed by the Canadian Copyright Act, R.S.C. 1970, c. C-30, and subsequent amendments.

AVIS

La qualité de cette microforme dépend grandement de la qualité de la thèse soumise au microfilmage. Nous avons tout fait pour assurer une qualité supérieure de reproduction.

S'il manque des pages, veuillez communiquer avec l'université qui a conféré le grade.

La qualité d'impression de certaines pages peut laisser à désirer, surtout si les pages originales ont été dactylographiées à l'aide d'un ruban usé ou si l'université nous a fait parvenir une photocopie de qualité inférieure.

La reproduction, même partielle, de cette microforme est soumise à la Loi canadienne sur le droit d'auteur, SRC 1970, c. C-30, et ses amendements subséquents.

Canada

A STUDY OF PRESSURE BUILDUP ANALYSIS FOR A GAS WELL IN A RECTANGULAR RESERVOIR

BY

PRASIT KOSARUSSAWADEE

A THESIS

SUBMITTED TO THE FACULTY OF GRADUATE STUDIES AND RESEARCH

IN PARTIAL FULFILLMENT OF THE REQUIREMENTS FOR THE DEGREE OF

MASTER OF SCIENCE

IN

PETROLEUM ENGINEERING

DEPARTMENT OF MINING, METALLURGICAL AND PETROLEUM ENGINEERING

EDMONTON, ALBERTA
FALL, 1992

National Library of Canada
Bibliothèque nationale du Canada

Canadian Theses Service
Service des thèses canadiennes

Ottawa, Canada
K1A 0N4

The author has granted an irrevocable non-exclusive licence allowing the National Library of Canada to reproduce, loan, distribute or sell copies of his/her thesis by any means and in any form or format, making this thesis available to interested persons.

The author retains ownership of the copyright in his/her thesis. Neither the thesis nor substantial extracts from it may be printed or otherwise reproduced without his/her permission.

L'auteur a accordé une licence irrévocable et non exclusive permettant à la Bibliothèque nationale du Canada de reproduire, prêter, distribuer ou vendre des copies de sa thèse de quelque manière et sous quelque forme que ce soit pour mettre des exemplaires de cette thèse à la disposition des personnes intéressées.

L'auteur conserve la propriété du droit d'auteur qui protège sa thèse. Ni la thèse ni des extraits substantiels de celle-ci ne doivent être imprimés ou autrement reproduits sans son autorisation.

ISBN 0-315-77306-5

Canada

RELEASE FORM

NAME OF AUTHOR: Prasit Kosarussawadee

TITLE OF THESIS: A STUDY OF PRESSURE BUILDUP ANALYSIS FOR A GAS WELL IN A RECTANGULAR RESERVOIR

DEGREE FOR WHICH THESIS WAS PRESENTED: MASTER OF SCIENCE

YEAR THE DEGREE WAS GRANTED: FALL, 1992

Permission is hereby granted to THE UNIVERSITY OF ALBERTA LIBRARY to reproduce single copies of this thesis and to lend or sell such copies for private, scholarly or scientific research purposes only.

The author reserves other publication rights, and neither the thesis nor extensive extracts from it may be printed or otherwise reproduced without the author's written permission.

(SIGNED) Prasit Kosarussawadee

PERMANENT ADDRESS:
249 PHRANAKAREDSE LANE,
RAMA 4 RD., BANGRAK
BANGKOK, 10500
THAILAND

DATED: April 30, 1992

THE UNIVERSITY OF ALBERTA

FACULTY OF GRADUATE STUDIES AND RESEARCH

The undersigned certify that they have read, and recommend to the Faculty of Graduate Studies and Research for acceptance, a thesis entitled "A STUDY OF PRESSURE BUILDUP ANALYSIS FOR A GAS WELL IN A RECTANGULAR RESERVOIR" submitted by Prasit Kosarussawadee in partial fulfillment of the requirements for the degree of MASTER OF SCIENCE in PETROLEUM ENGINEERING.

A. K. Ambastha (Supervisor)

J. M. Whiting

W. S. Tottike

K. Nandakumar

DATED: April 30 , 1992

ABSTRACT

For a gas well at the center of a circular reservoir, the use of pseudo-pressure and either pseudotime or normalized time, adequately linearizes the gas flow equation. Thus, accurate estimates of permeability, skin factor and average reservoir pressure can be obtained from a buildup test. Because of the non-linearity of the gas equation, however, superposition used in the analysis of the buildup test data for a gas well has to be verified for reservoir geometries other than circular.

By analyzing pressure data generated by a numerical simulator, Horner plots, using pseudo-pressure and modified Horner times, and MDH graphs, using pseudo-pressure and modified MDH times, provide accurate estimates of permeability, skin factor and average reservoir pressure for a well situated in a closed, rectangular reservoir.

Buildup data from a gas reservoir containing gas contaminants can be accurately analyzed using pseudo-pressure and either modified Horner time ratios or MDH times, provided that the gas properties used are corrected for the presence of the contaminants. Failure to correct for the contaminants significantly affects the accuracy of the estimate for permeability.

The time to the end of the semi-log straight line on Horner and MDH plots is approximately the same for the gas and liquid flow. The correlations developed for the liquid flow can be used as a guideline to estimate the time to the end of the semi-log straight line for the gas flow.

ACKNOWLEDGMENTS

The author wishes to express his gratitude and appreciation to Professor A. K. Ambastha for his guidance and support throughout this study. The graduate scholarship was provided by the Canadian International Development Agency, for which he is very thankful. Financial support for this work was provided by the Petroleum Graduate Research Program fund administered through the University of Alberta and NSERC Operating grant. Computer time for this work was provided by the Dept. of Mining, Metallurgical and Petroleum Engineering. Cooperation from M. W. Brown in developing the numerical simulator is appreciated. Finally, the author would like to thank Khun Nithiwadee Mapawongse for her encouragement and support during his graduate studies.

TABLE OF CONTENTS

Page

1. INTRODUCTION 1
2. LITERATURE REVIEW 3
3. REVIEW OF PRESSURE TRANSIENT ANALYSIS TECHNIQUES 11
   - 3.1 Pressure Transient Analysis for Liquid Flow 11
     - 3.1.1 Drawdown Solution 11
     - 3.1.2 Buildup Solution 13
   - 3.2 Pressure Transient Analysis for Gas Flow 18
4. STATEMENT OF THE PROBLEM 24
5. THE NUMERICAL SIMULATOR 25
   - 5.1 The Main Module 25
     - 5.1.1 The Numerical Approximation of Real Gas Flow 25
   - 5.2 The Grid Specification Module 27
   - 5.3 The Gas Correlation Module 28
   - 5.4 Verification of Pressure Responses During Short Producing Times 28
6. SENSITIVITY STUDY 30
   - 6.1 Sensitivity Analysis of Buildup Responses Following Long Producing Times ... 30
   - 6.2 Determination of The Producing Times When The Dimensionless Buildup Curves Become Sensitive to The Gas and Reservoir Properties 31
   - 6.3 Comparison of The Simulated Pressure With The Material Balance Pressure 33
7. PRESSURE TRANSIENT ANALYSIS FOR A GAS WELL IN A RECTANGULAR RESERVOIR 36
   - 7.1 Methodology 36
     - 7.1.1 The Well/reservoir Geometries to Be Studied 37
     - 7.1.2 Parameters Used in This Study 37

7.2 Effects of Well/reservoir Geometry 38

7.2.1 Analyses to Be Performed 38

7.3.1 Analyses of A Well Producing From The Center of A Square Reservoir 39

7.3.1.1 Drawdown Analysis 39

7.3.1.2 Analysis Based on Horner Plot 40

7.3.1.3 Analysis Based on MDH Graph 42

7.3.2 Analyses of A Well producing From A Corner of A Four-to-One Rectangular Reservoir 44

7.3.2.1 Drawdown Analysis 45

7.3.2.2 Analysis Based on Horner Plot 46

7.3.2.3 Analysis Based on MDH Graph 47

7.3.3 Analyses of Wells C, D and E 48

7.4 Buildup Analyses for A Well Shut in During The Transitional Period 49

7.5 Effects of Gas and Reservoir Properties 50

7.6 Effects of The Producing Rate 51

7.7 Effects of Gas Contaminants 53

7.8 The End of Semi-log Straight Line on Buildup Plots 56

8. CONCLUSIONS AND RECOMMENDATION 59

8.1 Conclusions 59

8.2 Recommendation 60

TABLES 61

FIGURES 67

REFERENCES 81

APPENDIX A Computer Programs 86

APPENDIX B Sample Input and Output Data 115

APPENDIX C An Investigation on The Average Pressure Determination for a Gas Well 119

Appendix D Gas Properties for Selected Compositions and Reservoir Temperatures 127

LIST OF TABLES

Page

Table 5.1 Gas and reservoir properties for the base case 61

Table 6.1 Analysis results for Figure 6.1 61

Table 6.2 Grid specifications for simulations run used in this study 61

Table 7.1 Analysis results of the buildup response for Well A (q_D=0.01, t_{pDA}=30) 62

Table 7.2 Analysis results of the buildup response for Well B (q_D=0.01, t_{pDA}=30) 62

Table 7.3 Analysis results of the buildup response for Wells C, D and E (q_D=0.01, t_{pDA}=30) 63

Table 7.4 Pseudo-reduced pressures and temperatures used in Figure 7.10 64

Table 7.5 Analysis results of the buildup responses for Figure 7.10 (q_D=0.01, t_{pDA}=10) 64

Table 7.6 Analysis results of the buildup responses for Figure 7.12 (q_D=0.1) 65

Table 7.7 Analysis results of the buildup responses for Figure 7.13 based on R_{H2} (H_2S=20%, t_{pDA}=30) 65

Table 7.8 Analysis results of the buildup responses for Figure 7.13 based on R_{H1} (H_2S=20%, t_{pDA}=30) 65

Table 7.9 Analysis results of the buildup responses for Figure 7.14 66

Table 7.10 Analysis results of the buildup responses for Figure 7.15 66

Table 7.11 Dimensionless times to the end of Horner and MDH straight line for Wells A and C 66

LIST OF FIGURES

Page

Figure 5.1 Area Subdivision for a square reservoir 68

Figure 5.2 Drawdown responses for short producing times 68

Figure 5.3 Buildup responses for short producing times, t_{pDA}=0.01 69

Figure 6.1 Horner plot for wells in the center of a square, t_{pDA}=10 70

Figure 6.2 Horner plot of a well in a center of a square 70

Figure 6.3 Horner plot of a well at (0.75,0.75) in a 4:1 reservoir 71

Figure 6.4 Differences between the average reservoir pressure from the simulator and the material balance equation 71

Figure 7.1 Well/reservoir configurations used in this study 72

Figure 7.2 Semi-log graph of the drawdown response for Well A (q_D=0.01) 73

Figure 7.3 Horner plot of the buildup response for well A (q_D=0.01, t_{pDA}=30) 73

Figure 7.4 MDH graph of the buildup response for Well A (q_D=0.01, t_{pDA}=30) 74

Figure 7.5 Semi-log graph of the drawdown response for Well B (q_D=0.01) 74

Figure 7.6 Horner plot of the buildup response for Well B (q_D=0.01, t_{pDA}=30) 75

Figure 7.7 MDH graph of the buildup response for Well B (q_D=0.01, t_{pDA}=30) 75

Figure 7.8 Horner plot of the buildup responses for Wells C, D and E (q_D=0.01, t_{pDA}=30) 76

Figure 7.9 Horner plot of the buildup response for Well B (q_D=0.01) 76

Figure 7.10 Horner plot of the buildup response for Well B with different gas and reservoir properties (q_D=0.01, t_{pDA}=10) 77

Figure 7.11 Semi-log graph of the drawdown response for Well A (q_D=0.1) 77

Figure 7.12 Horner plot of the buildup responses for Well A with different t_{pDA} (q_D=0.1) 78

Figure 7.13 Effects of contaminants on Horner plot of the buildup responses for Wells A and B (H_2S=20%,t_{pDA}=30) 78

Figure 7.14 Effects of the concentration of the contaminant on Horner plot of the buildup response for Well B (q_D=0.01, t_{pDA}=30) 79

Figure 7.15 Effects of the concentration of the contaminant on Horner plot of the buildup responses for Well B (q_D=0.1, t_{pDA}=0.2) 79

Figure 7.16 Dimensionless time to the end of Horner and MDH straight lines for Well A 80

Figure 7.17 Dimensionless time to the end of Horner and MDH straight lines for Well C 80

Figure C.1 Dimensionless graph of buildup responses of a gas and an oil well at the center of a square (base case properties except pi=5,000 psia and γ_g=1.0) 124

Figure C.2 Dimensionless graph of buildup responses of a gas and an oil well in a corner of a 4:1 reservoir (base case properties except pi=5,000 psia and γ_g=1.0) 124

Figure C.3 Dimensionless graph of buildup responses of a gas and an oil well at the center of a square (base case properties except T=250° F) 125

Figure C.4 Dimensionless graph of buildup responses of a gas and an oil well in a corner of a 4:1 reservoir (base case properties except T=250° F) 125

Figure C.5 Dimensionless graph of buildup responses for a gas well in a corner of a 4:1 reservoir, m(pi)=3.10*10^8 psi^2/cp and t_{pDA}=30 126

Figure D.1 Pseudo-pressure for selected compositions and reservoir temperatures 128

Figure D.2 Gas compressibility factor for selected compositions and reservoir temperatures 128

Figure D.3 Gas viscosity for selected compositions and reservoir temperatures 129

Figure D.4 Gas compressibility for selected compositions and reservoir temperatures 129

NOMENCLATURE

A	=	Area, ft^2
B	=	Oil formation volume factor, bbl/STB
c_g	=	Gas compressibility, psi^{-1}
c_t	=	Total compressibility, psi^{-1}
C_A	=	Dietz shape factor
Ei	=	Exponential-integral
h	=	Reservoir thickness, ft
k	=	Permeability, md
m_D	=	Dimensionless pseudo-pressure
m_{DMBH}	=	Dimensionless Matthews-Brons-Hazebroek pseudo-pressure function
m_s	=	Semi-log slope, $(psia^2/cp)$/cycle
m_{sD}	=	Dimensionless shut-in pseudo-pressure
m_{wD}	=	Dimensionless producing pseudo-pressure
m^*	=	Source term in the diffusivity equation, $lb/ft^3.sec$
$m(p_i)$	=	Initial pseudo-pressure, psi^2/cp
$m(p_{wf})$	=	Flowing wellbore pseudo-pressure, psi^2/cp
$m(p_{wfs})$	=	Flowing wellbore pseudo-pressure at the instant of shut-in, psi^2/cp
$m(p_{ws})$	=	Shut-in wellbore pseudo-pressure, psi^2/cp
$m(p^*)$	=	False pseudo-pressure, psi^2/cp
$m(\bar{p})$	=	Average pseudo-pressure, psi^2/cp
p	=	Pressure, psia
p_D	=	Dimensionless pressure = $\frac{kh}{141.3qB\mu}(p_i - p_w)$
p_{DMBH}	=	Dimensionless Matthews-Brons-Hazebroek pressure drop
p_i	=	Initial pressure, psia

p_{sc}	=	Pressure at standard condition, 14.7 psia
p_{sD}	=	Dimensionless shut-in pressure
p_w	=	Wellbore pressure, psia
p_{wf}	=	Wellbore flowing pressure, psia
p_{ws}	=	Shut-in wellbore pressure, psia
$\bar{p}$	=	Average reservoir pressure, psia
$\bar{p}_{sD}$	=	Dimensionless pressure defined by Equation C.2
q	=	Gas surface flow rate, Mscf/D or liquid surface flow rate, STB/D
q_D	=	Dimensionless flow rate
r_{inv}	=	Radius of investigation, ft
r_w	=	Wellbore radius, ft
R_H	=	Horner time ratio
s	=	Skin factor
t	=	Time, hr
t_A	=	Agarwal's pseudotime, hr.psi/cp
t_D	=	Dimensionless time
t_n	=	Scott's normalized time, hr.psi/cp
t_p	=	Producing time, hr
t_{pDA}	=	Dimensionless producing time based on area
T	=	Reservoir temperature, ° R
T_{sc}	=	Temperature at standard condition, 520° R
v	=	Velocity, ft/sec
x_{wD}	=	Dimensionless well location in the x-direction
y_{wD}	=	Dimensionless well location in the y-direction
z	=	Real gas compressibility factor

Greek Symbols

α	=	Viscosity-compressibility ratio = $\frac{\mu c_t - \mu_i c_{ti}}{\mu_i c_{ti}}$
γ	=	Exponential of Euler's constant = 1.781
γ_g	=	Gas specific gravity (air=1)
δ	=	Correction term for the gas diffusivity equation or partial
Δt	=	Shut-in time, hr
Δt_A	=	Pseudotime, hr.psi/cp
Δt_{DAesl}	=	Dimensionless time based on area to the end of the semi-log straight line on Horner or MDH graph
Δt_1, Δt_2, Δt_3	=	MDH shut-in time functions, hr.psi/cp
$\Delta t'_D$	=	Dimensionless MDH shut-in time function
μ	=	Viscosity, cp
ϕ	=	Porosity, fraction
ρ	=	Density, lb/ft^3

Subscripts

1hr	=	Evaluated at 1 hr.
A	=	Area
D	=	Dimensionless
f	=	Flowing
i	=	Initial
pr	=	Pseudoreduced
s	=	Shut-in
sc	=	Standard condition

w = Wellbore

1. INTRODUCTION

With the diminishing oil resources, as well as environmental concern about the release of green-house gases and the instability surrounding the marketing of crude oil, natural gas development projects are gaining increasing attention. For the parties involved, the gas development projects present finite pre-determined sources of revenue since the agreement on the production and pricing is usually laid down in the contract on a long-term basis.

Notwithstanding the favorable circumstances for the natural gas projects, the discovery of shallow, large gas bearing formations with good permeability has become a rare possibility. Companies nowadays have to deal with less favorable reservoir conditions. Low-permeability formations also have to be developed. Even reservoirs containing gas in small pockets, such as those disturbed by heavy faulting, are beginning to receive attention.

As far as reservoir engineering is concerned, vital information of a petroleum reservoir consists of the deliverability and the amount of producible hydrocarbon. For small reservoirs, this information can be secured effectively and inexpensively by pressure transient testing.

Pressure transient analysis is an established practice for the petroleum industry due to its fast, inexpensive and relatively simple procedure. Theory for oil well testing has received much attention as evidenced by the amount of the literature in that area. The theory of gas well testing, due to the non-linearity of gas flow, did not enjoy this privilege until the 1960's. Still, the literature on gas well testing relies heavily on the extension from the theory of oil well testing. As a consequence, the basic difference between the oil and gas pressure analysis - the non-linearity in the gas equation - has been overlooked to a large extent.

In recent years, new analysis techniques better addressing the nature of the gas flow have been developed. Most notable are the pseudo-pressure transformation by Al-Hussainy et al. (1966), the pseudotime transformation by Agarwal (1979) and the normalized time function by Scott (1979). These developments enable more accurate results to be obtained from gas well testing, especially in the situations where the effects of the non-linearity become pronounced, such as production from a tight formation.

One notable omission of the investigations on the analysis of gas well testing, however, is the study of the boundary effects. So far, most studies are restricted to the assumptions of a well in the center of a circular reservoir. The analysis techniques for other boundary configurations are traditionally extended from the available theory of the liquid well testing.

This study attempts to verify the applicability of the pressure transient analysis techniques in conjunction with the pseudo-pressure, pseudotime and normalized time to pressure buildup testing of a gas well producing from a closed, rectangular reservoir. Pressure responses are generated by a two-dimensional, single-phase gas simulator developed for this study. This numerical simulator is described in Section 5. A review of available analysis methods for gas well testing is presented in Section 3. In Section 7, the pressure responses generated are analyzed using the methods presented in Section 3. By comparing the results of the analysis for a variety of gas, reservoir and producing conditions, conclusions are drawn in Section 8 as to the accuracy and applicability of each analysis method.

2. LITERATURE REVIEW

Well testing is an engineering application of the diffusivity equation which describes the flow of fluids in porous media. The diffusivity equation is a partial differential equation that relates the pressure as a function of distance and time. For a slightly compressible fluid with small and constant compressibility, the linear form of the diffusivity equation is satisfactory. Consequently, the known solutions can be superposed to generate the solutions for more complicated problems and there are a large number of studies on the flow of slightly compressible liquids in the literature.

For the flow of gas in porous media, however, the linear diffusivity equation is inadequate due to the variation of the gas properties with pressure. Before 1966, approximation techniques, such as the pressure-squared method, were developed to partially linearize the diffusivity equation so that the available solutions for the liquid flow could be used. Nevertheless, the gas equation still contained some non-linearity and the superposition was not applicable a priori.

In 1966, Al-Hussainy et al. introduced the pseudo-pressure transformation to treat the non-linearity in the gas flow equation. The pseudo-pressure method partially linearized the gas diffusivity equation such that the solutions of the resulting equation could be better approximated by the corresponding liquid solutions, if the producing time was not too long. In the pseudo-pressure form, the drawdown response of gas flow prior to the start of boundary effects could be described accurately by the corresponding solution for liquid. After the onset of the boundary effects, the drawdown response of gas deviated from the liquid solution. For buildup analyses, Al-Hussainy et al. found that accurate estimates of permeability and skin factor could be obtained by plotting the pseudo-pressure with the Horner(1951) time ratio.

Al-Hussainy and Ramey (1966) suggested that the average reservoir pressure could be determined from a buildup analysis by either the Matthews-Brons-Hazebroek (MBH) method (1954) or the Dietz

method (1965). However, since Al-Hussainy et al. (1966) showed that the gas drawdown response deviated from the liquid solution after long producing times, both the MBH and Dietz methods might fail to accurately determine the average reservoir pressure for buildup analyses conducted after the effects of the boundary became significant.

For low production rates, Wattenbarger and Ramey (1968) showed that the permeability and skin factor could be accurately estimated from buildup analyses, even with the presence of non-Darcy flow effects around the wellbore. However, for high production rates, buildup analyses would yield low permeability values, even without non-Darcy effects.

Since the introduction of the pseudo-pressure transformation, other researchers have developed a number of techniques to more accurately estimate permeability, skin factor and average reservoir pressure for gas wells. In 1971, Odeh and Al-Hussainy proposed a method for average reservoir pressure determination which did not require the knowledge of permeability, compressibility and viscosity. Their method was to re-label the dimensionless producing time (t_{pDA}) with an equivalent term consisting of the slope of the Horner plot and the difference between the initial reservoir pressure and the average reservoir pressure. They showed, in an example problem, that their method provided accurate estimation of the average reservoir pressure. However, the pressure depletion, which was only 100 psi from the initial pressure of 3150 psi, was too small for the non-linearity in the gas flow equation to become significant.

In 1974, Kazemi presented a method to estimate the average reservoir pressure, permeability and skin factor for a buildup test run after a long producing time. He suggested replacing the producing time in the Horner time ratio with the time to pseudosteady state for the system of reservoir and gas composition under consideration. He claimed that this treatment achieved a longer straight line on the Horner plot. For the determination of the average reservoir pressure, he proposed an iterative method based on the material balance between an assumed initial reservoir pressure and the current

reservoir pressure.

The procedure proposed by Kazemi started by extrapolating the straight line section of the Horner plot to the Horner time ratio of unity for the false pressure. This pressure was used, together with the well/reservoir geometry factor and the corresponding time to pseudosteady state, to estimate an intermediate average reservoir pressure. The resulting pressure would then be used to determine another initial reservoir pressure, via the material balance equation. The compressibility and viscosity determined from the new initial reservoir pressure would be used in the MBH method to determine another average reservoir pressure. The procedure would be repeated until the solution converged. In the appendix, Kazemi (1974) verified the theoretical validity of the substitution of the producing time in the Horner time ratio. However, it was not clear how his method provided better estimation of the average reservoir pressure.

During 1980's, the methods for linearizing the gas diffusivity equation fell into two principal categories. The first was to evaluate a correction term based on the perturbation method and the second was to modify the Horner time ratio to incorporate the variation of the gas properties with pressure. The former was applicable for drawdown analyses, while the latter was applicable to buildup analyses after any duration of producing time.

Application of the perturbation method to linearize the gas diffusivity equation was first introduced by Kale and Mattar (1980). They modified the diffusivity equation with a variable α, which was defined as the ratio between the difference of the μc_t term at the initial and the present condition, and the μc_t term at the initial condition. The rearrangement of the resulting equation led to a correction term δ. Using the solution to the liquid equation, known to be in the exponential integral form (or the Ei solution), they determined the governing partial differential equation for δ. By neglecting two second-order terms, they numerically evaluated the values for δ. The δ term was shown to be a small negative number whose magnitude increased quickly and stabilized after a short

time. They concluded that the correction essentially behaved like a small negative skin. Thus, the stabilized value for the correction term could be added directly to the Ei solution to obtain a better estimation for the wellbore pressure. Since they did not consider the producing time effects in this study, their method was only applicable for the drawdown and the buildup solution after a long producing time. Kale and Mattar (1980) used the viscosity and compressibility at the initial condition in the dimensionless time.

Further modifications to the perturbation approach were developed by Ziauddin (1982), Toh et al. (1984) and Kabir and Hasan (1986). Ziauddin used Kale and Mattar's method to generate the perturbed solution for a well in a closed reservoir by superposing the Ei solutions of the image wells. Since the correction terms for the image wells were small, he proposed that the perturbation approach as developed by Kale and Mattar could be used to estimate the average reservoir pressure by adding the correction term to the Ei solution of the well considered. In the example given in the paper, he demonstrated that the average reservoir pressure calculated by this method was close to the result from the numerical simulator. Like Kale and Mattar's, his correction factor needed to be numerically determined due to its dependency on the gas and reservoir properties. Noting this deficiency, Toh et al. (1984) numerically evaluated the correction terms for different initial pressures, reservoir and gas properties. They found that the term stabilized at 0.2982α with time. This conclusion led to a development of an iterative method. First, the average reservoir pressure was determined from one of the conventional methods. Then, this pressure was used to estimate α and the correction was determined. This correction was used to obtain a new average reservoir pressure, which, in turn, would be used to estimate a new α. The procedure would be repeated until convergence was achieved.

In 1986, Kabir and Hasan presented a study which utilized the perturbation method and Agarwal's pseudotime (to be discussed later). They concluded that the drawdown solution for gas could be approximated by the addition of a correction term δ to the corresponding liquid solution and that the

use of pseudo-pressure and pseudotime completely linearized the buildup equation for gas. In the estimation of the correction term for drawdown, they also incorporated one of the second-order terms previously neglected by other investigators. However, inclusion of this term did not result in a significant change in the value of δ.

Subsequently, Aadnoy and Finjord (1986), and Ambastha (1986) made their respective observations on the paper by Kabir and Hasan. Aadnoy and Finjord pointed out that the omission of the second-order term was theoretically incorrect. They showed that if this term was included, the correction, far from being constant, would grow with time. They also argued that the use of both pseudotime and pseudo-pressure did not completely linearize the gas buildup equation. Ambastha observed that the omission of the second-order term implied dropping one of the boundary conditions. He numerically evaluated the correction factor and found that the magnitude of the term was higher with the second-order term included in the evaluation.

As mentioned earlier, two major methods were developed during 1980's to linearize the gas diffusivity equation. The second approach was to modify the Horner time ratio such that the correct permeability, skin factor and average reservoir pressure could be determined. For this purpose, the variation of gas viscosity and compressibility would be incorporated into the definition of the Horner time ratio.

Agarwal proposed the pseudotime function in 1979. With an analogy to the pseudo-pressure method, he defined the pseudotime function as an integration of the shut-in time divided by the compressibility-viscosity product at the corresponding shut-in pressure. The pseudotime time function was used with success to analyze pressure transient data from massively hydraulic fractured wells. Agarwal (1979) assumed long producing times. Therefore, the producing time effects were not considered.

Scott (1979) proposed a similar time function, called the normalized time, which he used to analyze the buildup tests of fractured gas wells in tight formations. He defined the normalized time as the shut-in time divided by the compressibility and viscosity at the corresponding wellbore pressure. Unlike Agarwal, Scott used his new time function in the Horner time ratio. This proved to be a vital step since the Horner time ratio accounted for the producing time effects. Consequently, the modified Horner time ratio could be used for either short or long producing period before shut-in.

In 1985, Lee and Holditch mathematically showed that the use of pseudo-pressure and pseudotime effectively (though not completely) linearized the gas buildup equation during the wellbore-storage-dominated flow regime. They pointed out that type-curve matching would yield correct wellbore storage coefficient and reservoir parameters, if pseudotime and pseudo-pressure were used in lieu of shut-in time and pressure, respectively. For the buildup analyses, they found that the shut-in time in both the numerator and denominator of the Horner time ratio should be replaced by pseudotime.

Spivey and Lee (1986a and b) compared the accuracy of the buildup analyses using the pseudotime and normalized time for different situations. They found that both treatments yielded equally good results for most circumstances. The analysis using pseudotime was more accurate only during the wellbore-storage-dominated flow period.

Aanonsen (1985) presented a detailed mathematical study of the pseudotime function during the buildup period. He showed that the buildup analysis for gas wells was not a result of superposition, but of a modification such that the gas diffusivity equation using pseudo-pressure and pseudotime possessed the same set of initial and boundary conditions as the liquid case. From the examples given in his paper, the pseudotime treatment yielded the least accurate estimates of the average reservoir pressure and skin factor when the reservoir shape was not symmetric and the well was off-center. However, in this research, we found that buildup analyses for a well located off-centered in an asymmetric reservoir also yield accurate estimates of skin factor and average reservoir pressure.

Reynolds et al. (1987) presented a thorough investigation for the use of pseudotime and normalized time for circular reservoirs. Using numerical simulation, they found that the analysis based on a modified Horner time ratio with the denominator replaced by either pseudotime or normalized time yielded accurate estimation of permeability, skin factor and average reservoir pressure. They confirmed that the wellbore-storage-dominated data were best analyzed using pseudo-pressure and pseudotime. They also suggested that when the producing time was long, the average reservoir pressure could be accurately determined, if the viscosity and compressibility used in modified Horner times based on pseudotime or normalized time were substituted by the corresponding values at the final shut-in pressure.

In summary, the perturbation method as introduced by Kale and Mattar (1980) does not correctly represent the nature of the diffusivity equation for gas flow. As pointed out by Aadnoy and Finjord, Ambastha, and Aanonsen, the second-order term has a significant effect on the nature of the correction factor. As discussed by Aanonsen and Reynolds et al., the second-order term affects the solution so that the permeability and skin factor calculated from the semi-log method are too low. The Horner time modification using pseudotime and normalized time is more amenable to engineering analyses.

The treatment of the non-linearity in the diffusivity equation of gas during the buildup period has been extensively examined for the case of a well situated in the center of a circular reservoir. However, to the author's knowledge, the two examples given in Aanonsen (1985) were the only investigations in the literature that presented the case of a well producing from a rectangular reservoir. Since the gas equation is not linear, the buildup responses for the rectangular shape should also be thoroughly investigated.

In this research, the available pressure buildup analysis techniques are studied to assess their accuracy in the estimation of the permeability and average reservoir pressure for a well situated in a

rectangular gas reservoir. The skin factor and non-Darcy effects are not considered. Since both the skin factor and non-Darcy flow effects occur close to the wellbore, these would not influence the effects due to the outer boundaries. Consequently, all the observations on the skin and non-Darcy flow effects for the circular reservoirs are also applicable for the rectangular reservoirs. This study is conducted with the modified Horner approach due to the method's distinct advantage for engineering applications.

3. REVIEW OF PRESSURE TRANSIENT ANALYSIS TECHNIQUES

The techniques in the area of pressure transient analysis were originally developed for liquid flow. For the liquid flow, the diffusivity equation describing the flow phenomenon can be assumed to be linear. The approximate linearity allows superposing the solutions for simple problems to create the solutions for more complicated problems. The developments in the area of gas well testing usually require modifying the existing analysis methods for the liquid flow. Most notable modifications include the pseudo-pressure transformation, the pseudotime and normalized time functions.

In this chapter, the fundamentals of pressure transient analysis will be discussed. The discussion begins with the drawdown analysis for liquid flow, which forms an important building block for more complicated situations, such as the buildup analysis. The buildup analysis for liquid flow is then discussed followed by the modification of the liquid solutions for gas flow.

3.1 Pressure Transient Analysis for Liquid Flow

3.1.1 Drawdown Solution

For a reservoir with constant thickness, porosity, and permeability, containing a liquid of small, constant compressibility, producing at a constant rate q with small pressure gradient everywhere, the solution for the producing pressure at the well is given by (van Everdingen and Hurst, 1949) :

$$\frac{kh}{141.3qB\mu}(p_i - p_{wf}) = p_D(t_D) + s \ , \qquad (3.1)$$

where:

$$t_D = \frac{0.0002637kt}{\phi\mu c_t r_w^2} \,. \tag{3.2}$$

The term p_D in Equation (3.1) depends on the well/reservoir geometry and the producing time. For a producing time when no boundary effects are felt at the well, the term p_D is given by:

$$p_D = \frac{1}{2}\left(\frac{4t_D}{\gamma}\right) = \frac{1}{2}(\ln t_D + 0.80907) \,, \tag{3.3}$$

where γ is the exponential of Euler's constant, and has a value of 1.781. For a reservoir with closed boundaries, when all boundaries are affecting the pressure responses at the well, the term p_D is given by:

$$p_D = \frac{1}{2}\left(\ln\frac{4A}{\gamma C_A r_w^2}\right) + 2\pi t_{DA} \,, \tag{3.4}$$

where C_A is the shape factor for a given well/reservoir geometry as defined by Dietz (1965), and :

$$t_{DA} = \frac{0.0002637kt}{\phi\mu c_t A} = t_D \frac{r_w^2}{A} \,. \tag{3.5}$$

The skin factor can be determined by rearranging Equation (3.1) :

$$s = \frac{kh}{141.3qB\mu}(p_i - p_{wf}) - p_D(t_D) \,. \tag{3.6}$$

The p_D term in Equation (3.6) should be replaced by the p_D term from Equation (3.3) for short producing times, and from Equation (3.4) for long producing times.

3.1.2 Buildup Solution

Superposition in time is used with the drawdown solutions to generate the solution for the pressure buildup at a well. The buildup solution describing the pressure at the well at a shut-in time of Δt following a producing time of t_p is given by :

$$\frac{kh}{141.3qB\mu}(p_i - p_{ws}) = [p_D(t_{pD} + \Delta t_D) + s] - [p_D(\Delta t_D) + s]$$

$$= p_D(t_{pD} + \Delta t_D) - p_D(\Delta t_D) \ . \qquad (3.7)$$

Again, both p_D terms are dependent upon the well/reservoir geometry as well as the producing and shut-in times. Ramey and Cobb (1971) suggested adding the terms $\frac{1}{2}\ln(t_{pD} + \Delta t_D) - \frac{1}{2}\ln(t_{pD} + \Delta t_D)$ to Equation (3.7). The resulting equation is :

$$\frac{kh}{141.3qB\mu}(p_i - p_{ws}) = p_D(t_{pD} + \Delta t_D) - p_D(\Delta t_D) + \frac{1}{2}\ln(t_{pD} + \Delta t_D) - \frac{1}{2}\ln(t_{pD} + \Delta t_D) \ . \quad (3.8)$$

If the shut-in time is short, the second p_D term on the right-hand side of Equation (3.8) can be assumed to have a solution given by Equation (3.3). Thus, Equation (3.8) becomes:

$$\frac{kh}{141.3qB\mu}(p_i - p_{ws}) = \frac{1}{2}\ln(\frac{t_p + \Delta t}{\Delta t}) + p_D(t_{pD} + \Delta t_D) - \frac{1}{2}\{\ln(t_{pD} + \Delta t_D) + 0.80907\} \quad (3.9)$$

Equation (3.9) describes the shut-in pressure at the well. The last two terms in Equation (3.9) cancel out when the p_D term is represented by Equation (3.3). This situation occurs when no boundary effects have been felt after a producing time of $t_p + \Delta t$. Usually, the well is produced long enough for the pressure at the well to be influenced by the boundary effects and the p_D term can be represented by Equation (3.4).

If $t_p >> \Delta t$, then $t_p + \Delta t \approx t_p$, and Equation (3.9) becomes :

$$\frac{kh}{141.3qB\mu}(p_i - p_{ws}) = \frac{1}{2}\ln(\frac{t_p + \Delta t}{\Delta t}) + p_D(t_{pD}) - \frac{1}{2}\{\ln t_{pD} + 0.80907\} \qquad (3.10)$$

Thus, a pressure buildup test can be analyzed by plotting the shut-in pressure vs. the time ratio in the first term on the right-hand-side of Equation (3.10). This type of plot was first introduced by Horner in 1951 and is known as the Horner plot. If the straight line represented by Equation (3.10) is extrapolated to an infinitely long shut-in time such that the ratio inside the ln term becomes unity, the well pressure p_{ws} at the infinite shut-in time is designated a new symbol p^*. The pressure p^* is known as the false pressure. At infinite shut-in time, Equation (3.10) becomes :

$$\frac{kh}{141.3qB\mu}(p_i - p^*) = p_D(t_{pD}) - \frac{1}{2}\{\ln t_{pD} + 0.80907\} \; . \qquad (3.11)$$

Matthews, Brons and Hazebroek (1954) defined a function to determine the average reservoir pressure. Their approach is to add a term $(p^* - \bar{p})$ into Equation (3.11).

The average reservoir pressure can be obtained from the material balance equation :

$$\frac{kh}{141.3qB\mu}(p_i - \bar{p}) = \frac{2\pi(0.0002637)kt_p}{\varphi\mu c_t A} = 2\pi t_{pDA} \,. \tag{3.12}$$

Introducing Equation (3.12) into Equation (3.11) yields:

$$\frac{kh}{141.3qB\mu}\{(p_i - \bar{p}) - (p_i - p^*)\} = 2\pi t_{pDA} - p_D(t_{pD}) + \frac{1}{2}\{\ln t_{pD} + 0.80907\} \,. \tag{3.13}$$

The Matthews-Brons-Hazebroek (MBH) dimensionless pressure is defined as twice the left hand side of Equation (3.13) :

$$p_{DMBH} = \frac{kh}{70.6qB\mu}(p^* - \bar{p}) = 4\pi t_{pDA} - 2p_D(t_{pD}) + \{\ln t_{pD} + 0.80907\} \,. \tag{3.14}$$

Depending on the producing time, p_D may be represented by Equation (3.3) for a short producing time, and by Equation (3.4) for a long producing time. Consequently, when the producing time is short, the last two terms in Equation (3.14) cancel and the false pressure is equal to the initial pressure. For a long producing time, the p_D term is represented by Equation (3.4). The equation for the dimensionless MBH pressure becomes :

$$\begin{aligned} p_{DMBH} &= \frac{kh}{70.6qB\mu}(p^* - \bar{p}) = 4\pi t_{pDA} - 2\{\frac{1}{2}\ln(\frac{4A}{\gamma C_A r_w^2}) + 2\pi t_{pDA}\} + \{\ln t_{pD} + 0.80907\} \\ &= \ln(C_A t_{pDA}) \end{aligned} \tag{3.15}$$

The average reservoir pressure can be read directly on the straight line of the Horner plot. Using Equation (3.9) and (3.12), the Horner time ratio satisfying the condition $p_{ws} = \bar{p}$ is:

$$\ln\left(\frac{t_p+\Delta t}{\Delta t}\right)_{p_{ws}=\bar{p}} = 4\pi t_{pDA} - 2p_D(t_{pD}+\Delta t_D) + \{\ln(t_{pD}+\Delta t_D) + 0.80907\} \qquad (3.16)$$

If the producing time is short, the p_D term in Equation (3.16) is given by Equation (3.3), and Equation (3.16) yields :

$$\left(\frac{t_p+\Delta t}{\Delta t}\right)_{p_{ws}=\bar{p}} = e^{4\pi t_{pDA}} \qquad (3.17)$$

If the producing time is long, then Equation (3.4) describes the p_D term in Equation (3.16) and Equation (3.16) becomes :

$$\left(\frac{t_p+\Delta t}{\Delta t}\right)_{p_{ws}=\bar{p}} = C_A t_{pDA} \,. \qquad (3.18)$$

Equations (3.17) and (3.18) are used to find the average reservoir pressure directly from the straight line portion of the Horner plot. This method of average reservoir pressure estimation is known as the Dietz (1965) method.

If $t_p >> \Delta t$, the first p_D term in Equation (3.7) is essentially constant. If the shut-in time is short, the second p_D term in Equation (3.7) is represented by Equation (3.3). Thus, for long producing times, Equation (3.7) becomes :

$$\frac{kh}{141.3qB\mu}(p_i - p_{ws}) = p_D(t_{pD}) - \frac{1}{2}\{\ln(\Delta t_D) + 0.80907\} \qquad (3.19)$$

Equation (3.19) suggests that a plot of the well pressure vs. logarithm of the corresponding shut-in time should appear as a straight line. This is known as Miller, Dyes and Hutchinson (1950) or the MDH graph.

For $t_p >> \Delta t$, Equation (3.18) simplifies to :

$$(\Delta t_{DA})_{p_{ws}=\bar{p}} = \frac{1}{C_A} . \tag{3.20}$$

Using Equation (3.20), average reservoir pressure can be estimated directly from the straight line portion of the MDH plot. The skin factor does not appear in either Equation (3.9) or (3.19). However, the skin factor can be introduced into a buildup analysis by subtracting the general buildup equation, Equation (3.7), from the drawdown equation, Equation (3.1). The resulting equation can be solved for the skin factor :

$$s = \frac{kh}{141.3qB\mu}(p_{ws} - p_{wf}) + p_D(t_{pD} + \Delta t_D) - p_D(t_{pD}) - p_D(\Delta t_D) . \tag{3.21}$$

If $t_{pD} >> \Delta t_D$, then :

$$p_D(t_{pD} + \Delta t_D) = p_D(t_{pD}) , \tag{3.22}$$

and the skin factor can be estimated from :

$$s = \frac{kh}{141.3qB\mu}(p_{ws} - p_{wf}) - p_D(\Delta t_D) . \tag{3.23}$$

3.2 Pressure Transient Analysis for Gas Flow

For gas flow, Al-Hussainy et al. (1966) defined the pseudo-pressure function as:

$$m(p) = 2\int_{o}^{p} \frac{p}{\mu z} dp \tag{3.24}$$

In their study, they found that, for the producing time before the onset of the boundary effects, the drawdown response of a gas well is given by an equation similar to the equation describing the drawdown response for the liquid :

$$m_{wD} = \frac{1}{2}(\ln \frac{4t_D}{\gamma}) + s \ . \tag{3.25}$$

With a standard condition at 14.7 psia and 60° F, the dimensionless pseudo-pressure is defined as :

$$m_{wD} = \frac{kh}{1423qT}\{m(p_i) - m(p_{wf})\} \ , \tag{3.26}$$

and :

$$t_D = \frac{0.0002637kt}{\phi(\mu c_t)_i \ r_w^2} \ . \tag{3.27}$$

Note that the viscosity and compressibility at the initial pressure have been used in Equation (3.27).

For long producing times, however, an equation similar to Equation (3.4) with the pressure terms replaced by the pseudo-pressure terms was found to be inaccurate. Reynolds et al. (1987) and Brown

(1992) presented analysis methods for a drawdown test for gas wells following a long producing time.

For buildup analyses, Al-Hussainy et al. found that an equation similar to Equation (3.9) with the pressure terms replaced by the pseudo-pressure terms describes the buildup response accurately if the producing time is short :

$$m_{sD} = \frac{kh}{1423qT}\{m(p_i) - m(p_{ws})\} = m_D(t_{pD}) - \frac{1}{2}\ln(\frac{4t_{pD}}{\gamma}) + \frac{1}{2}\ln(\frac{t_p + \Delta t}{\Delta t})$$

$$= \frac{1}{2}\ln(\frac{t_p + \Delta t}{\Delta t}) \qquad (3.28)$$

Wattenbarger and Ramey (1968) investigated the accuracy of the Horner analysis for a high producing rate well producing for a short time. They defined the dimensionless producing rate as :

$$q_D = \frac{1423qT}{kh\, m(p_i)} \qquad (3.29)$$

The producing rate is considered high for q_D greater than 0.1 and low for q_D of 0.01. For the cases of high producing rate, Wattenbarger and Ramey found that the drawdown analysis yields accurate estimates of the permeability and skin factor, but the permeability estimated from the buildup analysis can be as much as 10% too low.

Agarwal (1979) used a time function called pseudotime to analyze the buildup responses of hydraulically fractured wells with success. The pseudotime function is defined as :

$$t_A = \int_0^{\Delta t} \frac{dt}{\mu c_t} \,. \qquad (3.30)$$

In the same year, Scott used the normalized time function to analyze the buildup responses for fractured gas wells producing from tight reservoirs. The normalized time is defined as :

$$t_n = \frac{t}{\mu c_t} \,. \tag{3.31}$$

Reynolds et al. (1987) studied the applications of the pseudotime and normalized time for drawdown and buildup analyses for gas wells. They focused on the cases of a well in the center of a circular reservoir. Four Horner time ratios were investigated in their study :

$$R_{H1} = \frac{(t_p + \Delta t)}{\Delta t} \tag{3.32}$$

$$R_{H2} = \frac{(t_p + \Delta t)/(\mu c_t)_i}{\Delta t_n} \tag{3.33}$$

$$R_{H3} = \frac{(t_p + \Delta t)/(\mu c_t)_i}{\Delta t_A} \tag{3.34}$$

$$R_{H4} = \frac{(t_{pA} + \Delta t_A)}{\Delta t_A} \tag{3.35}$$

They found that the use of R_{H2} and R_{H3} provides satisfactory accuracy in the estimation of the permeability, skin factor for the high producing rate cases. In addition, the use of R_{H2} or R_{H3} in buildup analyses also provides accurate average reservoir pressure estimation after a long producing time by means of the MBH analysis.

They explained that the use of both R_{H2} and R_{H3} better reflects the gas properties in the area surrounding the well than the use of R_{H1}. After the well is put on production, a pressure profile is established in the reservoir. Since the viscosity and compressibility of a gas depend on the pressure, the gas has different properties at different points in the reservoir. For long producing times or high production rates, the gas viscosity and compressibility around the wellbore vary significantly from the values at the initial pressure due to the high pressure drawdown created by either producing condition. When the well is shut in, the pressure profile around the well becomes flat, and the gas compressibility and viscosity within the radius of investigation of the buildup are adequately represented by the gas properties evaluated at the well pressure.

The general buildup equation presented by Reynolds et al. is :

$$\frac{kh(m(p_i)-m(p_{ws}))}{1423qT} = 1.151\log(R_H) + m_D(t_{pD}) - 1.151\log(\frac{4t_{pD}}{\gamma}) \ , \qquad (3.36)$$

and the MBH function for long producing time is given by an equation similar to Equation (3.15) :

$$m_{DMBH} = \ln(C_A t_{pDA}) \ . \qquad (3.37)$$

For the determination of the skin factor, the drawdown solution is subtracted from the buildup solution to yield :

$$m(p_{ws}) - m(p_{wfs}) = -m_s \{\log[\frac{(t_p + \Delta t)/(\mu c_t)_i}{\Delta t_n}] - \log[\frac{kt_p}{\phi(\mu c_t)_i r_w^2}] + 3.23 - \frac{s}{1.151}\} \ , \qquad (3.38)$$

where :

$$m_s = slope = \frac{1637qT}{kh} \ . \tag{3.39}$$

At Δt = 1 hr, $t_p >> \Delta t$ so that $t_p + \Delta t \approx t_p$, the skin factor can be determined from :

$$s = 1.151\{\frac{m(p_{1hr}) - m(p_{wfs})}{m_s} - \log[\frac{k}{\phi(\mu c_t)_{1hr} r_w^2}] + 3.23\} \ . \tag{3.40}$$

Reynolds et al. pointed out that the use of R_{H2} and R_{H3} provides more accurate estimates of permeability, skin factor and average reservoir pressure than the use of R_{H1} because the variation of the gas viscosity and compressibility was accounted for in the definition of R_{H2} and R_{H3}. Referring to Bratvold (1984), Reynolds et al. (1987) stated that buildup analysis using MDH method can be carried out, if producing time is long. The MDH method plots the shut-in pseudo-pressure vs. the shut-in time on a semi-log graph. If the producing time is long, the first p_D term on the right hand side of Equation (3.19) can be assumed to be constant. Applying the pseudo-pressure analogy to Equation (3.19) yields :

$$\frac{kh}{1423qT}\{m(p_i) - m(p_{ws})\} = m_D(t_{pD}) - 1.151\{\log(\Delta t'_D) + 3.23\} \ . \tag{3.41}$$

In Equation (3.41), the dimensionless shut-in time $\Delta t'_D$ on the right-hand side can be substituted by any of the following :

$$\Delta t_{D1} = \frac{0.0002637k\Delta t}{\phi(\mu c_t)_i r_w^2} \tag{3.42}$$

$$\Delta t_{D2} = \frac{0.0002637k\Delta t_n}{\phi r_w^2} \tag{3.43}$$

$$\Delta t_{D1} = \frac{0.0002637 k \Delta t_A}{\phi r_w^2} \qquad (3.44)$$

The dimensionless shut-in time in Equation (3.42) is the form used for the liquid MDH analysis. The definitions in Equation (3.43) and (3.44) are a straightforward extension of Reynolds et al.'s concept to incorporate the variation in gas viscosity and compressibility to the MDH time variables. The definitions of $\Delta t'_D$ in Equations (3.43) and (3.44) employ Scott's (1979) normalized time and Agarwal's (1979) pseudotime to incorporate the change in viscosity and compressibility in the shut in time, respectively. The permeability and skin factor for the gas MDH analysis are determined from Equations (3.39) and (3.40), respectively.

To the best of the author's knowledge, the application of the MDH time functions as given by Equations (3.42) to (3.44) has not been investigated for a gas well in a rectangular reservoir. Bratvold (1984) used the MDH time functions to analyze buildup tests of a gas well in the center of a circular reservoir. Agarwal (1979) introduced the use of pseudotime as a parameter in the gas buildup analysis using liquid drawdown type curves. However, he did not suggest using the pseudotime function in the MDH analysis. The applicability of the pseudotime and normalized time for the MDH analysis to estimate permeability, skin factor and average reservoir pressure of a gas well in a rectangular reservoir is investigated in Chapter 7.

4. STATEMENT OF THE PROBLEM

The pressure transient analysis techniques used for gas producing wells are, to a large degree, an extension of the liquid flow equations with the modifications such as pseudo-pressure, pseudotime or normalized time to partially linearize the gas equation. The modified gas equations have been extensively studied for the configuration of a well in the center of a circular reservoir. The extension of the modified gas equations to other well/reservoir configurations have generally been assumed to be adequate without any validation.

The objectives of this study are :

1. To assess the applicability and accuracy of the modified gas equations for the problem of buildup tests conducted on a gas well producing from a rectangular reservoir.

2. To verify the extension of the liquid theory to the problem of buildup tests conducted on a gas well producing from a rectangular reservoir.

3. To gain insight into the nature of gas flow in rectangular reservoirs.

5. THE NUMERICAL SIMULATOR

A numerical simulator was developed to generate the pressure distribution for a gas well located in a homogeneous, isotropic, closed rectangular reservoir, containing a dry gas with constant gas composition. The program uses the pseudo-pressure approach to the diffusivity equation governing gas flow. A two-dimensional areal model is used to account for the flow in both the x- and y-directions. The wellbore skin, non-Darcy flow, and wellbore storage effects are not considered. The simulator consists of three modules - the main module, the grid specification module and the gas correlation module.

5.1 The Main Module

In addition to computing the pseudo-pressure distribution for each time step, the main module calculates the effective diffusivity terms for each grid location. All the time-dependent terms are treated with the fully-implicit scheme. The spatial and time derivatives are evaluated using a central-difference approximation in space and backward-difference approximation in time, respectively. This treatment results in a pentadiagonal matrix of equations. The resulting set of equations are solved simultaneously using the Waterloo Sparse Linear Equations Package (see George et al. (1980)). Due to the non-linearity of the equations, an iterative method has to be used. The calculated pseudo-pressures for the new time step are considered to be converged when the new pseudo-pressures calculated differ from the pseudo-pressures at the previous iteration by less than 0.001%. As the reservoir is modeled with the point centered grid scheme, the image method is used to generate the closed boundary effects.

5.1.1 The Numerical Approximation of Real Gas Flow

The differential equation describing the flow of a fluid through a porous medium in two dimensions can be written in terms of the density as:

$$\frac{\partial}{\partial x}(\rho v_x)+\frac{\partial}{\partial y}(\rho v_y)-m^{\bullet}+\phi\frac{\partial \rho}{\partial t}=0\ , \tag{5.1}$$

where m* is the source term.

Applying the gas law and the Darcy's law yields :

$$k\{\frac{\partial}{\partial x}(\frac{p}{\mu z}\frac{\partial p}{\partial x})+\frac{\partial}{\partial y}(\frac{p}{\mu z}\frac{\partial p}{\partial y})\}+m^{\bullet}\frac{RT}{M}=\phi\frac{\partial}{\partial t}(\frac{p}{z})\ . \tag{5.2}$$

Applying the pseudo-pressure transformation :

$$m(p)=2\int_0^p\frac{p}{\mu z}dp\ \text{, and} \tag{5.3}$$

$$\frac{\partial}{\partial t}(\frac{p}{z})=\frac{p}{z}c_g\frac{\partial p}{\partial t}\ , \tag{5.4}$$

yields :

$$\frac{\partial^2}{\partial x^2}m(p)+\frac{\partial^2}{\partial y^2}m(p)+\frac{2m^{\bullet}RT}{Mk}=\frac{\phi\mu c_g}{k}\frac{\partial m(p)}{\partial t}\ . \tag{5.5}$$

The derivatives on the left-hand side of Equation (5.5) are evaluated using a central difference approximation. Only the diffusivity term on the right-hand side is non-linear. Equation (5.5) suggests that the μc_g term should be averaged during the time interval considered. A simple arithmetic

average of the μc_g terms during the current and previous time steps, namely the n+1 and n time step, has been found to be adequate. The resulting equations are fully implicit with all the m(p) terms on the left-hand side set at time step n+1.

Once the matrix is set up, the SPARSPAK subroutine (George et al. (1980)) is used to solve the resulting set of equations. Due to the non-linear diffusivity term, the equations have to be solved iteratively. The convergence usually requires two to three iterations for the cases considered. With the tolerance of successive iterations of 10^{-5}, the material balance error is around 10^{-5}.

The program source code of the simulator is provided in Appendix A.

5.2 The Grid Specification Module

Apart from handling the input and output, this module computes the transmissibilities for each grid location. The reservoir is divided into three regions. For a square containing the well at the center (Fig 5.1), the first region is around the well and covering a distance of one-fifth of the reservoir length in the x- and y- directions. This region can be subdivided into two areas- Area I and Area II. Proper sizing of the grids for Area I and Area II is critical to the accuracy of the pressure response at the well . The grid size in Area I has to be small enough to minimize the numerical wellbore storage effect. The grid size for Area II has to be approximately comparable to the radius of investigation of the pressure transient responses during the first few time steps in the calculation for the pressure response to reflect the correct reservoir properties.

Immediately surrounding Area II is Area III which covers two-fifths of the length of the x- and y-directions. Area IV covers the rest of the reservoir. The grid size for Area III can be specified, but the grid size for Area IV is fixed as twice the grid size of Area III. Proper specification of the grid sizes in these two areas is critical to the accuracy of the average reservoir pressure.

For other well/reservoir geometries, the grid construction also starts at the well. The grid construction is performed for Areas I and II, then for the surrounding area. Depending on the distance of the well to the boundaries, Areas III and IV may not be present in some quadrants of the reservoir. The grid construction is described in more detail in Brown (1992).

The program listing for the grid specification module is provided in Appendix A.

5.3 The Gas Correlation Module

The program uses a number of gas property correlations given in Appendix D of the ERCB. manual (1975) . The following correlations are used in the subroutines :

- The gas viscosity by Carr et al. (1954)
- The gas compressibility and compressibility factor by Dranchuk et al. (1974)
- The sour gas correction factor for the compressibility factor by Wichert and Aziz (1972)

5.4 Verification of Pressure Responses During Short Producing Times

For short producing time with negligible non-Darcy flow effects around the wellbore, Al-Hussainy et al. (1966), Wattenbarger and Ramey (1968) and Reynolds et al. (1987) demonstrated that the pressure transient tests for gas wells could be accurately analyzed by plotting pseudo-pressure vs. time for drawdowns, and pseudo-pressure vs. Horner time ratio for buildups. Al-Hussainy et al. and Wattenbarger and Ramey showed that the dimensionless drawdown and buildup solutions for gas flow are the same as the corresponding liquid cases, when the producing time is short. Short producing time indicates that no boundary effects are felt at the well during the production.

Therefore, for short producing times, the verification of the simulator can be achieved by comparing the simulated data with the corresponding liquid solutions.

For long producing times, the verification can be accomplished by comparing the pressure response from a gas well producing from a closed square and the pressure response of a gas well producing from a closed circle. The approximate solutions for a gas well producing from a closed circular reservoir is readily available from Reynolds et al. (1987). This part of the verification will be presented in Chapter 6, since it overlaps with discussions in that chapter.

In Figure 5.2, a set of short producing time drawdown responses for different gas and reservoir properties are plotted with the liquid solution. The properties used in the base case are given in Table 5.1. The gas compressibility, compressibility factor and viscosity as a function of pressure for a number of selected gas and reservoir properties are given in Appendix C. All the gas cases considered trace the liquid solution very well, except at early producing times . The early-time data from the simulator are influenced by the numerical wellbore storage effects, which are not considered in the liquid solution used. The wellbore storage is inherently present in the simulated data due to the finite size of the well block used in the numerical simulator.

Figure 5.3 presents the buildup responses from the reservoirs in Figure 5.2 plotted with the liquid buildup solution. Good match of all data is observed except for the early and the late time data which are affected by the numerical wellbore-storage and pressure-stabilization effects, respectively. The dimensionless producing time used is defined with the viscosity and compressibility evaluated at the initial reservoir pressure :

$$t_{pDA} = \frac{0.0002637 k t_p}{\phi (\mu c_t)_i A} .$$

6. SENSITIVITY ANALYSIS

In this chapter, the effects of gas and reservoir properties on buildup responses following long producing times of a well in the center of a square are examined followed by a discussion on the dimensionless variables. In the last section of this chapter, the average reservoir pressures from the simulator are compared with the average reservoir pressures estimated from the material balance.

6.1 Sensitivity Analysis of Buildup Responses Following Long Producing Times

The buildup responses are generated for a well in the center of a square reservoir to approximate the responses for a well at the center of a circular drainage area. As discussed in the literature review, pressure transient response for a gas well located at the center of a circular reservoir was studied by Al-Hussainy et al. (1966) , Al-Hussainy and Ramey (1966), Wattenbarger and Ramey (1968), and Reynolds et al. (1987), among others. The buildup responses generated for a square are analyzed using the methods developed for the circular reservoirs presented in these papers to further validate the numerical model used. To limit the number of parameters to be studied, sensitivity analyses are performed using the base case parameters in Table 5.1. The gas properties as a function of pressure for the base case are presented in Appendix D.

The buildup responses for the sensitivity analysis are graphed in Figure 6.1. The producing time for each case corresponds to t_{pDA} of 10. Figure 6.1 highlights a fundamental difference between the liquid and gas cases. For the liquid flow, the dimensionless solution is completely general - the solution is independent of the parameters considered - and therefore would have fallen on the same curve. For the gas flow, however, the dimensionless solution is not completely general, as is evident from Figure 6.1. Each buildup curve is displaced distinctly from one another. This sensitivity to the parameters can be attributed to the change in gas properties with the change in pressure. For short producing times, the dimensionless pressure responses for different reservoir and gas properties

appear general (as in Figure 5.3) because the gas properties have not changed significantly from the initial values. However, the analysis of Figure 6.1 reveals that the permeability, skin factor and the stabilized pseudo-pressure are correct for every case. These results are summarized in Table 6.1. During the infinite-acting period (up to R_{H2} of approximately 10^3), all the buildup curves considered have a slope close to the characteristic value of 1.151 per log cycle and are correctly displaced such that the skin factor estimated from the semi-log straight line portion is correct. A modified Horner time ratio, R_{H2}, is used in the analysis. The use of R_{H2} for the analysis of a buildup test following long producing time was previously suggested by Reynolds et al.(1987).

Figure 6.1 shows the parameters used do not affect the accuracy of the analysis of the semi-log straight line portion of the buildup data. However, different parameters do cause the buildup responses to be displaced and stabilize at different pseudo-pressure. Here, it might be misleading to present the dimensionless buildup plots since the dimensionless presentation usually suggests that the behavior studied is general. The conventional buildup plots will be used throughout this investigation although the dimensionless presentation will still be used for some specific situations.

6.2 Determination of The Producing Times at Which The Dimensionless Buildup Curves Become Sensitive to The Gas and Reservoir Properties

Most of the investigations done in the area of well testing employed the dimensionless variable as a means of generalizing the studies. A comparison between Figures 5.3 and 6.1 shows that, for buildup plots of a gas well, the usual dimensionless variables are general only for short producing times but become sensitive to the parameters of the problem when the producing time is long. This observation has not been discussed before in the literature.

To determine when the dimensionless plots start to become sensitive to the gas and reservoir properties, a series of buildup responses is simulated. The reservoir and gas properties used are based

on the base case values in Table 5.1. The gas specific gravity and the reservoir temperature are selected as the variables for study since the buildup curves of these two cases define the upper and lower bounds in Figure 6.1, respectively. This observation may be different if other gas and reservoir properties were used. Two well/reservoir geometries are studied - that of a well in the center of a square and that of a well in a corner of a 4 :1 rectangle, with the relative well position of (0.75,0.75).

Figure 6.2 presents buildup plots for a well in the center of a square. The producing times considered correspond to t_{pDA} of 0.1,2.0 and 4.0. The viscosity and compressibility used in the dimensionless time definition is evaluated at the initial pressure. The t_{pDA} = 0.1 is the time for the system to reach pseudosteady state for the corresponding liquid case. Figure 6.3 is for the buildup plots for a well in a corner of a 4 to 1 rectangle. The producing times considered correspond to t_{pDA} of 2.0 and 4.0, where t_{pDA}=4 is the time for the corresponding liquid system to reach pseudosteady state.

Figures 6.2 and 6.3 demonstrate that the separation between the buildup data for the case with the gas specific gravity of 1.0 and the case with the reservoir temperature of 250° F become visibly distinct at t_{pDA} of 4.0. This conclusion is specific to the buildup responses of the set of reservoir and gas properties considered. The time of separation for other sets of reservoir and gas properties may be different. Based on the limited information in Figure 6.3, the dimensionless plots become sensitive to the gas and reservoir properties before the system reaches pseudosteady state for the case of a well in a corner of a 4:1 rectangle. This observation suggests that the dimensionless variables commonly used may not be suitable for the study of buildup analyses of gas wells.

Reynolds et al. (1987) used the dimensionless plots extensively in their study of pressure transient analysis for a gas well at the center of a circular reservoir. They demonstrated that the average reservoir pressure could be accurately determined from a pressure buildup test conducted after a long producing time. However, they did not compare the dimensionless graphs for different gas and reservoir conditions. The configurations of a well in the center of a circular reservoir can be

considered approximately the same as a well in the center of a square. Since the dimensionless plots of buildup responses following long producing times for a well in a square (Figure 6.1) are sensitive to the gas and reservoir properties, the dimensionless plots for buildup responses following long producing times for a well in the center of a circular reservoir would be sensitive to the gas and reservoir properties as well .

Despite the sensitivity of the buildup responses, the analysis results in Table 6.1 and the results of Reynolds et al. (1987) indicate that accurate average reservoir pressures can be estimated from buildup responses for a well in the center of a square and a well in the center of a circular reservoir, respectively. The fact that average reservoir pressures can be accurately estimated from buildup tests, despite the sensitivity of the buildup responses, justifies further investigation into this problem. This investigation is presented in Appendix C.

6.3 Comparison of The Simulated Pressure With The Material Balance Pressure

As production continues, the pressure inside the reservoir will decline due to the withdrawal of the fluid from the reservoir. The magnitude of the new average reservoir pressure can be obtained either by shutting in the well and letting the pressure profile stabilize or by the material balance relationship. If the pressure profile in the reservoir is known, the average reservoir pressure can be computed as the volumetric average of the pressure distribution in the reservoir at the time of shut-in. For the simulation data, the volume-averaged reservoir pressures obtained from the simulator and the average reservoir pressure estimated by the material balance equation are somewhat different due to the inherent material balance error in the simulator .

Figure 6.4 compares the percent difference between the average reservoir pressure estimated from the material balance with the average reservoir pressure obtained from volumetric-averaging of the block pressures. The base case parameters are used for the five reservoir/well geometries considered.

The x_w and y_w in Figure 6.4 indicate the well position relative to the length and width of the reservoir in the x- and y-directions, respectively. At the producing time corresponding to t_{pDA} of 30, which is the maximum producing time considered in this study, the percentage difference for all cases is less than 6%. The geometries with the well located off center seem to yield the least accurate volume-averaged reservoir pressure. This inaccuracy may be due to a greater proportion of large grid blocks used for the reservoir containing an off-centered well than the one containing a well in the center.

The average pressure difference presented for the five reservoir/well geometries in Figure 6.4 are the results of optimizing the computer time and memory with the accuracy of the pressure responses. The grid specifications for the cases in Figure 6.4 are given in Table 6.2. These grid specifications will be used throughout this study. As outlined in Section 5.2, the reservoir area is subdivided into three regions. The first region is made up of Area I and Area II. The second region is made up of Area III and the third region is made up of Area IV. Proper specification of the grid sizes in each region is critical to the overall accuracy of the pressure distribution in the reservoir. As an example, for the case of a 1:1 reservoir with the well at the center (the first case in Table 6.2), the grid blocks immediately surrounding the well is specified as a 1 ft x 1 ft square (Area I). These 1 ft x 1 ft grids cover 5% of the first region. The rest of the first region is covered by Area II which is composed of 2 ft x 2 ft grid blocks. The size of the grid in Area II is multiplied by three for the grid size in the second region (Area III). The grid size in the third region (Area IV) will be twice the grid size in the second region, a 12 ft square in this particular case.

For the five cases considered in Figure 6.4, the pseudo-pressures stabilize after a long shut-in time. The stabilized pressures are evaluated corresponding to these pseudo-pressures. Based on Figure 6.4, the maximum difference between the stabilized pressure and the volume-averaged reservoir pressure, obtained using grid-block pressures at the instant of shut-in, is less than 5 psi. Throughout this study,

the stabilized pressure is considered the correct average reservoir pressure and will be compared to the average reservoir pressure estimated from the buildup analysis .

7. PRESSURE TRANSIENT ANALYSIS FOR A GAS WELL LOCATED IN A RECTANGULAR RESERVOIR

In this chapter, the pressure responses generated for a well producing from a rectangular gas reservoir are studied to assess the accuracy of the analysis methods generally developed for the circular reservoir. Effects of the reservoir geometry, well location, reservoir condition, gas properties, producing time and producing rate on the accuracy of the analyses are investigated.

7.1 Methodology

Before attempting to analyze the buildup responses generated by the simulator, steps are taken to ensure that the grid specifications used provide accurate pressure responses. The grid configuration is considered adequate when the drawdown responses (before the onset of the boundary effects) can be accurately analyzed for the permeability and skin factor, and when the stabilized pressure from the simulator agrees well with the average reservoir pressure calculated by the material balance equation. For all the cases simulated, the difference between the stabilized pressure and the material-balance average pressure is less than 6% after t_{pDA} of 30 using the grid specifications in Table 6.2.

For each investigation performed, the pressure responses generated by the simulator are analyzed for the permeability, skin factor, and average reservoir pressure. The accuracy of each analysis method is then evaluated by comparing the analysis results with the input values of permeability and skin factor, and the stabilized pressure output from the simulator.

7.1.1 The Well/reservoir Geometries to Be Studied

Figure 7.1 (excerpted from Dietz, 1965) shows five well/reservoir geometries to be studied. The geometries are selected to cover various interactions between the pressure responses and the boundaries.

In Figure 7.1, Well A is located at the same distance from all boundaries. Therefore, the pressure response at the well has a very short transition time after the end of the infinite-acting radial flow regime, where the pressure transient behaves as if there were no boundaries, to the pseudosteady state flow regime, where the effects of all the boundaries are felt at the well. The well/reservoir geometry of Well A is the closest approximation to the geometry of a well at the center of a circular reservoir, which is the principal geometry investigated in the literature. Thus, Well A serves as a calibration tool for this study with the previous studies on the circular reservoirs.

For other well/reservoir geometries in Figure 7.1, the effects of all boundaries are not felt at the same time. For Well B, the effects of the boundaries are felt in succession. Therefore, Well B is an ideal geometry to study the effects of the boundaries on the buildup responses. For Well C and Well D, two boundaries are felt at the same time. However, The second pair of boundaries are felt later for Well D than Well C. Finally, for Well E the effects of three boundaries are felt concurrently.

7.1.2 Parameters Used in The Study

The reservoir and gas properties for the base case given in Table 6.2 are used for all well/reservoir geometries. The effects of each property can be determined by comparing the pressure response of the corresponding case with the base case.

It was shown earlier that the dimensionless graphs for gas become sensitive to the gas and reservoir properties very early in the production (see Section 6.2). For the configuration of Well B, the dimensionless buildup plots become sensitive to the parameters of the problem before t_{pDA} of 4.0, the producing time for an equivalent liquid system to reach pseudosteady state. Furthermore, the dimensionless presentation does not reflect the magnitude of the average reservoir pressure directly. Since one of the main objectives of the study is to determine the average reservoir pressure, most presentations are in dimensional forms.

7.2 Effects of Well/Reservoir Geometries

In this section, the pressure data generated for the five well/reservoir geometries in Figure 7.1 are analyzed. The gas and reservoir properties used are taken from Table 6.2 (the base case) and the production rate used is 34.85 Mscf/D which corresponds to q_D of 0.01.

7.2.1 Analyses to Be Performed

The following analyses are to be performed for each well :

For drawdown analysis :

- Permeability is determined by Equation (3.39)
- Skin factor is determined by Equation (3.6) with pseudo-pressure replacing pressure terms

For the Horner plot :

- Permeability from Equation (3.39)
- The skin factor from Equation (3.40)

- Average reservoir pressure from Equations (3.14) and (3.16) with pseudo-pressure replacing pressure terms

For the MDH plot:

- Permeability from Equation (3.39)

- The skin factor from Equation (3.40)

- Average reservoir pressure from Equations (3.19) and (3.20) with pseudo-pressure replacing pressure terms

7.3.1 Analyses of A Well Producing From The Center of A Square Reservoir

7.3.1.1 Drawdown Analysis

Figure 7.2 presents a semi-log graph of the drawdown response for Well A. A straight line develops on the plot starting at a producing time of 0.003 hours. The data points earlier than 0.003 hours are influenced by the numerical wellbore storage effect. Since the pressure data are simulated using a well block, which is one foot by one foot in size, a small portion of the data is distorted by the finite size of the well block.

The slope of the straight line is $3.53*10^7$ psi^2/cp. From the slope, the permeability is estimated using Equation (3.39) to be 0.98 md. Using Equation (3.6), with pseudo-pressure replacing pressure terms, the skin factor is calculated to be -0.06. The values of the permeability and skin factor match the simulator inputs quite well. Al-Hussainy et al. (1966) and Reynolds et al. (1987) also reported success of analyzing drawdown tests of a gas well using semi-log graphs.

In Figure 7.2, the data start to deviate from the straight line after a producing time of 5 hours. The dimensionless time for the boundary effects to be felt at the well for Well A (the fourth column in

Figure 7.1) is 0.1 with the corresponding producing time of 4.5 hours. Again, Al-Hussainy et al. and Reynolds et al. reported that drawdown response started to deviate from the infinite-acting behavior at a dimensionless producing time t_{pDA} of 0.1.

The estimates of permeability and skin factor, which appear to be slightly lower than the input values, were also reported in the literature. Finjord and Aadnoy (1986) pointed out that the low estimates of skin factor and permeability were caused by the non-linearity contained in the diffusivity equation for gas. This non-linearity, the μc_g term on the right-hand side of the diffusivity equation, is a function of pressure. If the drawdown around the wellbore is high, as is the case for high producing rate or a long producing time, the decrease in the permeability and skin factor estimated will be significant. Wattenbarger and Ramey (1968) reported that drawdown responses can be accurately analyzed up to q_D of 0.1. If q_D is higher than 0.1, the drawdown pseudo-pressure responses start to deviate from the liquid drawdown responses (Figure 3 in their paper.) Since the low producing rate used for Well A causes only a small pressure drawdown around the wellbore, the effects of the non-linearity are mild.

7.3.1.2 Analysis Based on The Horner Plot

Figure 7.3 is the Horner plot of Well A after a producing time corresponding to t_{pDA} of 30. Three Horner time ratios are used in the plot. The Horner time ratio R_{H1} given by Equation (3.32) is the conventional definition of the Horner time ratio used in buildup analyses for liquid flow while the Horner time ratios R_{H2} and R_{H3} are based on the formulation suggested by Reynolds et al (1987). Since the responses based on the Horner time ratio R_{H2} and R_{H3} are virtually indistinguishable, the analysis is performed using R_{H2}.

In Figure 7.3, the pseudo-pressure response graphed with R_{H2} and R_{H3} are located above the pseudo-pressure response graphed with R_{H1}. Due to the higher position of the R_{H2} and R_{H3} curves,

the extrapolation of these data points to the Horner time ratio of unity will yield higher false pseudo-pressure $m(p^*)$ for R_{H2} and R_{H3} than for R_{H1}. Consequently, the average reservoir pressures determined from R_{H2} and R_{H3} are higher than from R_{H1}. This observation is general for any Horner plot of a gas well producing for a long producing time, as mentioned by Reynolds et al. (1987).

After a few early data points affected by wellbore storage, the data points for each of the three Horner time ratios exhibit a straight line portion on which the analysis is performed. The analysis based on R_{H2} yields a permeability of 0.99 md, skin factor of -0.07, while the analysis on R_{H1} yields a permeability of 0.95 md, and a skin factor of -1.15.

The last portion of the pressure data shows pressure stabilization. The stabilized m(p) for Well A is $3.57*10^7$ psi^2/cp, corresponding to an average reservoir pressure of 2134 psia. The straight line portion of the data points for R_{H2} extrapolates to a false pseudo-pressure of $4.61*10^8$ psi^2/cp. The false pseudo-pressure for the data points plotted with R_{H1} is $4.4*10^8$ psi^2/cp. Both the MBH (Equation 3.14) and Dietz methods (Equation 3.16) are used to estimate the average reservoir pressure. For a given Horner time ratio, both methods yield the same average reservoir pressure. For the analysis based on R_{H2}, the average pseudo-pressure is $3.57*10^8$ psi^2/cp, which is equal to the stabilized pseudo-pressure from the simulator. For R_{H1}, the calculated pseudo-pressure at the average pressure is $3.32*10^8$ psi^2/cp corresponding to an average reservoir pressure of 2,050 psi. The average reservoir pressure as determined by R_{H1} is 84 psi lower than the average reservoir pressure from the simulator.

Based on the estimates of permeability, all the three Horner time ratios used appear to be satisfactory. However, the analysis based on R_{H1} yields an unrealistically low value for the skin factor. A skin factor of -1.15 suggests that the well is stimulated. Analyzing the gas buildup tests after a long producing time with R_{H1} can, therefore, lead to a gross misinterpretation. Similarly, the

average reservoir pressure calculated from R_{H2} is accurate while the average reservoir pressure estimated from R_{H1} is too low.

Similar conclusions regarding the accuracy of the three Horner time ratios in the estimation of permeability, skin factor and average reservoir pressure were previously reached by Reynolds et al. (1987) for the case of a well in the center of a circular reservoir.

The unrealistically low estimate of the skin factor based on R_{H1} can be explained by investigating Equation (3.40). In Equation (3.40), the logarithmic term on the right-hand side contains the gas viscosity and compressibility evaluated at the well pressure extrapolated to a shut-in time of 1 hour. The skin factor equation used for R_{H1} doesn't account for any change in the gas properties, and consequently the gas viscosity and compressibility are estimated at the initial pressure. On the contrary, the analysis based on R_{H2} and R_{H3} is designed to account for the change of the viscosity and compressibility. The viscosity and compressibility are evaluated corresponding to the shut-in time used in Equation (3.40). Since the compressibility increases drastically while the viscosity doesn't decrease significantly with a decrease in pressure, the magnitude of the viscosity-compressibility product is larger if evaluated at an extrapolated pressure corresponding to a shut-in time of 1 hour than if it is evaluated at the initial pressure. The overall effect of evaluating the viscosity and compressibility product at an extrapolated pressure corresponding to a shut-in time of 1 hour is to reduce the magnitude of the skin factor calculated with Equation (3.40). The significance of using the viscosity and compressibility corresponding to an extrapolated pressure at 1 hour is that the gas properties around the wellbore can be accurately represented in the skin factor estimation.

7.3.1.3 Analysis Based on MDH Graph

Figure 7.4 is an MDH graph of the pressure buildup for Well A using three MDH time parameters given by Equations (3.42) to (3.44). The shut-in pseudo-pressure graphed with Δt_2 and Δt_3 (the

normalized time and pseudotime, respectively) are not visually distinguishable. A straight line portion appears after a few data points distorted by the wellbore storage effect on all three MDH time functions. Since the data points for Δt_2 and Δt_3 are indistinguishable, the analysis is performed on Δt_2. The MDH analysis based on Δt_2 yields a permeability of 0.99 md and skin factor of -0.07. The permeability and skin factor analyzed by using the pseudo-pressure corresponding to Δt_1 are 1.02 md and -0.83, respectively.

The average reservoir pressure for the MDH plot is estimated using the Dietz(1965) method with the MDH time estimated from Equation (3.20). The wellbore pressure stabilizes at 2,134 psi with a corresponding pseudo-pressure of $3.57*10^8$ psi^2/cp. Using Equation (3.20) for Δt_2 yields a pseudo-pressure of $3.51*10^8$ psi^2/cp, which is in excellent agreement with the simulator's pseudo-pressure reached after a long shut-in time. The pseudo-pressure for Δt_1 corresponding to the MDH time calculated by Equation (3.21) is $3.28*10^8$ psi^2/cp, which corresponds to an average pressure of 2,037 psi, some 97 psi lower than the average reservoir pressure from the simulator.

From the permeability, skin factor, and average reservoir pressure obtained through Δt_1 and Δt_2, it can be concluded that the use of Δt_2 and Δt_3 in the MDH plot yields accurate estimates of permeability, skin factor and average reservoir pressure. The use of Δt_1 yields estimates of permeability, skin factor and average reservoir pressure that are too low.

Table 7.1 summarizes the results of the buildup analysis using the Horner time ratios and MDH times. The analysis using the modified Horner time ratios, R_{H2} and R_{H3} ,and the modified MDH times, Δt_2 and Δt_3, yields accurate estimates of permeability, skin factor, and average reservoir pressure. The use of the conventional Horner time ratio R_{H1} and MDH time Δt_1 yields permeability, skin factor and average reservoir pressure that are too low .

7.3.2 Analyses of A Well Producing From A Corner of A Four to One Rectangular Reservoir

In this section, the applicability of the buildup and drawdown analyses as given in Section 7.2.1 is assessed for the case of a well in a corner of a four to one reservoir - Well B. This well/reservoir geometry is an extreme test on all the analysis methods. The pressure profile established between the well and any boundary of the reservoir is different due to the different distance from the well to each boundary. Consequently, Well B does not have the symmetry of the pressure profile as in Well A .

As discussed earlier, the use of the modified Horner time ratios and the modified MDH times allows the variations of the gas viscosity and compressibility to be accounted for during a buildup test. Reynolds et al. (1987) justified the use of the modified Horner time ratios through the pressure profile established around the well during the buildup period. They stated that the pressure profile was flat within the radius of investigation of the pressure transient created during the buildup. The flat pressure profile allowed the gas viscosity and compressibility within the radius of investigation during the shut-in to be accurately represented with the corresponding gas properties at the well.

The argument presented by Reynolds et al. (1987) has been substantiated through their study of pressure buildup of a well producing from the center of a circular reservoir and the study of Well A in the previous section. For a well/reservoir geometry which is significantly different from that of a well in the center of a circular reservoir, the validity of Reynolds et al.'s argument is still debatable. If the analysis methods in Section 7.2.1 yield reasonably accurate estimates of permeability, skin factor and average reservoir pressure for the geometry of Well B, the analysis methods in Section 7.2.1 should yield satisfactory results for other well/reservoir geometries where the boundaries are located at different distances from the well.

7.3.2.1 Drawdown Analysis

Figure 7.5 is a semi-log graph of the drawdown test data for Well B. The data points start to fall on the semi-log straight line after the wellbore storage effect diminishes. When the boundary effects start to be felt at the well, the data points start to deviate from the straight line. From the semi-log straight line, a permeability of 0.95 md and the skin factor of -0.13 can be calculated. The permeability and skin factor are within an acceptable range of accuracy.

The first visible departure of the data point on Figure 7.5 from the semi-log straight line appears around a producing time of 3 hour. The radius of investigation of the pressure transient at a given producing time can be estimated from (Reynolds el al., 1987) :

$$r_{inv} = 0.029\sqrt{\frac{kt}{\phi(\mu c_t)_i}} \,. \qquad (7.1)$$

Based on Equation (7.1), the radius of investigation after 3 hours of producing time is 92 ft away from the wellbore. The distances from Well B to all the boundaries are 25, 75, 100 and 300 ft. The radius of investigation of 92 ft indicates that the third boundary is reached when the departure of pressure response from the semi-log straight line becomes visible. The first and second boundaries do not cause appreciable departure from the semi-log straight line. This observation can be attributed to the approximate nature of the estimation of the radius of investigation and might indicate the possible shortcomings of the application of pressure transient analysis methods to determine the distance of a boundary.

7.3.2.2 The Horner Plot

Figure 7.6 is a Horner plot of the buildup data from Well B. Again, the pseudo-pressures graphed with R_{H2} and R_{H3} lie above those for R_{H1}. The false pseudo-pressure for R_{H2} and R_{H3} should be higher than the false pseudo-pressure for R_{H1}. Once again, the data points corresponding to R_{H2} and R_{H3} are not distinguishable. Therefore, only the buildup data graphed with R_{H1} and R_{H2} are analyzed.

The features on Figure 7.6 are similar to those found in Figure 7.4. After a few data points distorted by the wellbore storage during early shut-in time , the straight line portion is established. Following a long transition period, the pseudo-pressure eventually stabilizes. The transition period in Figure 7.6 is around three logarithmic cycles long. The corresponding period in Figure 7.4 lasts around one logarithmic cycle. The long transition period in Figure 7.6 is due to the location of Well B with respect to the boundaries.

A straight line can be observed from the Horner time of $7*10^2$ to $1*10^6$ for the pseudo-pressures graphed with R_{H2} and from $1*10^3$ to $2*10^5$ for the pseudo-pressures graphed with R_{H1}. The permeability calculated from the straight line is 0.99 md for the analysis using R_{H2} and 0.95 md for the analysis using R_{H1}. The skin factor is -0.15 and -1.15 for the analysis using R_{H2} and R_{H1}, respectively. The buildup analysis based on R_{H2} yields accurate estimates of permeability and skin factor. As for the buildup analysis based on R_{H1}, the permeability is less accurate than the analysis with R_{H2}. The skin factor for the analysis based on R_{H1} is unacceptable, however.

For the estimation of the average reservoir pressure, the false pseudo-pressures for R_{H2} and R_{H1} are $4.25*10^8$ and $4.02*10^8$ psi^2/cp, respectively. Using the MBH function, the pseudo-pressures corresponding to the average reservoir pressure are calculated to be $4.06*10^8$ and $3.82*10^8$ psi^2/cp for the analysis using R_{H2} and R_{H1}, respectively. The pseudo-pressure from the simulator stabilizes at $4.05*10^8$ psi^2/cp, which corresponds to a pressure of 2267 psia. The average reservoir pressures from the analysis using R_{H2} and R_{H1} are 2,271 and 2,213 psi, respectively. The average reservoir

pressure estimated from R_{H2} is within 4 psi of the simulator pressure, while the average reservoir pressure based on R_{H1} is 54 psi lower than the simulator pressure.

Using the Dietz method to estimate the average reservoir pressure, the pseudo-pressures corresponding to the average reservoir pressures for R_{H2} and R_{H1} are found to be $4.06*10^9$ and $3.82*10^8$ psi^2/cp, respectively, which are in excellent agreement with the pseudo-pressures corresponding to the average reservoir pressures estimated with the MBH method for both Horner time ratios.

7.3.2.3 The MDH Graph

Figure 7.7 is the MDH graph of the buildup response for Well B. The buildup data are plotted with three MDH times. Again, the data points plotted with Δt_2 and Δt_3 are indistinguishable. The analysis using Δt_2 yields a permeability of 0.99 md and a skin factor of -0.15, whereas the analysis using Δt_1 yields a permeability of 1.03 md and a skin factor of -1.13.

As to the determination of the pseudo-pressure corresponding to the average reservoir pressure from the MDH plots, the analyses using Δt_2 and Δt_1 yield pseudo-pressures corresponding to the average reservoir pressure of $4.06*10^8$ and $3.81*10^8$ psi^2/cp, respectively. The average reservoir pressure estimated from the conventional Horner time ratio is the same as the average reservoir pressure estimated from the conventional MDH time, and so are the average reservoir pressures estimated from the modified Horner time ratios and the modified MDH times. This observation is true for all the buildup tests analyzed in this study. The average reservoir pressures based on the Dietz method for Δt_2 and Δt_1 are within 4 and 54 psi of the stabilized pressure from the simulator, respectively.

The analysis results for Well B are given in Table 7.2. From Table 7.2, the analysis based on the modified Horner time ratios, R_{H2} and R_{H3}, and the modified MDH times, Δt_2 and Δt_3, yields

accurate estimates of permeability, skin factor and average reservoir pressure. The analysis using the conventional Horner time ratio, $R_{H1,}$ and the conventional MDH time, Δt_1 yields a reasonably accurate permeability. However, the skin factor and average reservoir pressure estimated from Δt_1 or R_{H1} are unacceptably low.

7.3.3 The Analysis of Wells C, D, And E

Figures 7.8 presents the Horner plots for Well C, D and E. Pressure transient responses at the three wells are affected by the boundaries with respect to the distance between the wells and the boundaries. All the characteristic features noted from the Horner plots for Wells A and B are present in Figures 7.8. The pseudo-pressure data points graphed with the modified Horner time ratios R_{H2} and R_{H3} lie above the pseudo-pressure data graphed with R_{H1}. The buildup responses graphed with R_{H2} and R_{H3} are virtually indistinguishable.

After a brief period when the buildup responses are distorted by the numerical wellbore-storage effects, the responses show a semi-log straight line from which the permeability and skin factor can be calculated. This portion of semi-log straight line corresponds to the infinite-acting radial flow regime for the buildup tests. After the semi-log straight line portion, the pseudo pressures deviate from the semi-log straight line, indicating that the effects of the boundaries start to become significant. In the last portion of the buildup data, the pseudo-pressures stabilize when the pressure reaches the average reservoir pressure everywhere in the reservoir.

Table 7.3 summarizes the results for the buildup in Figure 7.8. In addition, Table 7.3 also provides the results of the MDH analysis of the buildup responses in Figure 7.8. From Table 7.3, the buildup analyses using the modified Horner time ratios, R_{H2} and R_{H3}, as well as the modified MDH times, Δt_2 and Δt_3, yield accurate estimates of permeability, skin factor and average reservoir pressure for Wells C, D and E. The average reservoir pressures determined from the MBH and Dietz methods

using the modified Horner time ratios and the modified MDH times are also in excellent agreement with the corresponding average reservoir pressures from the simulator. The analysis using R_{H1} and Δt_1 yields a skin factor and average reservoir pressure that are too low.

Based on the results of the investigation on the accuracy of the Horner and MDH plots for all the five well configurations, the analyses using the modified Horner time ratios and the modified MDH times yield accurate estimates of the permeability, skin factor and average reservoir pressure. The analyses using conventional Horner time ratio and MDH time yield reasonable estimates of permeability but low estimates of the skin factor and average reservoir pressure.

7.4 Buildup Analyses for A Well Shut in During The Transitional Period

Figure 7.9 presents Horner plots of the buildup response for Well B following three short producing times. These three producing times are selected so that the corresponding radii of investigation are beyond the boundaries at 25, 50 and 100 ft during the respective producing time. Due to the relatively short producing times, the plots using R_{H1}, R_{H2} and R_{H3} are practically identical.

For all the three producing times, permeability of 0.99 md and a skin factor of -0.15 is estimated from the Horner plot. The average reservoir pressures estimated using the MBH method agree within 2 psi of the stabilized pressure.

Although not shown here, buildup analyses for the shut-in during the transitional period have been performed for Wells C, D and E. The permeability, skin factor and average reservoir pressure estimated from the buildup analyses using R_{H1}, R_{H2} ,or R_{H3} are satisfactorily accurate for all the three wells considered. The permeabilities estimated are within 2% of the input values. The skin factors are no worse than -0.2 and the average reservoir pressure agree within 3 psi with the average pressure from the simulator. For all practical purposes, the Horner analysis yields accurate estimates

of permeability, skin factor and average reservoir pressure for a buildup test of a well in a rectangular gas reservoir following producing times between the infinite acting period and pseudosteady state.

For a well shut-in before the system reaches pseudosteady state, the μc_g at the well has not changed appreciably from the initial condition. Therefore, the MDH analysis using Δt_1, Δt_2 ,or Δt_3 would also yield accurate estimates of permeability, skin factor and average reservoir pressure for the buildups conducted when the producing well is shut in during the transition period. However, for producing times shorter than the time for the system to reach pseudosteady state, the duration of the semi-log straight line for an MDH graph would be significantly shorter than for the corresponding Horner plot. The short semi-log straight line on the MDH graph may cause difficulty in the analysis. Thus, a buildup analysis using the Horner plot is preferable. The times to the end of the semi-log straight lines on Horner and MDH graphs will be discussed in more detail in Section 7.8.

7.5 Effects of Gas And Reservoir Properties

The effects of well/reservoir geometries and the producing time are investigated in Sections 7.3 and 7.4 using the base case gas and reservoir properties given in Table 7.1. It has been shown that the gas and reservoir properties do not have significant impacts on the accuracy of buildup analysis of tests conducted after a producing time shorter than the time for a corresponding liquid system to reach pseudosteady state (Section 7.3 for the producing time during the transition period and Section 4.4 for infinite-acting.) This section covers the effects of gas and reservoir properties on the accuracy of analyses for buildup tests conducted after long producing times.

The reservoir and gas properties are varied from the base case values to assess the effects of each property on the buildup analyses. Figure 7.10 presents Horner plots of the buildup responses for the cases simulated for Well B. The dimensionless rate, $q_{D,}$ is maintained at 0.01 and the producing

times used correspond to a dimensionless time t_{pDA} of 10 in Figure 7.10. Table 7.4 presents the values of the properties varied from the base case as well as the pseudo-reduced initial pressure and pseudo-reduced reservoir temperature for each case.

In Figure 7.10, the pseudo-pressure data from each case are graphed using both R_{H1} and R_{H2}. The pseudo-pressure response graphed using R_{H3} would be indistinguishable from the data graphed with R_{H2} and are consequently not considered. The dimensionless shut-in pseudo-pressure m_{sD} is used in Figure 7.10 to show that all the slopes obtained from the semi-log straight lines, regardless of the choice of R_{H1} or R_{H2}, are approximately equal to the characteristic slope of 1.151. Thus, the permeability calculated from the slopes is correct . Determining the skin factor and average reservoir pressure requires the use of Equations (3.40) and (3.36). The estimated permeabilities, skin factors and average reservoir pressures from the analyses are given in Table 7.5. The results of the analyses performed emphasize the accuracy of the analysis using R_{H2} over R_{H1} for long producing times. Analyzing a buildup with R_{H1} generally yields the skin factor and average reservoir pressure that are too low, whereas the analysis with R_{H2} yield accurate estimates of permeability, skin factor and average reservoir pressure.

7.6 Effects of The Producing Rate

All previous investigations are conducted for a producing rate corresponding to q_D of 0.01. Wattenbarger and Ramey (1968) and Reynolds et al. (1987) studied the buildup and drawdown analyses for a well producing at a high producing rate corresponding to q_D of 0.1. They concluded that the drawdown analyses using the semi-log plots of pseudo-pressure and producing time yielded accurate estimates of permeability and skin factor. Wattenbarger and Ramey also reported that the buildup analysis for q_D of 0.1 using R_{H1} did not yield accurate estimates of the permeability and skin factor. Reynolds et al. reported successful applications of R_{H2} and R_{H3} to analyze buildup

tests for q_D of 0.1 for permeability and skin factor. However, Reynolds et al.'s results for q_D=0.1 pertain to short producing times only.

In this section, the pressure response for a well producing at q_D of 0.1 is simulated for producing times t_{pDA} of 0.03, 0.1 and 0.93. The well/reservoir geometry used is that of Well A to ensure the longest possible producing time. The t_{pDA} of 0.93 is the longest producing time for which this high flow rate can be sustained before the wellbore flowing pressure reaches atmospheric pressure. For Well A, the pseudosteady state flow regime is reached after t_{pDA} of 0.1.

Figure 7.11 is a graph of a portion of the drawdown data for t_{pDA} of 0.93. The liquid drawdown solution as given by Equation (3.3) is also presented. The gas drawdown data cross the liquid drawdown solution at t_D of 10^5, which corresponds to t_{pDA} of 0.1 (r_w is 0.2 ft and the reservoir area is 40,000 ft^2.) Since the change in the slope suggests a change in the flow regime from infinite acting to pseudosteady state, the gas drawdown data prior to the cross-over are analyzed using the liquid drawdown solution. The analysis yields a dimensionless slope of 1.164 which is within 2% of the correct dimensionless slope of 1.151. The gas drawdown data are below the liquid drawdown solution during the infinite-acting radial flow period. The location below the liquid solution indicates that a negative skin factor will be estimated from the analysis. A skin factor of -0.18 is obtained, which is within acceptable range of accuracy.

Figure 7.12 graphs the buildup responses .for producing times t_{pDA} of 0.03, 0.1 and 0.93. The data are plotted using R_{H1} and R_{H2}. Again, the data plotted using R_{H3} would overlay the data plotted with R_{H2}. Even with a small t_{pDA} of 0.03, the data points plotted with R_{H1} and R_{H2} do not overlay. It was shown earlier that the data points plotted with R_{H1} and R_{H2} for Well A overlay well until pseudosteady state is attained for a producing rate q_D of 0.01. With the high producing rate used in this section, the pressure drawdown around the wellbore is much larger than the pressure drop induced by q_D of 0.01. The large pressure drawdown causes the pressure dependent gas

properties, the viscosity, compressibility and compressibility factor, to vary significantly from the initial values.

The results of the buildup analyses for the three producing times considered are summarized in Table 7.6. Unlike the analysis results for q_D=0.01, even the permeability and skin factor estimated for q_D=0.1 using R_{H2} are less accurate for buildup tests conducted after longer producing time than for shorter producing times. The results in Table 7.6 also indicate that the analysis of buildup tests using R_{H2} provides results that are more accurate than the analysis using R_{H1}. The permeability estimated with R_{H1} falls out of an acceptable range of accuracy at t_{pDA} of 0.93. At a t_{pDA} of 0.93, the analysis based on R_{H2} still yields accurate estimates of permeability and skin factor. At t_{pDA} of 0.93, the average reservoir pressure estimated with R_{H1} is some 200 psi lower than the correct pressure while the average reservoir pressure estimated using R_{H2} is in excellent agreement with the average reservoir pressure from the simulator.

7.7 Effects of Gas Contaminants

The presence of gas contaminants, such as hydrogen sulfide (H_2S), carbon dioxide (CO_2), and nitrogen (N_2), affects the properties of the natural gas. The correlations for the viscosity, compressibility, and compressibility factor in the industry are developed for uncontaminated natural gas using the gas specific gravity as a primary input. Corrections of the estimated gas properties are required for accurate prediction of the properties for the contaminated natural gas (Wichert and Aziz, 1972; Carr et al., 1954.) These corrections require the knowledge of the mole percent of the contaminants contained. Since the formulation of the pseudo-pressure and modified Horner and MDH times requires the knowledge of gas properties as a function of pressure, failure to correct the gas properties for the presence of gas contaminants will lead to error in the pseudo-pressure, modified Horner time ratios and MDH times. The error thus introduced will lead to error in the estimation of reservoir properties from well test analyses.

Zana and Thomas (1970) studied the effects of the contaminants on well test analyses using the pseudo-pressure and R_{H1}. By comparing the results of the buildup analyses using pseudo-pressure with and without the correction for the contaminants, they concluded that the permeability, skin factor and average reservoir pressure can be accurately estimated from the buildup analyses, if the gas properties were corrected for the contaminants. However, the permeability and skin factor estimated from the buildup analyses using the pseudo-pressure without gas property corrections for the contaminants were too low. For the situation of a well at the center of a circular reservoir, they did not find a significant difference between the average reservoir pressures estimated from the MBH method with and without the corrections for the contaminants.

Zana and Thomas (1970) assumed that the buildup analysis using R_{H1} and pseudo-pressure with gas property corrections yielded accurate estimates of the reservoir parameters. However, the buildup tests given as examples were limited to the tests conducted after relatively short producing times (t_{pDA} of 0.1 and 2.7, respectively). Due to the short producing times used in their study, their observations of the accuracy of the permeability, skin factor and average reservoir pressure should be tested for long producing times.

To extend Zana and Thomas' (1970) conclusions regarding the accuracy of buildup analyses of a gas well with contaminants to the rectangular geometry and long producing times, a number of buildup responses are generated for the study. The buildup responses from Wells A and B are graphed in Figure 7.13. The gas for both wells contains 20% H_2S. The wells are produced with q_D of 0.01 for a t_{pDA} of 30. The results of the buildup analyses for Figure 7.13 are given in Table 7.7.

In Table 7.7, the permeabilities and skin factors estimated with the analysis using gas properties without the corrections for gas contaminants are lower than the corresponding figures estimated from analysis using the gas properties with corrections for the gas contaminants. The average reservoir

pressures estimated from the buildup analyses using the gas properties with and without the corrections for contaminants appear to be accurate. This observation from Table 7.7 agrees with the observation made by Zana and Thomas (1970).

Table 7.8 presents the analysis results of the buildup data in Figure 7.13, if R_{H1} is used. From Table 7.8, the analysis based on R_{H1}, even with gas properties corrections, yields permeabilities, skin factors, and average reservoir pressures that are too low. However, the average reservoir pressures estimated are approximately the same for the analysis with and without gas properties corrections for the contaminants.

Based on the results in Table 7.7 and 7.8, it can be concluded that, for a buildup test conducted following a long producing time, the analysis using modified Horner time ratios will provide more accurate estimates of permeability, skin factor and average reservoir pressure than the analysis using conventional Horner time ratio. For a given Horner time ratio, failure to correct the gas properties for the presence of contaminants will not affect the estimates of the average reservoir pressures, but will affect the estimates of the permeabilities.

To illustrate the effects of the concentration of gas contaminants on the pressure buildup analyses for other configurations, a number of buildup cases following a t_{pDA} of 30 for Well B are generated. The data points corresponding to 10%, 20% and 30% H_2S concentrations of gas contaminants are plotted in Figure 7.14. The data points without correction are displaced above the corresponding data with correction. This displacement might suggest that the average reservoir pressures estimated from pressure data without corrections for the contaminants should always be higher than from the pressure data with corrections. However, the results summarized in Table 7.9 indicate that the average reservoir pressures determined from the analysis using gas properties with and without the corrections for the contaminants are about the same. This confusion stems from the fact that the different gas properties are used to calculate the pseudo-pressures. The location of the pressure data

without corrections for the contaminants above the data with the corrections only indicates that the average pseudo-pressures determined from the data without corrections are higher. However, the corresponding pressures to the pseudo-pressures estimated with and without corrections for the contaminants are about the same. For example, the average pseudo-pressures for the gas with H_2S content of 20% are $2.69*10^8$ and $2.55*10^8$ psi^2/cp based on the pseudo-pressure data with and without corrections for the contaminants, respectively. However, the corresponding pressures are almost the same, 1833 and 1834 psia, for the data with and without corrections for the contaminants, respectively.

Figure 7.15 is used to study the combined effects of high producing rate q_D=0.1, gas contaminants and boundaries. The pressure buildup responses are simulated for Well A following a t_{pDA} of 0.2 to take the flow regime into pseudosteady state. The results of the analysis are given in Table 7.10. The permeability and skin factor can still be accurately estimated from the buildup data if R_{H2} is used in the analysis. However, the average reservoir pressures seem to be inaccurate, about 60 psi different from the stabilized pressure. This inaccuracy is caused by the rapid change in pressure with the change of pseudo-pressure around 8,000 psi for the gas and reservoir conditions used (see Figure D.1) For example, the pseudo-pressure corresponding to the average reservoir pressure from the simulator for the case with 20% H_2S is $2.55*10^9$ and the average pseudo-pressure estimated by the MBH method is $2.53*10^9$ psi^2/cp. The MBH average pseudo-pressure is very close to the pseudo-pressure corresponding to the average reservoir pressure from the simulator. The relatively big discrepancy in the average reservoir pressures, therefore, is caused by the relationship between pressure and pseudo-pressure around the pressure range under consideration and not by the method of calculation.

7.8 The End of Semi-log Straight Line on Buildup Plots

The existence of a semi-log straight line on an Horner or MDH plot is crucial for the estimation of permeability, skin factor and average reservoir pressure. Therefore, every effort should be spent to ensure the validity of the semi-log straight line used for the analysis. A number of correlations have been developed to ascertain the time when the semi-log straight line begins and ends for liquid flow. One of the investigations was performed by Cobb and Smith in 1975. They generated pressure buildup responses for a well in several locations of a rectangular reservoir. Using the difference between the generated data and the theoretical infinite-acting responses, they determined the time when the semi-log straight line ends for both Horner and MDH plots. Earlougher (1977) adapted the results by Cobb and Smith and presented the correlations in Figures 5.6 and 5.7 of his monograph.

Figure 7.16 presents the time when the semi-log straight line ends, Δt_{DAesl} as a function of the producing time t_{pDA}, on the Horner and MDH plots for the configuration of Well A. The liquid correlations for Δt_{DAesl} are taken from Cobb and Smith (1975). The criterion used to determine the end of the semi-log straight line for the liquid case is when the computed pressure differs from the theoretical pressure by 5%. According to Cobb and Smith, this amount of error was approximately equivalent to a slope difference of 10%. The data for the gas cases have been obtained from the semi-log derivative analysis using the reservoir and gas properties of the base case. The Δt_{DAesl} for gas is selected when the semi-log derivative differs by more than 10% from the characteristic value of 0.5 (as suggested by Equation 3.25.) The semi-log derivative was calculated using the method suggested by Bourdet et al. (1989). From the derivative study, it is found that Δt_{DAesl} corresponding to each well/reservoir configuration is the same for three Horner time ratios. This observation also applies for the MDH times.

Figure 7.16 shows that Horner plots always produce a longer semi-log straight line than MDH plots. The shape and location of the gas and liquid curves in Figure 7.16 appear to be quite similar. Another feature on both the liquid and gas curves in Figure 7.16 is that after t_{pDA} of 0.1 (the time to reach pseudosteady state for this well/reservoir configuration), Δt_{DAesl} remains essentially constant.

Figure 7.17 shows a similar comparison for Well C. The criterion used in determining Δt_{DAesl} is the same as for Figure 7.16. Again, the gas and liquid curves appear to be in good agreement. The data points for the liquid case, however, were adapted from Earlougher (1977).

The correlations of the time to the end of the semi-log straight line presented are approximate. The correlations will be slightly different if different gas properties are used to generate the gas buildup responses. Table 7.11 presents the Δt_{DAesl} when different gas and reservoir properties are used for the configurations of Wells A and C. However, the range of the Δt_{DAesl} values for the gas cases cover the liquid correlations. Consequently, the liquid correlations for Δt_{DAesl} can be used as a guideline for determining the end of semi-log straight line for gas flow.

8. CONCLUSIONS AND RECOMMENDATION

8.1 Conclusions

1. The incorporation of gas viscosity and compressibility into the Horner time ratio or the shut-in time partially linearizes the gas flow equations so that the buildup analyses using pseudo-pressure in conjunction with R_{H2}, R_{H3}, Δt_2 and Δt_3 yield accurate estimates of permeability, skin factor and average reservoir pressure. The non-linearity in the gas flow equation is significant when there is a large pressure drawdown around the wellbore, such as the situations of high producing rates or long producing times.

2. Analyses using conventional Horner time ratio or shut-in time yield low estimates of permeability, skin factor and average reservoir pressure when there is a large pressure drawdown around the wellbore.

3. The MBH and Dietz methods of average reservoir pressure estimation are found to provide accurate results for the cases of a well producing from a rectangular reservoir provided that the modified Horner time ratio or the modified shut-in time is used in the analysis in conjunction with the pseudo-pressure.

4. Buildup analyses for a well producing from a rectangular gas reservoir containing a significant concentration of impurities yield accurate estimates of permeability, skin factor and average reservoir pressure provided that the gas properties used in pseudo-pressure, R_{H2}, R_{H3}, Δt_2 and Δt_3 are corrected for the presence of the impurities.

5. The time to the end of the semi-log straight line on the Horner and MDH plots for gas and liquid flow is approximately the same. The time to the end of the semi-log straight line for

liquid can be used as a guideline for a gas well producing from a similar well/reservoir configuration.

5. The dimensionless producing time t_{pDA} is not a good indication of the depletion level for a gas reservoir. However, the dimensionless pseudo-pressure corresponding to the average reservoir pressure still provides accurate indication of the depletion level for a gas reservoir. The graph of buildup responses using modified Horner or MDH times, in conjunction with the MBH or Dietz method of average pressure determination, is shown to be a good approximation of a liquid system with comparable depletion level.

8.2 Recommendation

The problem of interference tests of gas reservoirs should be addressed. Since gas properties are functions of pressure, the pressure profile established in the reservoir might have a significant impact on the storativity estimated from interference tests.

TABLES

γ_g (air=1)	0.6
T (°F)	150
p_i (psia)	9,000
k (md)	1
q_D	0.01

Table 5.1 Gas and reservoir properties for the base case

	k (md)	s	p_{stab}, psia	p_{MB}, psia
Base case	1.01	0.08	5,432	5,436
γ_g=1.0	1.00	0.01	4,662	4,677
T=250° F	1.02	0.02	5,527	5,533
k=10 md	1.01	-0.14	5,432	5,436
p_i=6000 psia	1.00	-0.12	3,795	3,809

Table 6.1 Analysis results for Figure 6.1

y:x	(y_{wD}, x_{wD})	x, ft	Grid Area I, ft	Area I fraction	Grid Area II	Area II multiplier
1:1	(0.5,0.5)	200	1	0.05	2	3
1:1	(0.75,0.75)	200	1	0.05	2	5
2:1	(0.75,0.5)	141.4	1	0.1	2	2
4:1	(0.5,0.5)	100	1	0.15	1.5	3
4:1	(0.75,0.75)	100	1	0.15	2	1.5

Table 6.2 Grid specifications for simulation runs used in the study

	k, md	s	$\bar{p}$, *psia*
Simulator	1	0	2,134
R_{H1}	0.95	-1.15	2,050
R_{H2} & R_{H3}	0.99	-0.07	2,134
Δt_1	1.02	-0.83	2,037
Δt_2 & Δt_3	0.99	-0.07	2,129

Table 7.1 Analysis results of the buildup response for Well A (q_D=0.01, t_{pDA}=30)

	k, md	s	$\bar{p}$, *psia*
Simulator	1	0	2,267
R_{H1}	0.95	-1.15	2,213
R_{H2} & R_{H3}	0.99	-0.15	2,271
Δt_1	1.03	-1.18	2,213
Δt_2 & Δt_3	0.99	-0.83	2,271

Table 7.2 Analysis results of the buildup response for Well B (q_D=0.01, t_{pDA}=30)

		k, md	s	$\bar{p}$, *psia*
Well C	Simulator	1	0	2,256
1:1	R_{H1}	0.97	-1.06	2,194
(0.75,0.75)	R_{H2}& R_{H3}	0.99	-0.15	2,256
	Δt_1	0.97	-1.06	2,194
	Δt_2& Δt_3	0.99	-0.15	2,256
Well D	Simulator	1	0	2,082
4:1	R_{H1}	0.97	-1.06	2,008
(0.5,0.5)	R_{H2}& R_{H3}	0.99	-0.12	2,100
	Δt_1	0.97	-1.06	2,008
	Δt_2& Δt_3	0.99	-0.12	2,100
Well E	Simulator	1	0	2,085
2:1	R_{H1}	0.97	-1.09	2,015
(0.5,0.75)	R_{H2}& R_{H3}	0.99	-0.14	2,102
	Δt_1	0.97	-1.09	2,015
	Δt_2& Δt_3	0.99	-0.15	2,102

Table 7.3 Analysis results of the buildup responses for Wells C, D and E (q_D=0.01, t_{pDA}=30)

	p_{pr}	T_{pr}
Base case	13.39	1.69
γ_g=1.0	13.79	1.26
p_i=6,000 psia	8.93	1.69
T=250° F	13.39	1.97
γ_g=1.0, p_i=5,000 psia	7.66	1.26

Table 7.4 Pseudo-reduced pressures and temperatures used in Figure 7.10

		k, md	s	$\bar{p}$, *psia*
Base case and k=10 md	Simulator	1.00	0	5,527
	R_{H1}	0.99	-0.45	5,490
	R_{H2}&R_{H3}	1.00	-0.09	5,527
γ_g=1.0	Simulator	1.00	0	4,772
	R_{H1}	0.99	-0.26	4,741
	R_{H2}&R_{H3}	1.00	0.12	4,772
p_i=6,000 psia	Simulator	1.00	0	3,869
	R_{H1}	0.99	-0.40	3,854
	R_{H2}&R_{H3}	1.00	-0.07	3,864
T=250° F	Simulator	1.00	0	5,627
	R_{H1}	0.99	-0.51	5,601
	R_{H2}&R_{H3}	1.00	-0.19	5,627
γ_g=1.0, p_i=5,000 psia	Simulator	1.00	0	2,985
	R_{H1}	0.99	-0.52	2,974
	R_{H2}&R_{H3}	1.00	-0.06	2,985

Table 7.5 Analysis results of the buildup responses for Figure 7.10 (q_D=0.01, t_{pDA}=10)

		k, md	s	$\bar{p}$, *psia*
$t_{pDA} = 0.03$	Simulator	1.00	0	8,953
	R_{H1}	0.90	-0.32	9,000
	R_{H2}&R_{H3}	0.98	-0.20	9,000
$t_{pDA} = 0.10$	Simulator	1.00	0	8,519
	R_{H1}	0.93	-0.70	8,525
	R_{H2}&R_{H3}	1.00	-0.30	8,519
$t_{pDA} = 0.93$	Simulator	1.00	0	5,617
	R_{H1}	0.84	-1.30	5,423
	R_{H2}&R_{H3}	0.95	0.08	5,617

Table 7.6 Analysis results of the buildup responses for Figure 7.12 (q_D=0.1)

		k, md	s	$\bar{p}$, *psia*
Well A	Simulator	1.00	0	1,923
	with correction	0.99	-0.16	1,916
	without correction	0.93	-0.13	1,926
Well B	Simulator	1.00	0	2,067
	with correction	0.99	-0.13	2,090
	without correction	0.93	-0.13	2,094

Table 7.7 Analysis results of the buidup responses for Figure 7.13 based on R_{H2} (H_2S=20%, t_{pDA}=30)

		k, md	s	$\bar{p}$, *psia*
Well A	Simulator	1.00	0	1,923
	with correction	0.96	-1.87	1,830
	without correction	0.90	-1.19	1,833
Well B	Simulator	1.00	0	2,067
	with correction	0.96	-1.14	2,014
	without correction	0.90	-1.19	2,014

Table 7.8 Analysis results of the buidup responses for Figure 7.13 based on R_{H1} (H_2S=20%, t_{pDA}=30)

		k, md	s	$\bar{p}$, *psia*
H_2S=10%	Simulator	1.00	0	1,974
	with correction	0.99	-0.15	1,897
	without correction	0.95	-0.14	1,897
H_2S=20%	Simulator	1.00	0	1,806
	with correction	0.99	-0.16	1,834
	without correction	0.93	-0.14	1,833
H_2S=30%	Simulator	1.00	0	1,762
	with correction	0.98	-0.18	1,789
	without correction	0.91	-0.15	1,793

Table 7.9 Analysis results of the buidlup responses for Figure 7.14

		k, md	s	$\bar{p}$, *psia*
H_2S=10%	Simulator	1.00	0	8,084
	with correction	1.02	-0.15	8,022
	without correction	0.95	-0.13	8,038
H_2S=20%	Simulator	1.00	0	8,083
	with correction	0.98	-0.16	8,035
	without correction	1.02	-0.15	8,036

Table 7.10 Analysis results of the buildup responses for Figure 7.15

	Δt_{DAesl}			
	Well A		Well C	
	Horner	MDH	Horner	MDH
Liquid	0.010	0.008	0.010	0.010
Base case	0.018	0.018	0.018	0.018
γ_g=1.0	0.019	0.019	0.019	0.022
T=250° F	0.013	0.013	0.057	0.015
k=10 md	0.015	0.015	0.013	0.018
p_i=6,000 psia	0.013	0.012	0.011	0.011
γ_g=1.0 p_i=5,000 psia	0.013	0.012	0.013	0.012

Table 7.11 Dimensionless times to the end of Horner and MDH straight line for Wells A and C

FIGURES

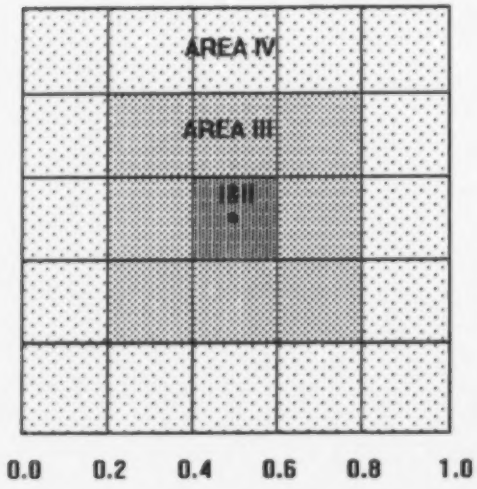

Figure 5.1 Area subdivision for a square reservoir

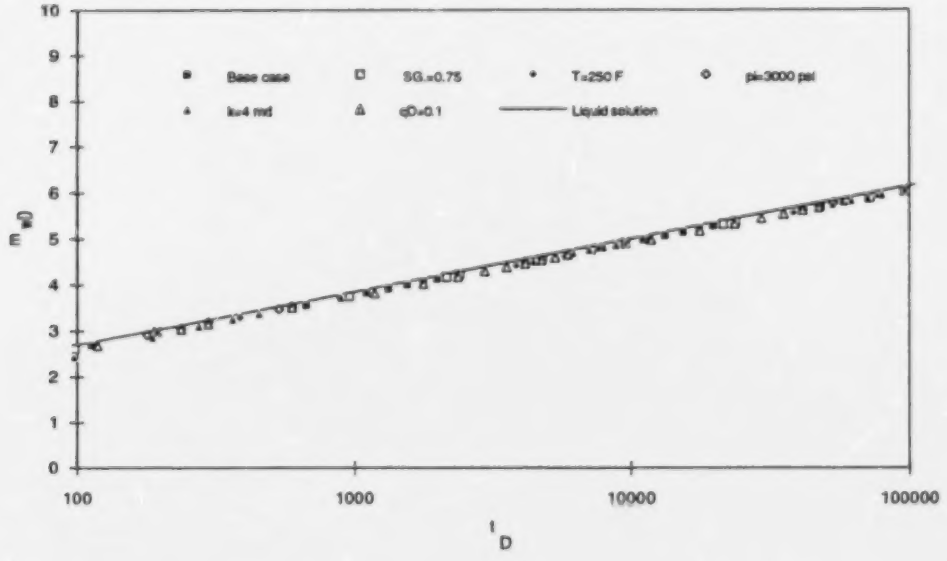

Figure 5.2 Drawdown responses for short producing times

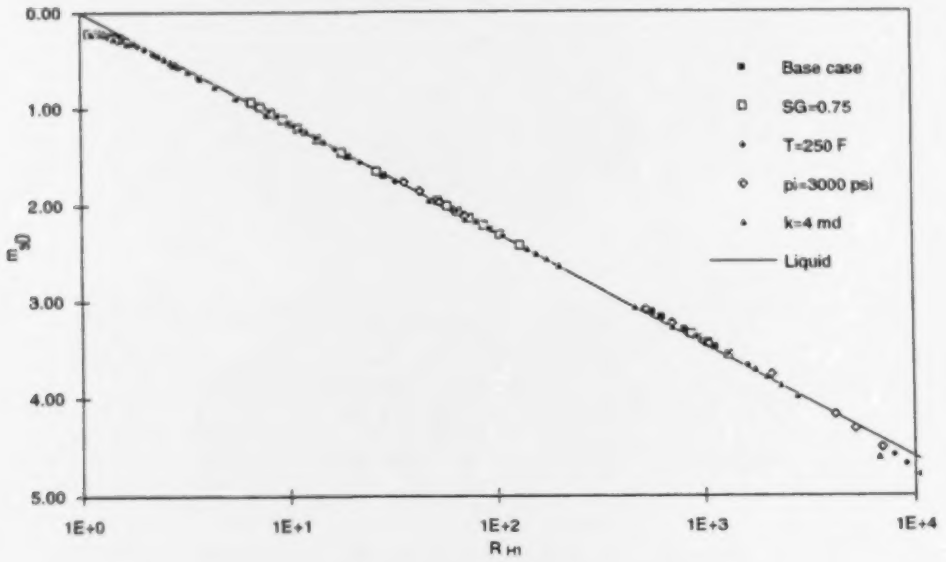

Figure 5.3 Buildup responses for short producing times, tpDA=0.01

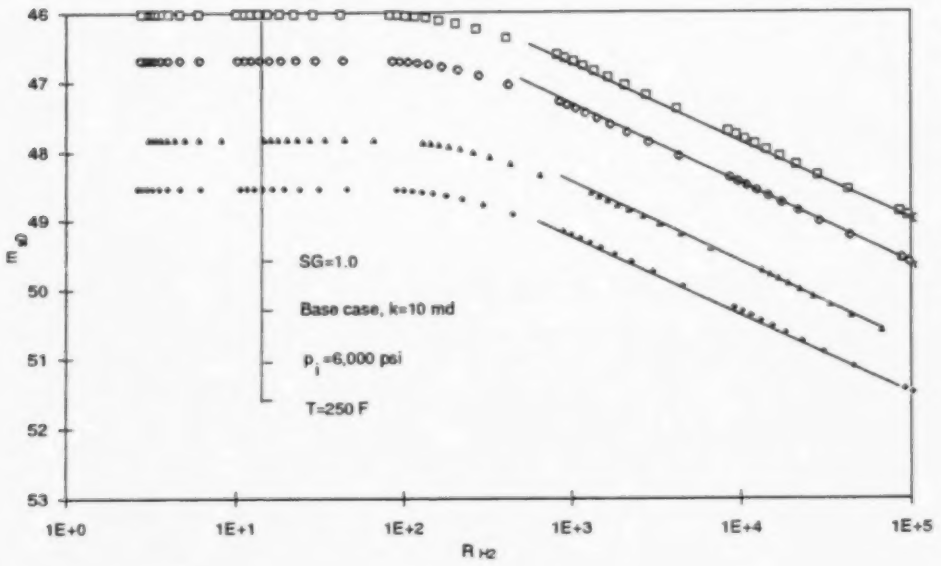

Figure 6.1 Horner plot for wells in the center of a square, t_{pDA}=10

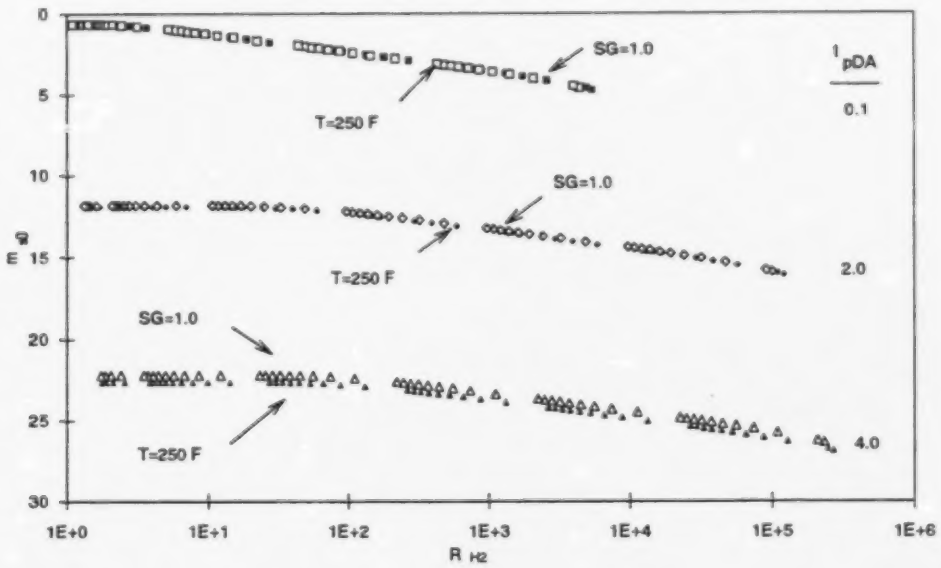

Figure 6.2 Horner plot for a well in the center of a square

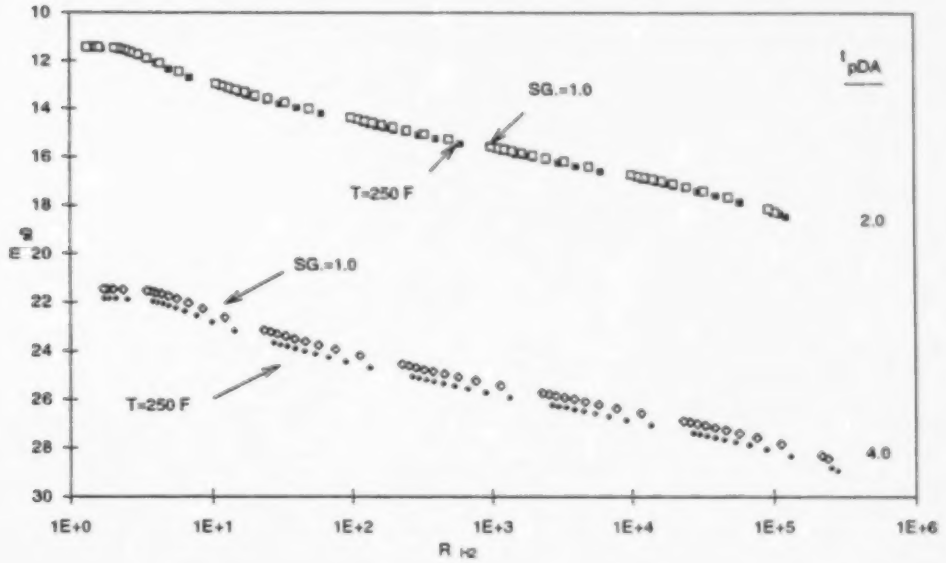

Figure 6.3 Horner plot for a well at (0.75,0.75) in a 4:1 reservoir

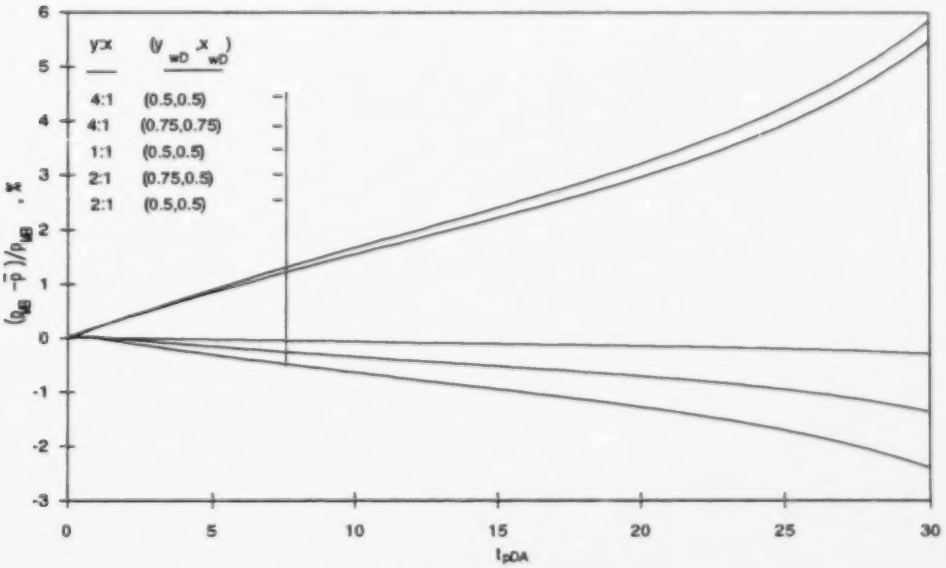

Figure 6.4 Differences between the average reservoir pressure from the simulator and the material balance equation

		C_A	Exact for t_{pDA} >	Less than 1% error when t_{pDA} >	Infinite system solution less than 1% error when t_{pDA} <
Well A		30.8828	0.1	0.05	0.09
Well B	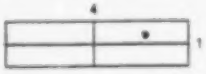	0.1155	4.0	2.00	0.01
Well C	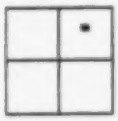	4.5132	0.6	0.30	0.025
Well D		5.3790	0.8	0.30	0.01
Well E	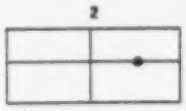	4.5141	1.5	0.50	0.06

Figure 7.1 Well/reservoir configurations used in this study.

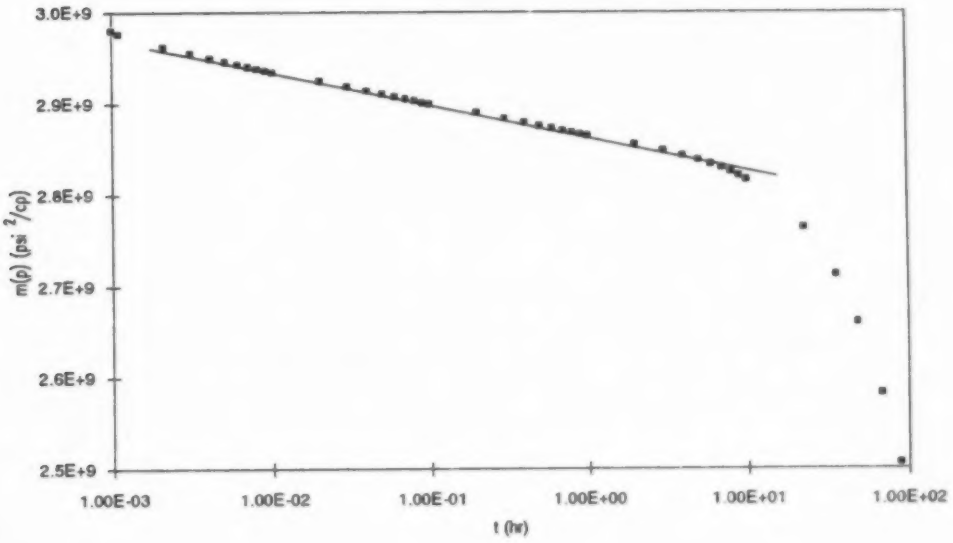

Figure 7.2 Semi-log graph of the drawdown response for Well A (q_D=0.01)

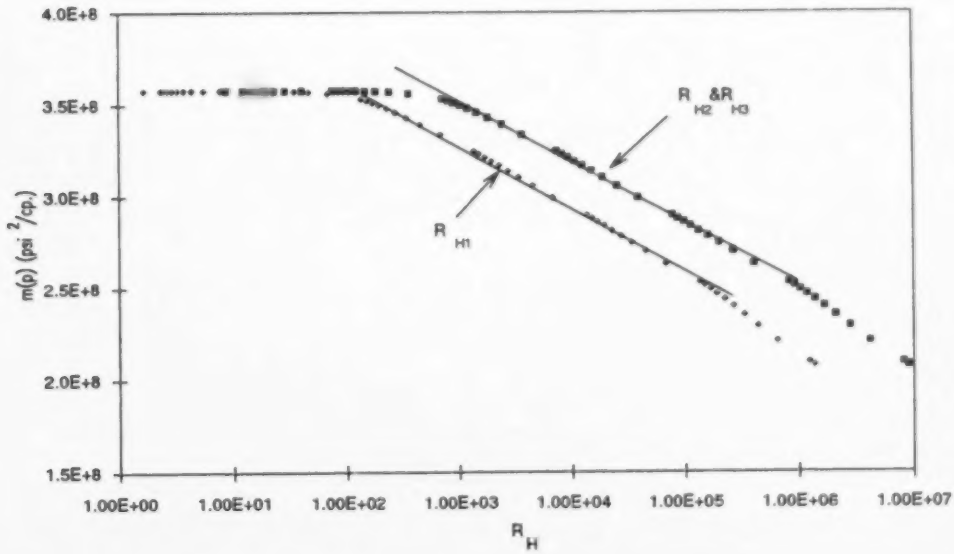

Figure 7.3 Horner plot of the buildup response for Well A (q_D=0.01, t_{pDA}=30)

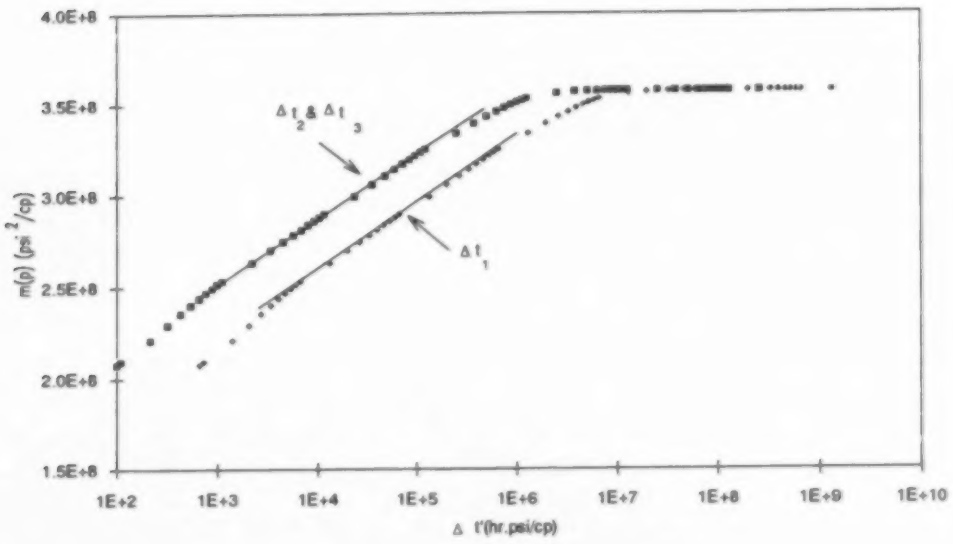

Figure 7.4 MDH graph of the buildup response for Well A (q_D=0.01, t_{pDA}=30)

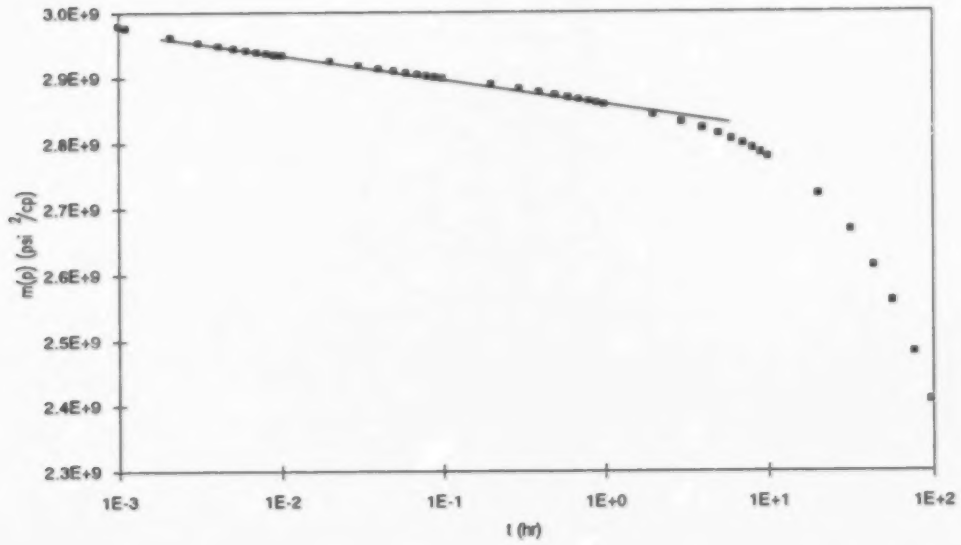

Figure 7.5 Semi-log graph of the drawdown response for Well B (q_D=0.01)

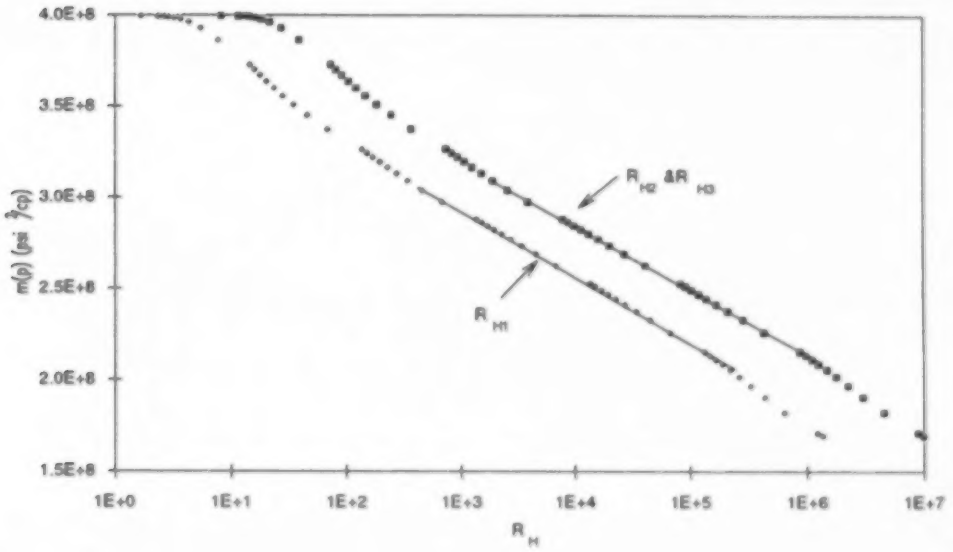

Figure 7.6 Horner plot of the buildup response for Well B (q_D=0.01, t_{pDA}=30)

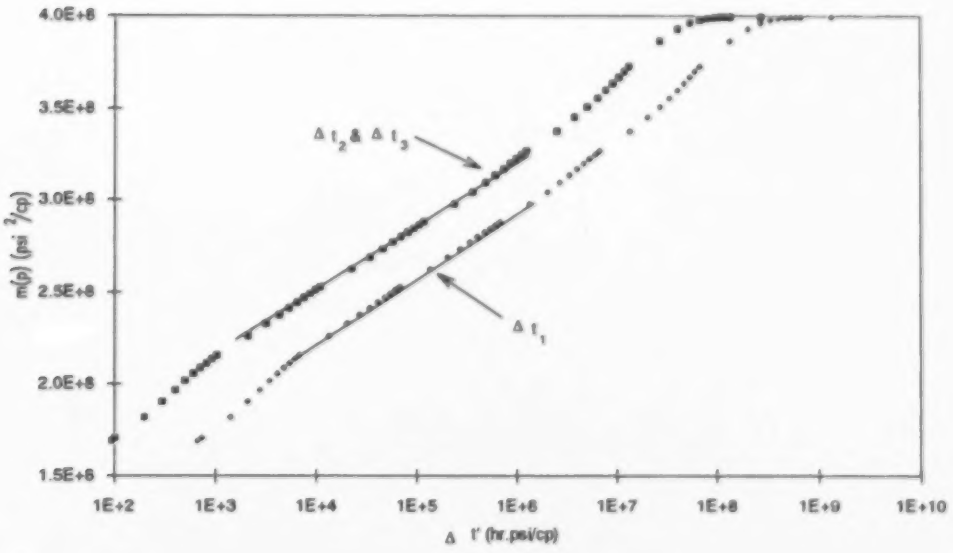

Figure 7.7 MDH graph of the buildup response for Well B (q_D=0.01, t_{pDA}=30)

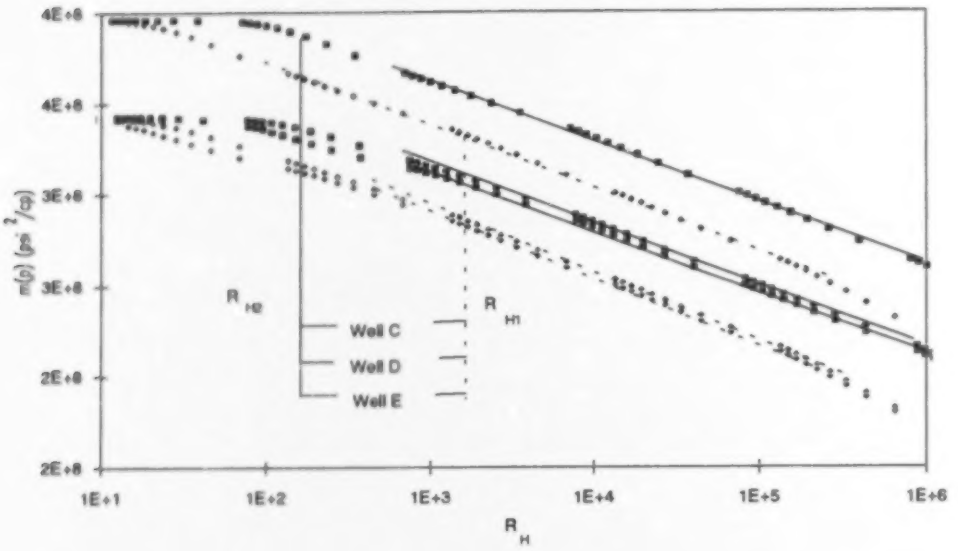

Figure 7.8 Horner plot of the buildup responses for Wells C, D and E (q_D=0.01, t_{pDA}=30)

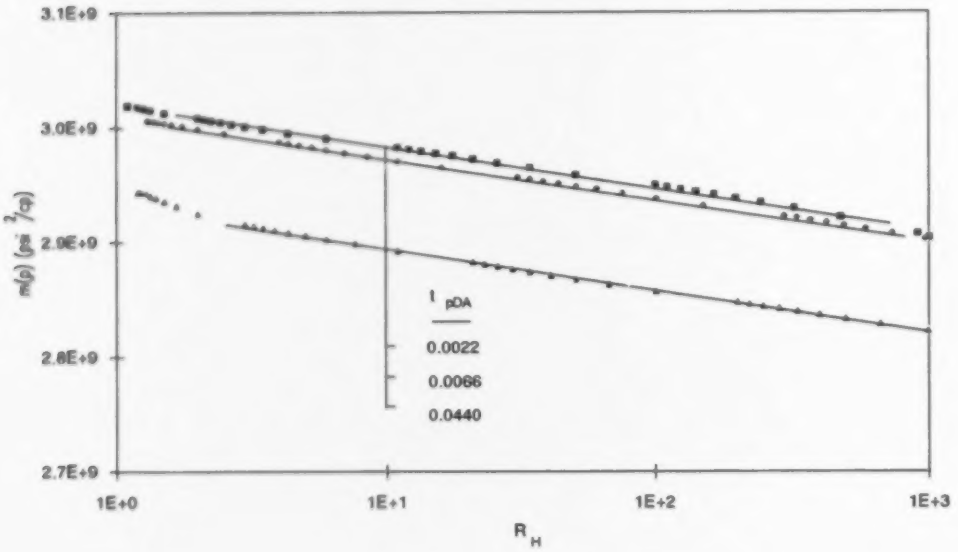

Figure 7.9 Horner plot of the buildup response for Well B (q_D=0.01)

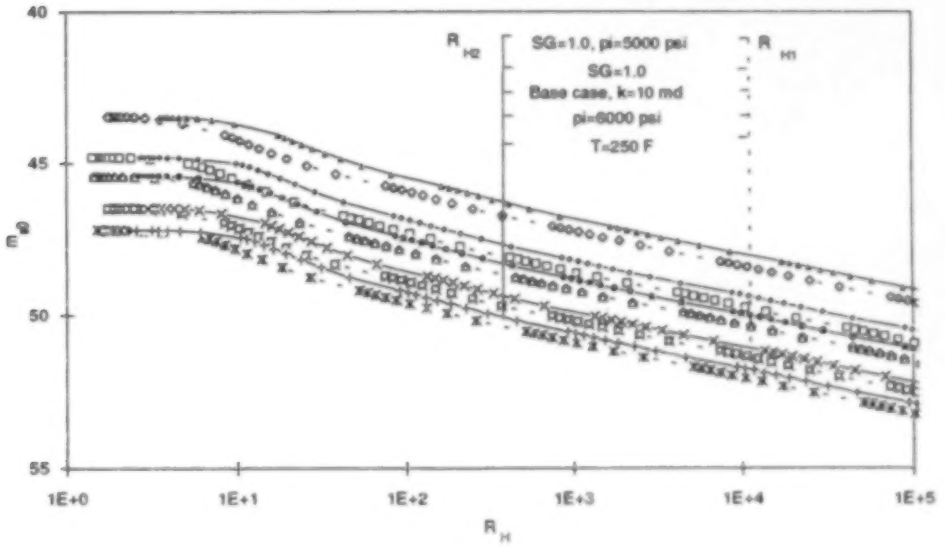

Figure 7.10 Horner plot of the buildup responses for Well B with different gas and reservoir properties (q_D=0.01, t_{pDA}=10)

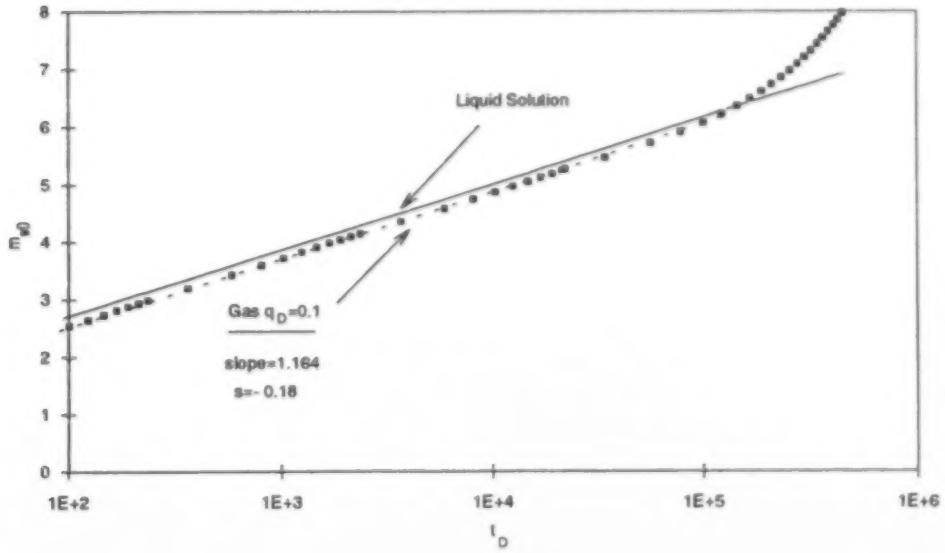

Figure 7.11 Semi-log graph of the drawdown response for Well A (q_D=0.1)

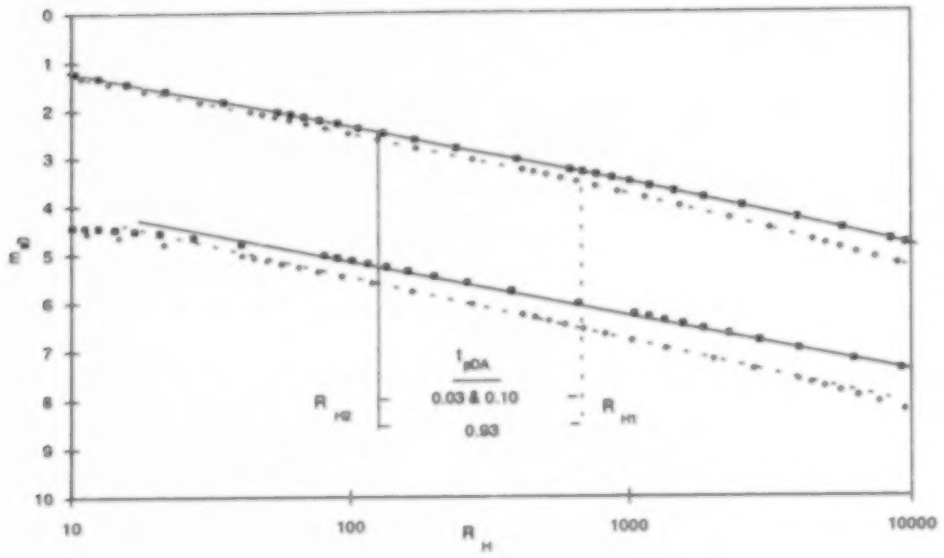

Figure 7.12 Horner plot of the buildup responses for Well A with different t_{pDA} (q_D=0.1)

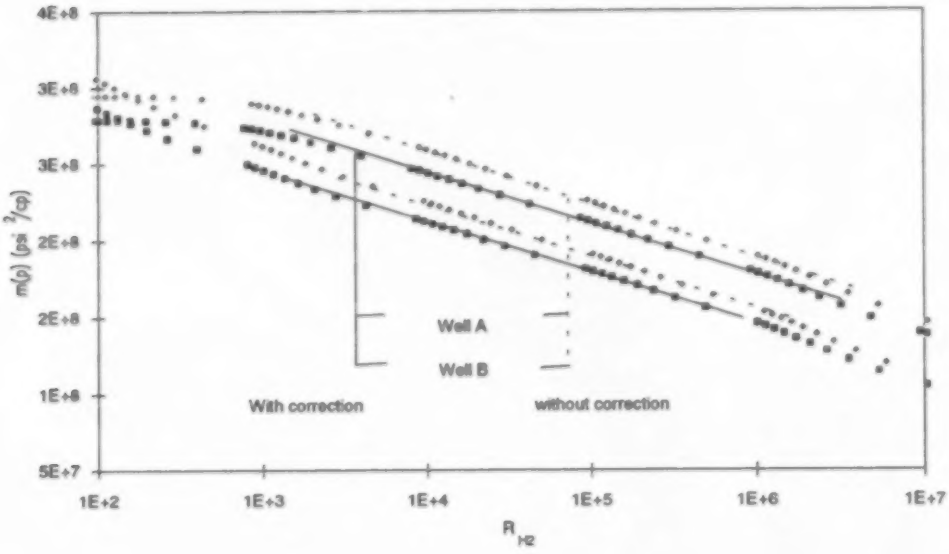

Figure 7.13 Effects of contaminants on Horner plot of the buidlup responses for Wells A and B (H_2S =20%, t_{pDA}=30)

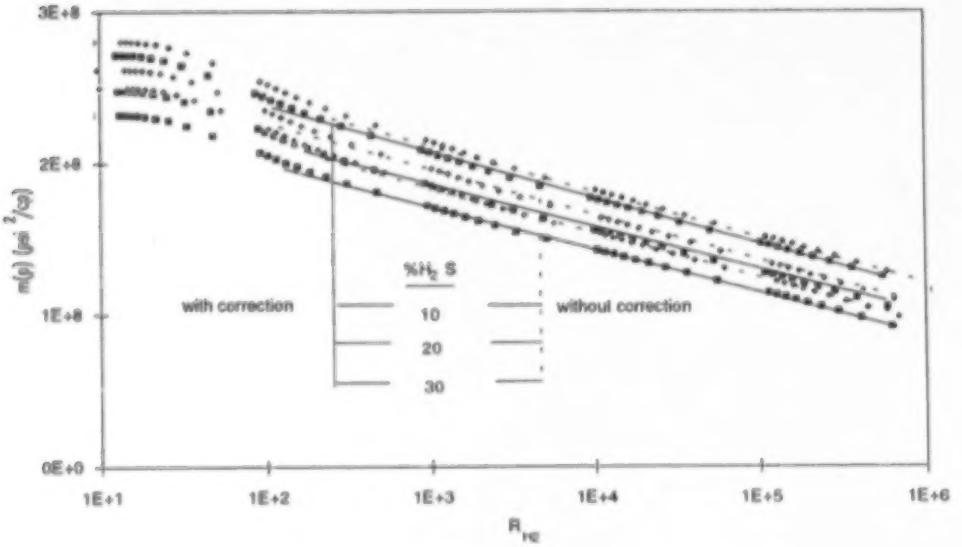

Figure 7.14 Effects of the concentration of the contaminant on Horner plot of the buidlup response for Well B (q_D=0.01, t_{pDA}=30)

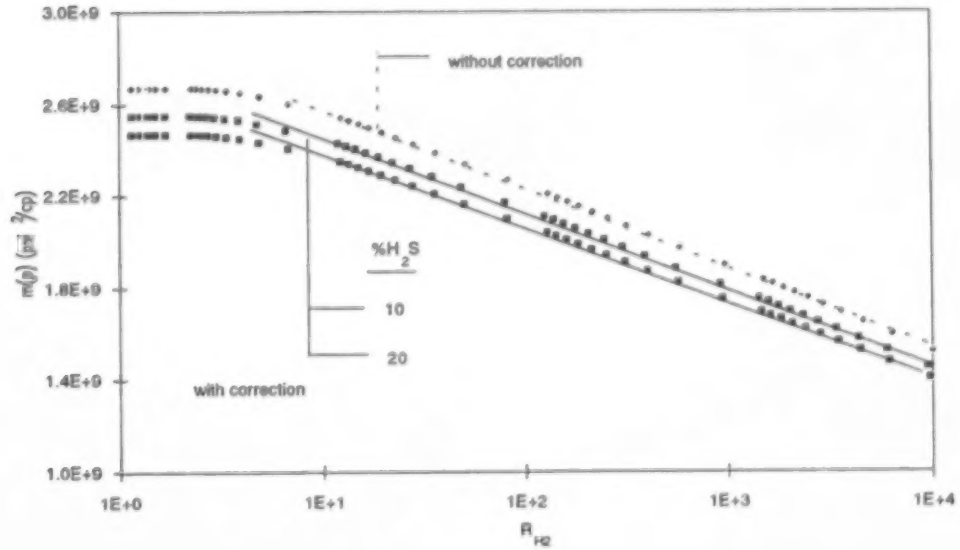

Figure 7.15 Effects of the concentration of contaminants on Horner plot of the buildup responses for Well B Buildup plot for Well B (q_D=0.1 , t_{pDA}=0.2)

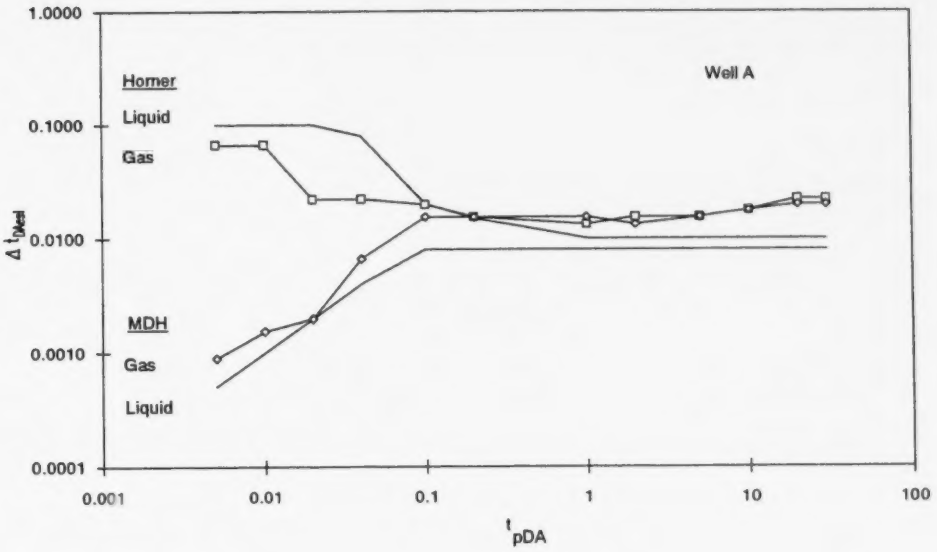

Figure 7.16 Dimensionless time to the end of Horner and MDH straight line for Well A

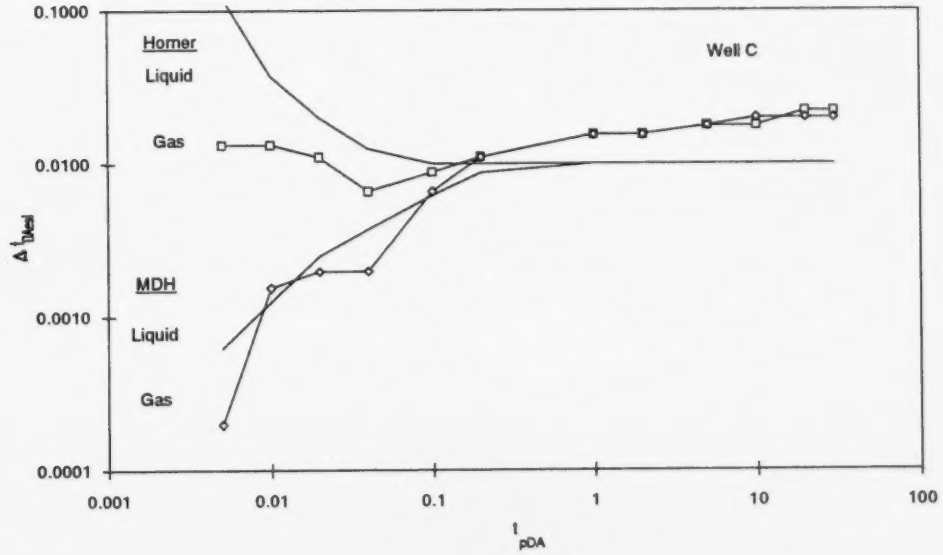

Figure 7.17 Dimensionless time to the end of Horner and MDH straight line for Well C

REFERENCES

Aadnoy, B.S. and Finjord, J.: "Discussion of Prefracture Testing in Tight Gas Reservoirs" *SPE Form. Eval.* (Dec. 1986) 628-9.

Aanonsen, S.: "Application of Pseudotime to Estimate Average Reservoir Pressure," paper SPE 14256 presented at the 60th Ann. Mtg. of SPE of AIME, Las Vegas, NV (Sept 22-25, 1985).

Agarwal, R.G.: " 'Real Gas Pseudo-Time' - A New Function of Pressure Buildup Analysis of MHF Gas Wells," paper SPE 8279 presented at the 54th Ann. Mtg. of SPE of AIME, Las Vegas, NV (Sept 23-26, 1979).

Agarwal, R.G.: "A New Method to Account for Producing Time Effects when Drawdown Type Curves are Used to Analyze Pressure Buildup and Other Test Data," paper SPE 8289 presented at the 55th Ann. Mtg. of SPE of AIME in Dallas, TX (Sept. 21-24, 1980).

Al-Hussainy, R., Ramey, H.J. Jr., and Crawford, P.B. : "The Flow of Real Gases Through Porous Media," *J. Pet. Tech.* (May 1966) 624-36.

Al-Hussainy R. and Ramey, H.J. Jr. : "Application of Real Gas Flow Theory to Well Testing and Deliverability Forecasting," *J. Pet. Tech.* (May, 1966) 110-5.

Ambastha, A.K.: "Discussion of Prefracture Testing in Tight Gas Reservoirs", *SPE Form. Eval.* (Dec. 1986) 630.

Bratvold, R.B.: "A Simulation Study of Gas Wells Under Radial Flow Conditions," MS thesis, U. of Tulsa, Tulsa, OK (June 1984).

Bourdet, D., Ayoub, J.A., and Pirard, Y.M.: "Use of Pressure Derivative in Well Test Interpretation," *SPE Form. Eval.* (June 1989) 293-302.

Brown, M.W.: "Reservoir Limit Testing for Gas Wells in Rectangular Reservoirs," M.Sc. thesis, U. of Alberta, Edmonton, Alberta (1992).

Carr, N.L., Kobayashi, R., and Burrows, D.B.: "Viscosity of Hydrocarbon Gases Under Pressure," *Trans.*, AIME (1954), **201,** 264-272.

Cobb, W.M. and Smith, J.T.: "An Investigation of Pressure-Buildup Tests in Bounded Reservoirs," *J. Pet. Tech.* (Aug. 1975) 991-6.

Dietz, D.N.: "Determination of Average Reservoir Pressure From Build-up Surveys," *J. Pet. Tech.* (Aug. 1965), 955-59; *Trans*, AIME, **234**.

Dranchuk, P.M., Purvis, R.A., and Robinson, D.B.: "Computer Calculation of Natural Gas Compressibility Factors Using the Standing and Katz Correlations," *Inst. of Pet. Tech.*, IP 74-008, 1974.

Earlougher, R.C., Jr.: "Advances in Well Test Analysis", Monograph Series, SPE, Dallas (1979) **5**.

ERCB: "Gas Well Testing Theory and Practice," Third Edition, 1975.

George, A., Liu J., and Ng, E.: "User Guide for SPARSPAK: Waterloo Sparse Linear Equation Package," U. of Waterloo (Jan. 1980).

Horner, D.R.: "Pressure Build-up in Wells," *Proc.*, Third World Pet. Cong., E.J. Brill, Leiden (1951) **II**, 503.

Kabir, C.S. and Hasan, A.R.: "Prefracture Testing in Tight Gas Reservoirs," *SPE Form. Eval.* (April 1986) 63-67.

Kale, D. and Mattar, L: "Solution of a Non-Linear Gas Flow Equation by the Perturbation Technique", *J. Can. Pet. Tech.* (Oct.-Dec. 1980) 63-67.

Kazemi, H. : "Determination of Average Reservoir Pressure from Pressure Buildup Tests", *Soc. Pet. Eng. J.* (Feb. 1974) 55-62; *Trans.*, AIME, **234**.

Lee, W.J. and Holditch, S.A.: "Application of Pseudotime to Buildup Test Analysis of Low-Permeability Gas Wells with Long-Duration Wellbore Storage Distortion," *J. Pet. Tech.* (Dec. 1982) 2877-87.

Matthews, C.S., Brons, F., and Hazebroek, P.: "A Method for Determination of Average Pressure in a Bounded Reservoir," *Trans*, AIME (1954) **201**, 182-91.

Miller, C.C., Dyes, A.B. and Hutchinson, C.A., Jr.: "The Estimation of Permeability and Reservoir Pressure From Bottom-Hole Pressure Build-up Characteristics," *Trans*, AIME, (1950) **198**, 91-104.

Odeh, A.S. and Al-Hussainy, R.: "A Method for Determining the Static Pressure of a Well from Buildup Data," *J. Pet. Tech.* (May 1971) 621-24: *Trans.*, AIME, **251**.

Ramey, H.J., Jr. and Cobb, W.M.: "A General Pressure Buildup Theory for a Well in a Closed Drainage Area," *J. Pet. Tech.* (Dec 1971) 1493-1505 : *Trans.*, AIME, **251**.

Reynolds, A. C., Bratvold, R.B., and Ding, W. : "Semilog Analysis of Gas Well Drawdown and Buildup Data," *SPE Form. Eval.* (Dec 1987) 657-670.

Scott, J.O. :"Application of a New Method for Determining Flow Characteristics of Fractured Gas Wells in Tight Gas Sands," paper SPE 7931 presented at the SPE Symposium on Low-Permeability Gas Reservoirs, Denver, CO (May 20-22 1979).

Spivey, L.J. and Lee, W.J.: "The Use of Pseudotime: Wellbore Storage and Middle Time Region," paper SPE 15229 presented at the Unconventional Gas Tech. Symposium, Louisville, KY (May 18-21, 1986a).

Spivey, L.J. and Lee, W.J.: "A Comparison of the Use of Pseudotime and Normalized Time for Gas Well Buildup Analysis in Various Geometries," paper SPE 15580 presented at the Ann. Mtg. of SPE of AIME, New Orleans, La. (Oct 5-8, 1986b).

Toh, C.H., Farshad, F.F. and LeBlanc, L.J.: "A New Iterative Technique with Updated Curves for Estimating Average Reservoir Pressure of Gas Wells from Pressure Buildup Tests," paper SPE 13235 presented at the Ann. Mtg. of SPE of AIME, Houston, TX (Sept 16-19, 1984).

van Everdingen, A.F., and Hurst, W.: " The Application of the Laplace Transformation to Flow Problems in reservoirs," *Trans.*, AIME (1949) **186**, 305-324.

Wattenbarger, R.A. and Ramey, H.J. Jr.: "Gas Well Testing with Turbulence, Damage and Wellbore Storage," *J. Pet. Tech.* (Aug 1968) 877-87.

Wichert, E., and Aziz, K.: "Calculate Z's for Sour Gases," *Hydrocarbon Processing* (May 1972) 119-122.

Zana, E.T. and Thomas, G.W.: "Some Effects of Contaminants on Real Gas Flow," *J. Pet. Tech.* (Sept 1970) 1157-68.

Ziauddin, Z.: "Determination of Average Pressure in Gas Reservoirs from Pressure Buildup Tests," paper SPE 11222 presented at the 57th Ann. Mtg. of SPE of AIME, New Orleans, La. (Sept. 26-29, 1982).

APPENDIX A

Program GSRECT :	Pressure response for a gas well in a closed rectangular reservoir
Subroutines :	Gas properties correlations
Program RH_DERV :	Semi-log derivative for Horner plots
Program MDH_DERV :	Semi-log derivative for MDH plots

```
      PROGRAM GSRECT
CCCCCCCCCCCCCCCCCCCCCCCCCCCCCCCCCCCCCCCCCCCCCCCCCCCCCCCCCCCCCCCCCCCCCCCCCC
C
C       THIS PROGRAM CLACULATES THE PRESSURE RESPONSES OF
C       A GAS PRODUCING WELL IN A CLOSED RECTANGULAER RESERVOIR.
C
C       THE MAIN MODULE IS DEVELOPED BY : PRASIT KOSARUSSAWADEE
C       THE GRID SEPCIFICATION AND INPUT MODULE
C                                       : MURRAY W. BROWN
C
C       FOR PARTIAL FULFILLMENT OF THE REQUIREMENTS FOR THE
C       DEGREE OF MASTER OF SCIENCE.
C
C
C       UNIVERSITY OF ALBERTA
C       FIRST VERSION OCTOBER, 1991.
C
CCCCCCCCCCCCCCCCCCCCCCCCCCCCCCCCCCCCCCCCCCCCCCCCCCCCCCCCCCCCCCCCCCCCCCCCCC

C       THIS PROGRAM USES THE SPARSPAK SUBROUTINE TO SOLVE
C       FOR THE UNKNOWNS. THE SUBROUTINE IS AVAILABLE FROM
C       U OF ALBERTA'S MTS SYSTEM.
C
C
C       DECLARATION
C
        IMPLICIT REAL*8 (A-H,O-Z)
        PARAMETER (MAX=100,MAXMAX=10000,MAXTAB=200,
     A             TOLEMB=1.D-3,TOLEPP=1.D-5,DELPMX=2.D2,
     B             C1=5.1169126531327D11,
     C             C2=8.0857805766753D13,
     D             C3=1.9405873384021D15,
     E             PSC=14.7D0, TSC=519.7D0,
     F             TEMRAK=459.7D0, ZATOL=1.D-4)
C
C
C     MAX:  MAXIMUM NUMBER OF GRID BLOCKS IN EITHER DIRECTION
C     MAXMAX: MAXIMUM NUMBER OF BLOCKS IN THE RESERVOIR
C     MAXTAB: MAXIMUM NUMBER OF ENTRIES IN P-M(P) TABLE
C     TOLEMB: TOLERANCE FOR THE MATERIAL BALANCE ERROR
C     TOLEPP: TOLERANCE FOR THE THE M(P) ERROR
C     DELPMX: MAXIMUM PRESSURE DROP ALLOWED FOR EACH TIME STEP
C     C1-C3 : CONVERSION FACTORS IN THE DIFFUSIVITY EQUATION
C     ZATOL : Z FACTOR TOLERANCE FOR THE AVERAGE RESERVOIR
C             PRESSURE CALCULATION FROM MATERIAL BALANCE
C
C
        DIMENSION TABP(0:MAXTAB),TABMP(0:MAXTAB),S(12*MAXMAX),
     A            IR(5),VISCGN(MAXMAX),
     B            VISCGO(MAXMAX),PPRESO(MAXMAX),
     B            PPRESI(MAXMAX),
     C            PPRESN(MAXMAX),ACOEF(MAXMAX,5),
     D            XG(MAX),YG(MAX),DX(MAX),DY(MAX),
     E            VALUES(5),BVEC(MAXMAX),TEMPO(4)
C
C
C     TABP,TABMP : ARRAYS CONTAINING PRESSURE AND M(P)
C     S : THE AMOUNT OF STORAGE FOR ORDERING AND CALCULATION
C         USED BY SPARAPAK
C     IR : ARRAY SPECIFYING THE LOCATIONS OF THE NON ZERO MATRIX
C          ELEMENTS
C     VISCGO,VISCGN : ARRAYS CONTAING THE VISCOSITY*COMPRESESSIBILITY
C                     PRODUCTS FOR THE PREVIOUS AND CURRENT TIME STEP
C     PPRESO,PPRESI,PPRESN : ARRAYS CONAINING THE M(P) VALUES
```

```
C                    FOR THE PREVIOUS,INTERMEDIAT AND CURRENT TIME
C     ACOEF : NON ZERO COEFFICIENT MATRIX
C     XG,YG : GRID BOUNDARIES IN X AND Y DIRECTIONS
C     DX,DY : BLOCK SIZES IN X AND Y DIRECTIONS
C     VALUES : THE VALUES OF MATRIX ELEMENTS WHOSE LOCATIONS
C              ARE GIVEN IN IR
C     BVEC   : THE RHS VECTOR OF THE EQUATIONS
C     TEMPO : TEMPORARY STORAGE FOR GAS PROPERTIES
C
C
        LOGICAL FTDEL,FBUP
        CHARACTER*8 OUTFIL
        COMMON /SPKUSR/MSGLVL,IERR,MAXS,NEQNS
C
C     FTDEL : INITIATE BACK TRACKING IF TRUE
C     FBUP  : TRUE IF BUILDUP TEST IS REQUESTED
C
C     VARIABLES IN THE COMMON STATEMENT ARE REQUIRED BY SPARSPAK
C
C
C       INITIALIZING
C
C       CALL SUBROUTINE FOR READING INPUT FILES
C
        CALL INPUT(PC,TC,PERM,PINIT,TEM,RW,POROS,TEMPO,
     A       PDEL,OUTFIL,MAXX,MAXY,IWELL,JWELL,XG,YG,
     B       FBUP,TFDD,TSLD,TCONS,TSI,TFBU,TSLB,QINPT)
        SPG=TEMPO(1)
C
C       CONVERSION TO MOLE PERCENT
C
        CNCN2=TEMPO(2)*1.D2
        CNCH2S=TEMPO(3)*1.D2
        CNCCO2=TEMPO(4)*1.D2
C
C     CALCULATE THE WELL LOCATION USING NATURAL ORDERING
C
       LWELL=(IWELL-1)*MAXY+JWELL
        FTDEL=.FALSE.
C
C       CALCULATE P,M(P) TABLE (ARRAYS TABP & TABMP)
C
        PRSMAX=PINIT+4.D0*PDEL
        CALL PSUDOP(PRSMAX,PDEL,TEM,SPG,TC,PC,CNCH2S,CNCCO2,
     A  CNCN2,TABP,TABMP,NSTEP)
C
C       DETERMINE M(P) INITIAL & CALCULATE VIS*COM @ P INITIAL
C
        CALL TABSEQ(PINIT,TABP,TABMP,NSTEP,PP)
        CALL VISCY((TEM+TEMRAK)/TC,PINIT/PC,SPG,TEM,CNCH2S,
     A  CNCCO2,CNCN2,VISGR,VISG,JERR)
        CALL ZANDC(TEM,TC,PINIT,PC,CNCH2S,CNCCO2,ZED,CMPG,JERR)
        DO 20 I=1,MAXX*MAXY
           PPRESN(I)=PP
           PPRESI(I)=PP
           PPRESO(I)=PP
           VISCGO(I)=VISG*CMPG
           VISCGN(I)=VISCGO(I)
20      CONTINUE
C
C       CALCULATE DX AND DY FOR BLOCK SIZING
C
        XCUM=0.D0
        DO 22 I=1,MAXX
```

```
            DX(I)=2.D0*(XG(I)-XCUM)
            XCUM=XCUM+DX(I)
22        CONTINUE
          YCUM=0.D0
          DO 24 J=1,MAXY
            DY(J)=2.D0*(YG(J)-YCUM)
            YCUM=YCUM+DY(J)
24        CONTINUE
C
C       CALCULATE THE ORIGINAL GAS IN PLACE (OGIP) IN MSCF.
C
          SUMINT=PINIT/ZED
          SUMOLD=SUMINT
          ZIN=ZED
          OGIP=POROS*XCUM*YCUM*PINIT*TSC/PSC/(TEM+TEMRAK)/ZIN/1.D3
C
C         INITIALIZE SPARSPAK
C         SET THE MAXIMUM STORAGE (MAXS)
C         SUPPRESS THE ON SCREEN MESSAGES FROM SPARSPAK (MSGLVL=0)
C
          CALL SPRSPK
          MAXS=12*MAXMAX
          MSGLVL=0
C
C         SAVE STRUCTURE OF MATRIX A - CALL SPARSPAK ROUTINE
C
          CALL IJBEGN
C
C         GIVING LOCATION OF NON-ZERO ELEMENTS
C         MATRIX A OBTAINED BY SCROLLING THROUGH ALL RESERVOIR
C         GRID BLOCKS. FIXING I AND FIRST VARING J.
C
          DO 10 I=1,MAXX
             DO 15 J=1,MAXY
                NORD=(I-1)*MAXY+J
                NIR=1
                IR(NIR)=NORD
                IF(I.GT.1) THEN
                   NIR=NIR+1
                   IR(NIR)=NORD-MAXY
                ENDIF
                IF(I.LT.MAXX) THEN
                   NIR=NIR+1
                   IR(NIR)=NORD+MAXY
                ENDIF
                IF(J.GT.1) THEN
                   NIR=NIR+1
                   IR(NIR)=NORD-1
                ENDIF
                IF(J.LT.MAXY) THEN
                   NIR=NIR+1
                   IR(NIR)=NORD+1
                ENDIF
                CALL INROW(NORD,NIR,IR,S)
15           CONTINUE
10        CONTINUE
C
C         FINISH GIVING LOCATION OF NON-ZEROS TO SPARSPAK
C
          CALL IJEND(S)
C
C         GIVE ORDERING FOR A - A4 IS THE OPTIMUM ORDERING
C         REFER TO THE SPARSPAK MANUAL FOR OTHER SCHEMES
C
```

```
      CALL ORDRA4(S)
C
C     CONSTRUCTION OF MATRIX ACOEFF(MAXX*MAXY,5)
C
      DO 100 I=1,MAXX
         DO 110 J=1,MAXY
           NORD=(I-1)*MAXY+J
           IF(I.NE.1.AND.I.NE.MAXX) THEN
              CDELX=XG(I+1)-XG(I)
              SDELX=XG(I)-XG(I-1)
              ACOEF(NORD,1)=1.0D0/(SDELX*(SDELX+CDELX))
              ACOEF(NORD,3)=-1.0D0/(SDELX*CDELX)
              ACOEF(NORD,5)=1.0D0/(CDELX*(SDELX+CDELX))
           ELSE
              IF(I.EQ.1) THEN
                 CDELX=XG(I+1)-XG(I)
                 ACOEF(NORD,1)=0.0D0
                 ACOEF(NORD,3)=-0.5D0/(CDELX*CDELX)
                 ACOEF(NORD,5)=0.5D0/(CDELX*CDELX)
              ELSE
C     I=MAXX
                 SDELX=XG(I)-XG(I-1)
                 ACOEF(NORD,1)=0.5D0/(SDELX*SDELX)
                 ACOEF(NORD,3)=-0.5D0/(SDELX*SDELX)
                 ACOEF(NORD,5)=0.0D0
              ENDIF
           ENDIF
           IF(J.NE.1.AND.J.NE.MAXY) THEN
             CDELY=YG(J+1)-YG(J)
             SDELY=YG(J)-YG(J-1)
             ACOEF(NORD,2)=1.0D0/(SDELY*(SDELY+CDELY))
             ACOEF(NORD,3)=ACOEF(NORD,3)-1.0D0/(SDELY*CDELY)
             ACOEF(NORD,4)=1.0D0/(CDELY*(SDELY+CDELY))
           ELSE
             IF(J.EQ.1) THEN
              CDELY=YG(J+1)-YG(J)
              ACOEF(NORD,2)=0.0D0
              ACOEF(NORD,3)=ACOEF(NORD,3)-0.5D0/(CDELY*CDELY)
              ACOEF(NORD,4)=0.5D0/(CDELY*CDELY)
             ELSE
C     J=MAXY
              SDELY=YG(J)-YG(J-1)
              ACOEF(NORD,2)=0.5D0/(SDELY*SDELY)
              ACOEF(NORD,3)=ACOEF(NORD,3)-0.5D0/(SDELY*SDELY)
              ACOEF(NORD,4)=0.0D0
             ENDIF
           ENDIF
           DO 120 K=1,5
             ACOEF(NORD,K)=ACOEF(NORD,K)*C1/C3
120        CONTINUE
110      CONTINUE
100   CONTINUE
C
C     CALCULATE Q (Q IS INPUT AS MSCF/D)
C
      CALL ZANDC(TSC,TC,PSC,PC,CNCH2S,CNCCO2,ZED,CMPG,
     A           JERR)
      QSOR=(-QINPT)*1.D3*(TEM+TEMRAK)/PERM/ZED*C2/C3*
     A     PSC/TSC/(DX(IWELL)*DY(JWELL))
C
C    QSOR IS THE SOURCE TERM IN THE DIFFUSIVITY EQUATION
C
C
C     CALCULATE QSORMB TO BE USED IN MB. CHECK
```

```
C
      QSORMB=(-QINPT)*1.D3*(TEM+TEMRAK)*PSC/ZED/TSC/24.D0
C
C     OPEN THE OUTPUT FILE AS UNIT 9 AND 10
C     R. CONATAINS THE M(P)'S AND RESIDUALS
C     A. CONATAINS THE AVERAGE RESERVOIR PRESSURES
C
      OPEN(UNIT=9,FILE='R.'//OUTFIL,STATUS='NEW')
      OPEN(UNIT=10,FILE='A.'//OUTFIL,STATUS='NEW')
C
C     DETERMINATION OF delT & EXIT TIME
C
      TEXIT=TSI
      TCUM=0.D0
      TDEL=TFDD
      TSLE=TSLD
      GOTO 500
C
C     REENTRY POINT FOR SUBSEQUENT CALCULATIONS
C
C     FIRST CHECK IF BACK TRACKING IS ACTIVATED
C     IF THE EXIT TIME ON DRAWDOWN IS REACHED, CHECK
C     WHETHER BUILDUP OPTION IS REQUESTED.
C     IF IT IS, PERFORM BUILDUP CALCULATION BY CHANGING
C     THE SOURCE TERM (QSOR) TO 0.
C
C     LOGARITHMIC TIME INCREMENTS ARE USED FOR EARLY TIME DRAWDOWN
C     ARITHMETIC INCREMENTS ARE USED FOR LATE TIME DRAWDOWN
C     LOGARITHMIC INCREMENTS ARE ALWAYS USED FOR BUILDUPS.
C
600   IF(FTDEL) THEN
         TCUM=TCUM-TDEL
      ENDIF
      IF(TCUM.EQ.TEXIT) THEN
          IF( .NOT.FBUP) THEN
             STOP
          ELSE
             FBUP=.FALSE.
             TEXIT=TSLB
             TSLE=TSLB
             TDEL=TFBU
             TCUM=0.0D0
             QSOR=0.0D0
             GOTO 500
          ENDIF
      ENDIF
      IF(TCUM.LT.TSLE) THEN
          IPOWR=INT(DLOG10(TCUM))
          IF(IPOWR.LT.0) THEN
             IPOWR=IPOWR-1
          ELSE
             IF(IPOWR.EQ.0) THEN
                  IF(DLOG10(TCUM).LT.0.D0) THEN
                      IPOWR=-1
                  ELSE
                      IPOWR=0
                  ENDIF
              ENDIF
          ENDIF
              TDEL=(10.0D0)**IPOWR
              IF((TCUM+1.2*TDEL).GE.TSLE) THEN
                   TDEL=TSLE-TCUM
              ENDIF
      ELSE
```

```
          TDEL=TCONS
          IF((TCUM+1.2*TDEL).GE.TEXIT) THEN
             TDEL=TEXIT-TCUM
          ENDIF
        ENDIF
        IF (FTDEL) THEN
        TDEL=TDELS
        ENDIF
500     TCUM=TCUM+TDEL
C
C       AFTER CONVERGENCE REPLACE VARIABLES AT OLD TIME
C       LEVEL WITH NEW TIME LEVEL IF FTDEL REMAINS FALSE.
C       OTHERWISE DO BACK TRACKING BY SKIPPING THIS STEP
C       AND REASSIGN OLD VARIABLES TO NEW ONES.
C
        IF(.NOT.FTDEL) THEN
           DO 30 I=1,MAXX*MAXY
             PPRESO(I)=PPRESN(I)
             PPRESI(I)=PPRESN(I)
             VISCGO(I)=VISCGN(I)
30         CONTINUE
        ELSE
           FTDEL=.FALSE.
           DO 35 I=1,MAXX*MAXY
             PPRESI(I)=PPRESO(I)
             VISCGN(I)=VISCGO(I)
35         CONTINUE
        ENDIF
C
C       GIVE VALUES FOR MATRIX A & B
C
300     DO 40 I=1,MAXX
         DO 50 J=1,MAXY
           NORD=(I-1)*MAXY+J
           NIR=1
           IR(NIR)=NORD
           VALUES(NIR)=ACOEF(NORD,3)-POROS/PERM/TDEL*
     A                 (VISCGO(NORD)+VISCGN(NORD))/4.D0
           IF(I.GT.1) THEN
             NIR=NIR+1
             IR(NIR)=NORD-MAXY
             VALUES(NIR)=ACOEF(NORD,1)
           ENDIF
           IF(I.LT.MAXX) THEN
             NIR=NIR+1
             IR(NIR)=NORD+MAXY
             VALUES(NIR)=ACOEF(NORD,5)
           ENDIF
           IF(J.GT.1) THEN
             NIR=NIR+1
             IR(NIR)=NORD-1
             VALUES(NIR)=ACOEF(NORD,2)
           ENDIF
           IF(J.LT.MAXY) THEN
             NIR=NIR+1
             IR(NIR)=NORD+1
             VALUES(NIR)=ACOEF(NORD,4)
           ENDIF
           CALL INROW4 (NORD,NIR,IR,VALUES,S)
50       CONTINUE
40      CONTINUE
C
C
C       FOR VECTOR B
```

```
C
      DO 60 I=1,MAXX*MAXY
        BVEC(I)=-POROS/PERM/TDEL/4.0D0*(VISCGO(I)+VISCGN(I))
     A          *PPRESO(I)
60    CONTINUE
      BVEC(LWELL)=BVEC(LWELL)-QSOR
      CALL INRHS(BVEC,S)
C
C     SOLVE FOR THE SOLUTION MATRIX
C
      CALL SOLVE4 (S)
C
C     CALL PSTATS TO OBTAIN CRUCIAL INFORMATION SUCH AS
C     THE DIMENSION OF S REQUIRED BY SPARSPAK.
C
C     CALL PSTATS
C
      DO 65 I=1,MAXX*MAXY
          PPRESN(I)=S(I)
65    CONTINUE
C
C     TEST OF CONVERGENCE
C
      ERRMAX=0.D0
      DO 62 I=1,MAXX*MAXY
           DMP=DABS((PPRESN(I)-PPRESI(I))/PPRESN(I))
           IF (DMP.GT.ERRMAX) THEN
              ERRMAX=DMP
           ENDIF
62    CONTINUE
      IF (ERRMAX.LT.TOLEPP)
     A THEN
C
C     CHECK IF delPmax IS EXCEEDED, IF YES, CALCULATE
C     A NEW TIME INCREMENT TO BE USED. IF NOT, CALCULATE
C     THE MAXIMUM RESIDUAL FOR THE TIME SEP.
C
200   CALL TABSEQ(PPRESO(LWELL),TABMP,TABP,NSTEP,PO)
      CALL TABSEQ(PPRESN(LWELL),TABMP,TABP,NSTEP,PN)
      IF(DABS(PN-PO).GT.DELPMX) THEN
          FTDEL=.TRUE.
          TDELS=TDEL*DELPMX/1.5D0/DABS(PN-PO)
      ELSE
           RESMAX=0.D0
           RESINT=0.D0
           DO 42 I=1,MAXX
           DO 52 J=1,MAXY
            NORD=(I-1)*MAXY+J
            SMLHS=(ACOEF(NORD,3)-POROS/PERM/TDEL*
     A                (VISCGO(NORD)+VISCGN(NORD))/4.D0)
     B                 *PPRESN(NORD)
            IF(I.GT.1) THEN
            SMLHS=ACOEF(NORD,1)*PPRESN(NORD-MAXY)+SMLHS
            ENDIF
            IF(I.LT.MAXX) THEN
            SMLHS=ACOEF(NORD,5)*PPRESN(NORD+MAXY)+SMLHS
            ENDIF
            IF(J.GT.1) THEN
            SMLHS=ACOEF(NORD,2)*PPRESN(NORD-1)+SMLHS
            ENDIF
            IF(J.LT.MAXY) THEN
            SMLHS=ACOEF(NORD,4)*PPRESN(NORD+1)+SMLHS
            ENDIF
            RESINT=DABS((SMLHS-BVEC(NORD))/BVEC(NORD))
```

```
                IF (RESINT.GT.RESMAX) THEN
                    RESMAX=RESINT
                    IRESMX=I
                    JRESMX=J
                ENDIF
52            CONTINUE
42            CONTINUE
C
C       MATERIAL BALANCE CHECK WILL BE PERFORMED
C       ON DRAWDOWN CALCULATION ONLY.
C
           IF(QSOR.NE.0.0D0) THEN
        GPRO=QINPT*TCUM/24.0D0
        SUMPZA=SUMINT*(1-GPRO/OGIP)
        PAVGO=SUMPZA
        ZAVGO=1.0
91      CALL ZANDC(TEM,TC,PAVGO,PC,CNCH2S,CNCCO2,ZAVG,CMPGA,JERR)
        ZACH=ABS(ZAVGO-ZAVG)
        IF(ZACH.LE.ZATOL) THEN
        GOTO 90
        ELSE
        PAVGO=SUMPZA*ZAVG
        ZAVGO=ZAVG
        GOTO 91
        ENDIF
90      CONTINUE
        PAVG=SUMPZA*ZAVG
              SUM=0.0D0
              SUMP=0.D0
              SUMPZ=0.D0
              DO 70 I=1,MAXX
                  DO 72 J=1,MAXY
                    NORD=(I-1)*MAXY+J
                    SUM=SUM+(VISCGN(NORD)+VISCGO(NORD))*
     A                   (PPRESN(NORD)-PPRESO(NORD))*
     B                    DX(I)*DY(J)
               CALL TABSEQ(PPRESN(NORD),TABMP,TABP,NSTEP,P)
             CALL ZANDC(TEM,TC,P,PC,CNCH2S,CNCCO2,ZED,CMPG,JERR)
                SUMP=P*DX(I)*DY(J)+SUMP
                SUMPZ=P/ZED*DX(I)*DY(J)+SUMPZ
72                 CONTINUE
70              CONTINUE
                SUM=SUM*POROS/4.0D0/TDEL
                SUMP=SUMP/XCUM/YCUM
                SUMPZ=SUMPZ/XCUM/YCUM
                CALL ZANDC(TEM,TC,SUMP,PC,CNCH2S,CNCCO2,ZED,CMPG,
     A                    JERR)
C               SUMP=SUMP/ZED
                EMBL=TSC*POROS/PSC/(TEM+TEMRAK)*(SUMPZ-SUMOLD)
     A               /QSORMB/TDEL
                EMBG=TSC*POROS/PSC/(TEM+TEMRAK)*(SUMPZ-SUMINT)
     A               /QSORMB/TCUM
                SUMOLD=SUMPZ
                 IF(TCUM.EQ.TDEL) THEN
                     WRITE(10,*)'TCUM,PB,PMB,(P/Z)B,PB/ZB,MBG,MGL'
                     WRITE(10,*)TCUM-TDEL,PINIT,PINIT,SUMINT,SUMINT,
     A                          EMBG-EMBG,EMBL-EMBL
                     WRITE(10,*)TCUM,SUMP,PAVG,SUMPZ,SUMP/ZED,
     A                          EMBG,EMBL
                 ELSE
                     WRITE(10,*)TCUM,SUMP,PAVG,SUMPZ,SUMP/ZED,
     A                          EMBG,EMBL
                 ENDIF
               ENDIF
```

```
                IF (TCUM.EQ.TDEL) THEN
                    WRITE(9,*)TCUM-TDEL,TDEL-TDEL,PPRESO(LWELL),
     A                        PO,RESMAX-RESMAX,
     B                        IRESMX-IRESMX,JRESMX-JRESMX
                    WRITE(9,*)TCUM,TDEL,PPRESN(LWELL),PN,
     A                        RESMAX,IRESMX,JRESMX
                ELSE
                    WRITE(9,*)TCUM,TDEL,PPRESN(LWELL),PN,
     A                        RESMAX,IRESMX,JRESMX
                ENDIF
C
C             THE BLOCK BELOW SHOULD BE TURNED ON IF M(P)
C             DISTRIBUTION IS DESIRED :
C
C               DO 82 I=1,MAXX
C                   NORD=(I-1)*MAXY+JWELL
C                   IF (I.EQ.1) THEN
C                        WRITE(11,*)TCUM,PPRESN(NORD),XG(I)
C                   ELSE
C                        WRITE(11,*)'         ',PPRESN(NORD),
C    A                       XG(I)
C                   ENDIF
C82                CONTINUE
C                  DO 84 J=1,MAXY
C                   NORD=(IWELL-1)*MAXY+J
C                   WRITE(11,*)'         ',PPRESN(NORD),YG(J)
C84                CONTINUE
           ENDIF
           GOTO 600
           ELSE
              DO 75 I=1,MAXX*MAXY
                  PPRESI(I)=PPRESN(I)
75            CONTINUE
C
C          PERFORM M(P) - P - VIS*CG COMPUTATION
C          FOR NEXT ITERATION IF NOT CONVERGED
C
           DO 80 I=1,MAXX*MAXY
C             WRITE(6,*)I,PPRESN(I),'CALLING TABSEQ'
              CALL TABSEQ(PPRESN(I),TABMP,TABP,NSTEP,P)
C             WRITE(6,*)P,'CALLING VISCY'
              CALL VISCY((TEM+TEMRAK)/TC,P/PC,SPG,TEM,CNCH2S,
     A                   CNCCO2,CNCN2,VISGR,VISG,JERR)
C             WRITE(6,*)'CALLING ZANDC'
              CALL ZANDC(TEM,TC,P,PC,CNCH2S,CNCCO2,ZED,CMPG,JERR)
              VISCGN(I)=VISG*CMPG
80         CONTINUE
           ENDIF
           GOTO 300
           END

CCCC
```

```
      DATA TC /
     A227.0,672.3,547.54,342.99,549.77,665.68,734.63,765.29,828.70
     B,845.28,913.32,972.36 /
      DATA PC /
     A493.,1306.,1072.,667.8,707.8,616.3,529.1,550.7,490.4,488.6,
     B436.9,396.8 /
      WRITE(6,*)'INPUT DATA FILE OUTPUT NAME'
      READ(5,*)OUTFIL
C
C     INPUTTING TYPE OF SIMULATION ANALYSIS - BUILD-UP OR DRAWDOWN
C
      WRITE(6,*)'TYPE OF SIMULATION ANALYSIS'
      WRITE(6,*)'1 - FOR BUILD-UP , 2 - FOR DRAWDOWN'
      READ(5,*)ITSA
       IF(ITSA.EQ.1) THEN
        FBUP=.TRUE.
       ELSE
        FBUP=.FALSE.
       ENDIF
C
C     INPUTTING TIMES FOR RESPECTIVE ANALYSIS
C
      WRITE(6,*)'INPUT FIRST TIME TO COMPUTE DRAWDOWN PRESSURE - HRS'
      READ(5,*)TFDD
      WRITE(6,*)'INPUT FINAL LOGARITHMIC TIME INCREMENT - HRS'
      READ(5,*)TSLD
      WRITE(6,*)'INPUT TIME CONSTANT INCREMENT FOR DRAWDOWN  - HRS'
      READ(5,*)TCONS
      WRITE(6,*)'INPUT TIME WELL SHUT-IN - HRS'
      READ(5,*)TSI
      IF(FBUP) THEN
      WRITE(6,*)'INPUT FIRST TIME TO COMPUTE BUILD-UP PRESSURE - HRS'
      READ(5,*)TFBU
      WRITE(6,*)'INPUT FINAL TIME TO COMPUTE BUILD-UP PRESSURE - HRS'
      READ(5,*)TSLB
      ENDIF
C
C     INPUTTING DELTA P (PSI) FOR P-M(P) TABLE
C
      WRITE(6,*)'INPUT DELTA P FOR P-M(P) TABLE - PSI'
      READ(5,*)PDEL
C
C     INPUTTING FLOWRATE TERM - QSOR
C
      WRITE(6,*)'INPUT FLOWRATE - MSCF/D'
      READ(5,*)QSOR
C
C     SUBROUTINE INPUT CONTAINS GAS PROPERTIES, RESERVOIR DATA,
C     RESERVOIR GRID SIZING, AND WELL LOCATION INFORMATION.
C
C     ARRAY DESCRIPTION
C
C             X , Y - block locations from well to respective x,y
C                     origins
C             XG,YG - grid block x,y locations from 0,0 at lower left
C                     corner
C             YM    - mole fracitons of gas analysis components
C             RD    - reservoir properties
C             SG    - gas SG and mole fractions of N2, H2S, CO2
C             GM    - molar mss of gas components
C             PC,TC - critical pressure, temperature of gas component
C
C
C     FILE DEFINITION  -  FILE        DESCRIPTION
```

```
C
C                       SGDAT        gas specific gravity and mole
C                                    fractions of N2, H2S, CO2.
C                       RDAT         reservoir properties
C                       FDAT         mole fractions of gas analysis
C                                    components
C                       SIMDAT       reservoir geometry data
C
C                       E.//OUFIL    Input Echo
C
      OPEN(UNIT=3,FILE='SGDAT')
      OPEN(UNIT=4,FILE='RDAT')
      OPEN(UNIT=7,FILE='FDAT')
      OPEN(UNIT=8,FILE='SIMDAT')
C     OPEN(UNIT=9,FILE='RAWDATA')
      OPEN(UNIT=9,FILE='E.'//OUTFIL,STATUS='NEW')
C
C     INPUTTING GAS PROPERTIES - BY EITHER GAS SG OR MOLE FRACTION
C
C             VARIABLE DESCRIPTION
C
C     VARIABLE        TYPE        DESCRIPTION
C
C     IGP              flag     identifies type of gas input, i.e. by
C                               mole fraction or specific gravity
C     ISGC             flag     identifies if new or old gas data to be
C                               used
C     YMC              real     sum. of mole fractions
C
      WRITE(6,*)'GAS PROPERTIES CALCULATIONS'
      WRITE(6,*)'BY MOLE FRACTIONS OR BY SPECIFIC GRAVITY ?'
      WRITE(6,*)'1 - FOR MOLE FRACTION, 0 - FOR SPECIFIC GRAVITY'
      READ(5,*)IGP
      IF(IGP.EQ.1) GOTO 7
              IF(IGP.EQ.0) THEN
              WRITE(6,*)'GAS ANALYSIS - INPUT NEW SPECIFIC GRAVITY ?'
              WRITE(6,*)'1 - FOR "YES", 0 - FOR "NO"'
              READ(5,*)ISGC
                      IF(ISGC.EQ.1) THEN
                      WRITE(6,*)'GAS SPECIFIC GRAVITY'
                      READ(5,*)SG(1)
                      WRITE(3,*)SG(1)
                      WRITE(6,*)'M. F. NITROGEN, N2 - Y'
                      READ(5,*)SG(2)
                      WRITE(3,*)SG(2)
                      WRITE(6,*)'M. F. HYDROGEN SULFIDE, H2S - Y'
                      READ(5,*)SG(3)
                      WRITE(3,*)SG(3)
                      WRITE(6,*)'M. F. CARBON DIOXIDE, CO2 - Y'
                      READ(5,*)SG(4)
                      WRITE(3,*)SG(4)
                      PCP=700.55-47.94*SG(1)
                      TCP=175.59+307.97*SG(1)
                      GOTO 3
                      ELSE
                       DO 9 I=1,4
                       READ(3,*)SG(I)
9                       CONTINUE
                      PCP=700.55-47.94*SG(1)
                      TCP=175.59+307.97*SG(1)
                      GOTO 3
                      ENDIF
               ENDIF
7     CONTINUE
```

```
      WRITE(6,*)'GAS ANALYSIS - INPUT NEW MOLE FRACTIONS ?'
      WRITE(6,*)'1 - FOR "YES", 0 - FOR "NO"'
      READ(5,*)ISGC
11    CONTINUE
            IF(ISGC.EQ.1) THEN
            WRITE(6,*)'INPUTTING GAS ANALYSIS MOLE FRACTIONS'
            WRITE(6,*)'NITROGEN, N2 - Y'
            READ(5,*)YM(1)
            WRITE(7,*)YM(1)
            WRITE(6,*)'HYDROGEN SULFIDE, H2S - Y'
            READ(5,*)YM(2)
            WRITE(7,*)YM(2)
            WRITE(6,*)'CARBON DIOXIDE, CO2 - Y'
            READ(5,*)YM(3)
            WRITE(7,*)YM(3)
            WRITE(6,*)'METHANE, CH4 - Y'
            READ(5,*)YM(4)
            WRITE(7,*)YM(4)
            WRITE(6,*)'ETHANE, C2H6 - Y'
            READ(5,*)YM(5)
            WRITE(7,*)YM(5)
            WRITE(6,*)'PROPANE, C3H8 - Y'
            READ(5,*)YM(6)
            WRITE(7,*)YM(6)
            WRITE(6,*)'ISO-BUTANE, i-C4H10 - Y'
            READ(5,*)YM(7)
            WRITE(7,*)YM(7)
            WRITE(6,*)'N-BUTANE, n-C4H10 - Y'
            READ(5,*)YM(8)
            WRITE(7,*)YM(8)
            WRITE(6,*)'ISO-PENTANE, i-C5H12 - Y'
            READ(5,*)YM(9)
            WRITE(7,*)YM(9)
            WRITE(6,*)'N-PENTANE, n-C5H12 - Y'
            READ(5,*)YM(10)
            WRITE(7,*)YM(10)
            WRITE(6,*)'HEXANES, C6 - Y'
            READ(5,*)YM(11)
            WRITE(7,*)YM(11)
            WRITE(6,*)'HEPTANES +, C7 - Y'
            READ(5,*)YM(12)
            WRITE(7,*)YM(12)
            ELSE
             DO 2 I=1,12
             READ(7,*)YM(I)
2             CONTINUE
            ENDIF
      YMC=0.
       DO 8 I=1,12
       YMC=YMC+YM(I)
8     CONTINUE
       YMC=1.-YMC
            IF(YMC.LE.0.000001) GOTO 22
       WRITE(*,*)YMC
       WRITE(6,*)'SUM. OF MOLE FRACTIONS NOT EQUAL TO 1.0'
       GOTO 11
22     CONTINUE
C
C     READING IN DATA FOR GAS MOLAR MASS & CRITICAL PROPERTIES
C     NOTE: IN OILFIELD UNITS
C
C              VARIABLE DESCRIPTION
C
C     VARIABLE       TYPE       DESCRIPTION
```

```
C
C       SGM             real    SG calculated from mole fractions
C       SGM1            real    increment SG of gas components
C       TCP             real    gas critical temperature
C       TC1             real    increment TC of gas components
C       PCP             real    gas critical pressure
C       PC1             real    increment PC of gas components
C
        SGM1=0.
        TC1=0.
        PC1=0.
         DO 21 I=1,12
         SGM=SGM1+(YM(I)*GM(I)/28.96)
         SGM1=SGM
         TCP=TC1+(YM(I)*TC(I))
         TC1=TCP
         PCP=PC1+(YM(I)*PC(I))
         PC1=PCP
21       CONTINUE
        SG(1)=SGM
        SG(2)=YM(1)
        SG(3)=YM(2)
        SG(4)=YM(3)
3       CONTINUE
C
C       INPUTTING RESERVOIR PROPERTY DATA
C
C               VARIABLE DESCRIPTION
C
C       VARIABLE        TYPE        DESCRIPTION
C
C       IRDC             flag    for input of old or new reservoir data
C       PERM             real    reservoir permeability (md)
C       P                real    reservoir pressure (psia)
C       T                real    reservoir temperature (R)
C       PHI              real    reservoir porositye (decimal)
C       RW               real    well radius (ft.)
C
        WRITE(6,*)'RESERVOIR DATA - INPUT NEW PROPERTIES ?'
        WRITE(6,*)'1 - FOR "YES", 0 - FOR "NO"'
        READ(5,*)IRDC
              IF(IRDC.EQ.0) GOTO 4
        WRITE(6,*)'INPUTTING RESERVOIR DATA'
        WRITE(6,*)'RESERVOIR PERMEABILITY - MD'
        READ(5,*)RD(1)
        WRITE(4,*)RD(1)
        WRITE(6,*)'RESERVOIR PRESSURE - PSIA'
        READ(5,*)RD(2)
        WRITE(4,*)RD(2)
        WRITE(6,*)'RESERVOIR TEMPERATURE - F'
        READ(5,*)RD(3)
        WRITE(4,*)RD(3)
        WRITE(6,*)'RESERVOIR POROSITY - (decimal)'
        READ(5,*)RD(4)
        WRITE(4,*)RD(4)
        WRITE(6,*)'WELL RADIUS - FT'
        READ(5,*)RD(5)
        WRITE(4,*)RD(5)
        GOTO 52
4             CONTINUE
         DO 51 J=1,5
         READ(4,*)RD(J)
51       CONTINUE
52      CONTINUE
```

```
      PERM=RD(1)
      P=RD(2)
      T=RD(3)
      PHI=RD(4)
      RW=RD(5)
C
C
C
C           RESERVOIR DIMENSIONS & GRID DEFINITION
C
C           VARIABLE DESCRIPTION
C
C     VARIABLE        TYPE        DESCRIPTION
C
C     XL(FT.)          real     reservoir length
C     YL(FT.)          real     reservoir width
C     XP(FT.)          real     well X location from 0.
C     YP(FT.)          real     well Y location from 0.
C     IG               flag     indicates grid spacing not fine enough
C                               for well location
C     XWB1(FT.)        real     wellblock AREA 1 grid spacing
C       XWB2(FT.)        real     wellblock AREA 2 grid spacing
C       XWB1F            real     wellblock AREA 1 fraction
C     XBM              real     X grid spacing multiplier
C     XYR              real     ratio XL/YL
C     YBM              real     Y grid spacing multiplier
C     XGM              real     multiplier defining grid sections
C     YGM              real     multiplier defining Y grid sections
C     XGM1             real     initial value of XGM
C     YGM1             real     initial value of YGM
C     XWB              real     X grid spacing around wellbore
C     YWB              real     Y grid spacing around wellbore
C     XSM,YSM          real     X,Y multipliers for adding half block
C                               lengths when changing block size
C     GMX,GMY          real     X,Y multipliers for changing the end
C                               grid point observed before changing
C                               block lengths
C     XEC,YEC          real     incremental length added when changing
C                               block lengths
C     XGC,YGC          real     grid sections identifier
C     GC,CC            real     dividers for calculating block lengths
C                               when changing block size
C     NX,NY   interger          well block X,Y location in XG,YG
C     XED,YED(FT.)     real     end X,Y locations before changing
C                               grid size
C     XE1,YE1          real     last XEC,YEC value
C     XCH,YCH          real     summ of XG,YG to ensure equal to XL,YL
C     MX,MY   interger          number of X,Y blocks in XG,YG
C
        WRITE(6,*)'RESERVOIR DIMENSIONS & GRID CONFIGURATION'
        WRITE(6,*)'INPUT NEW DATA ?'
        WRITE(6,*)'1 - FOR "YES" , 0 - FOR "NO"'
        READ(5,*)IRGC
         IF(IRGC.EQ.1) THEN
         CALL EMPTYF(8)
      WRITE(6,*)'Input reservoir length, xl'
      READ(5,*)XL
      WRITE(6,*)'Input reservoir width, yl'
      READ(5,*)YL
      WRITE(6,*)'Input well location, xp'
      READ(5,*)XP
      WRITE(6,*)'Input well location, yp'
      READ(5,*)YP
      IG=0
```

```
C
C       CHECK FOR PROPER GRID SET-UP
C
5       CONTINUE
              IF(IG.EQ.1) THEN
              WRITE(6,*)'1st block nonexistent-DECREASE GRID SPACING'
              IG=0
              ENDIF
        WRITE(6,*)'Input GRID SPACING AROUND WELL - AREA 1 (FT)'
        READ(5,*)XWB1
          WRITE(6,*)'INPUT AREA 1 GRID FRACTION - 0 TO 1.0 '
          READ(5,*)XWB1F
          WRITE(6,*)'INPUT GRID SPACING AROUND WELL - AREA 2 (FT)'
          READ(5,*)XWB2
          XWB1FI=XWB1F
6       CONTINUE
        WRITE(6,*)'Input GRID SPACING MULTIPLIER'
        READ(5,*)XBM
        XYR=XL/YL
        YBM=XBM/XYR
              IF(YBM.LT.1.) YBM=1.
        X(1)=XP
        Y(1)=YP
        XGM1=1.
        YGM1=1.
        XWB=XWB1
        YWB=XWB1
        XGM=XGM1
        YGM=YGM1
        XSM=0.
        YSM=0.
        XECS=0.
        YECS=0.
        GMX=1.
        GMY=1.
        GC=2.
        CC=1.
         DO 10 I=2,100
         NX=I
         X(I)=X(I-1)-XWB/CC-XSM*XECS
                 IF(X(I).LE.0.) THEN
                 X(I)=(X(I-1)-XEC)/2.
                 GOTO 15
                 ENDIF
         XGC=XP-(XL/(2.*5.))*XGM*XWB1F
         XEC=(X(I-1)-X(I))/GC-XSM*XECS
         XSM=0.
         GC=2.
         CC=1.
         XGC=XGC+XEC
                IF(X(2).LE.0.) THEN
                IG=1
                GOTO 5
                ENDIF
        IF(X(I).LE.XGC) THEN
            IF(XWB1F.LT.1.) THEN
            XWB=XWB2
            XWB1F=1.
            ELSE
        XGM=XGM+2
        XWB=XWB*XBM
            ENDIF
        XSM=1.
        GC=1.
```

```
      CC=2.
      GMX=0.75
      XECS=XEC
      ENDIF
       XED=2.*XEC*GMX
      IF(X(I).LE.XED) THEN
      X(I)=(X(I-1)-XE1)/2.
      GOTO 15
      ENDIF
      XE1=XEC
10     CONTINUE
15    DO 20 J=1,NX
        XG(J)=X(I)
        I=I-1
20     CONTINUE
      XWB=XWB1
      XGM=XGM1
      XSM=0.
      GMX=1.
      GC=2.
      CC=1.
        XWB1F=XWB1FI
      DO 25 I=NX+1,100
      MX=I
      XG(I)=XG(I-1)+XWB/CC+XSM*XECS
      XBC=XL-XG(I)
      IF(XG(I).GE.XL) THEN
      XG(I)=(XL-(XG(I-1)+XEC))/2.+XG(I-1)+XEC
      GOTO 30
      ENDIF
      XGC=XP+(XL/(2.*5.))*XGM*XWB1F
      XEC=(XG(I)-XG(I-1))/GC-XSM*XECS
      XSM=0.
      GC=2.
      CC=1.
      XGC=XGC-XEC
      IF(XG(NX+1).GE.XL) THEN
      IG=1
      GOTO 5
      ENDIF
      IF(XG(I).GE.XGC) THEN
          IF(XWB1F.LT.1.) THEN
          XWB=XWB2
          XWB1F=1.
          ELSE
      XGM=XGM+2.
      XWB=XWB*XBM
          ENDIF
      XSM=1.
      GC=1.
      CC=2.
      GMX=0.75
      XECS=XEC
      ENDIF
      XED=2.*XEC*GMX
      IF(XBC.LE.XED) THEN
      XG(I)=(XL-(XG(I-1)+XE1))/2.+XG(I-1)+XE1
      GOTO 30
      ENDIF
      XE1=XEC
25    CONTINUE
30    CONTINUE
      GC=2.
      CC=1.
```

```
        XWB1F=XWB1FI
      DO 35 I=2,100
      NY=I
      Y(I)=Y(I-1)-YWB/CC-YSM*YECS
      IF(Y(I).LE.0.) THEN
      Y(I)=(Y(I-1)-YEC)/2.
      GOTO 40
      ENDIF
      YGC=YP-(YL/(2.*5.))*YGM*XWB1F
      YEC=(Y(I-1)-Y(I))/GC-YSM*YECS
      YSM=0.
      GC=2.
      CC=1.
      YGC=YGC+YEC
      IF(Y(2).LE.0.) THEN
      IG=1
      GOTO 5
      ENDIF
      IF(Y(I).LE.YGC) THEN
          IF(XWB1F.LT.1.) THEN
          YWB=XWB2
          XWB1F=1.
          ELSE
      YGM=YGM+2.
      YWB=YWB*YBM
          ENDIF
      YSM=1.
      GC=1.
      CC=2.
      GMY=0.75
      YECS=YEC
      ENDIF
      YED=2.*YEC*GMY
      IF(Y(I).LE.YED) THEN
      Y(I)=(Y(I-1)-YE1)/2.
      GOTO 40
      ENDIF
      YE1=YEC
35    CONTINUE
40   DO 45 J=1,NY
      YG(J)=Y(I)
      I=I-1
45    CONTINUE
      YWB=XWB1
      YGM=YGM1
      YSM=0
      GMY=1.0
      GC=2.
      CC=1.
        XWB1F=XWB1FI
      DO 50 I=NY+1,100
      MY=I
      YG(I)=YG(I-1)+YWB/CC+YSM*YECS
      YBC=YL-YG(I)
      IF(YG(I).LE.0.) THEN
      YG(I)=(YL-(YG(I-1)+YEC))/2.+YG(I-1)+YEC
      GOTO 55
      ENDIF
      YGC=YP+(YL/(2.*5.))*YGM*XWB1F
      YEC=(YG(I)-YG(I-1))/GC-YSM*YECS
      YSM=0
      GC=2.
      CC=1.
      YGC=YGC-YEC
```

```
      IF(YG(NY+1).GE.YL) THEN
      IG=1
      GOTO 5
      ENDIF
      IF(YG(I).GE.YGC) THEN
          IF(XWB1F.LT.1.) THEN
          YWB=XWB2
          XWB1F=1.
          ELSE
      YGM=YGM+2.
      YWB=YWB*YBM
          ENDIF
      YSM=1.
      GC=1.
      CC=2.
      GMY=0.75
      YECS=YEC
      ENDIF
      YED=2.*YEC*GMY
      IF(YBC.LE.YED) THEN
      YG(I)=(YL-(YG(I-1)+YE1))/2.+YG(I-1)+YE1
      GOTO 55
      ENDIF
      YE1=YEC
50    CONTINUE
55    CONTINUE
      WRITE(8,*)XL,YL
      WRITE(8,*)XP,YP
      WRITE(8,*)XWB1,XWB1FI,XWB2,XBM,YBM,XYR
      WRITE(8,*)MX,MY
      DO 60 I=1,MX
      WRITE(8,*)XG(I)
 60   CONTINUE
      DO 65 I=1,MY
      WRITE(8,*)YG(I)
 65    CONTINUE
      XCH=0.
      YCH=0.
      DO 70 I=2,MX
      XCH=XCH+XG(I)-XG(I-1)
70    CONTINUE
      DO 75 I=2,MY
      YCH=YCH+YG(I)-YG(I-1)
75    CONTINUE
      XCH=XCH+XG(1)+(XL-XG(MX))
      YCH=YCH+YG(1)+(YL-YG(MY))
      WRITE(8,*)XCH,YCH
      WRITE(8,*)XG(NX),NX
      WRITE(8,*)YG(NY),NY
         ELSE
          DO 110 I=1,3
           READ(8,*)DUMM
110       CONTINUE
          READ(8,*)MX,MY
           DO 111 I=1,MX
            READ(8,*)XG(I)
111         CONTINUE
           DO 112 J=1,MY
            READ(8,*)YG(J)
112         CONTINUE
          READ(8,*)DUMM
          READ(8,*)DUMM,NX
          READ(8,*)DUMM,NY
         ENDIF
```

```
      WRITE(9,*)'CASE NAME : ',OUTFIL
      IF (FBUP) THEN
         WRITE(9,*)'BUILDUP ANALYSIS'
      ELSE
         WRITE(9,*)'DRAWDOWN ANALYSIS'
      ENDIF
      WRITE(9,*)'Tfdd Tflog Tcons Tsi,',TFDD,TSLD,TCONS,TSI
      IF (FBUP) THEN
      WRITE(9,*)'Tfbup Tslb,',TFBU,TSLB
      ENDIF
      WRITE(9,*)'Dp in p vs M(p),',PDEL
      WRITE(9,*)'Q (MSCFD),',QSOR
      WRITE(9,*)'SG %H2S CO2 N2,',SG(1),SG(3),SG(4),SG(2)
      WRITE(9,*)'k (md),',PERM
      WRITE(9,*)'Pi,',P
      WRITE(9,*)'Tres (F),',T
      WRITE(9,*)'Por (frac),',PHI
      WRITE(9,*)'Rw ,',RW
      WRITE(9,*)'xl (Ft),',XL
      WRITE(9,*)'yl (Ft),',YL
      WRITE(9,*)'Xwell,',XP
      WRITE(9,*)'Ywell,',YP
      WRITE(9,*)'Grid Area I,',XWB1
      WRITE(9,*)'Area I Grid Fraction,',XWB1FI
      WRITE(9,*)'Grid Area II,',XWB2
      WRITE(9,*)'Space Multiplier,',XBM
      WRITE(9,*)'Blocks x y,',MX,MY
      WRITE(9,*)'Well Block #,',NX,NY
    CLOSE(3)
    CLOSE(4)
    CLOSE(7)
    CLOSE(8)
    CLOSE(9)
    RETURN
    END
```

```
CCCCCCCCCCCCCCCCCCCCCCCCCCCCCCCCCCCCCCCCCCCCCCCCCCCCCCCCCCCCCCCCCCCCCCCCCCC
C
C     THE COLLECTION OF THE FOLLOWING SUBROUTINES ARE TAKEN FROM :
C     (WITH THE EXCEPTION OF TABSEQ)
C
C     GAS WELL TESTING - THEORY AND PRACTICE (3RD EDITION)
C     PUBLISHED BY THE ENERGY CONSERVATION BOARD
C     CALGARY, ALBERTA
C     1976.
C
C     REFER TO THE ABOVE REFERENCE FOR MORE INFORMATION
C
CCCCCCCCCCCCCCCCCCCCCCCCCCCCCCCCCCCCCCCCCCCCCCCCCCCCCCCCCCCCCCCCCCCCCCCCCCC
C
C     LAGRANGE INTERPOLATION
C
      SUBROUTINE XLGR4(X,X1,X2,X3,X4,Y,Y1,Y2,Y3,Y4)
C
C     Y IS TO BE ESTIMATED FOR X WHICH LIES BETWEEN (X1,Y1) TO (X4,Y4)
C
      IMPLICIT REAL*8 (A-H,O-Z)
      A1=X1-X2
      A2=X1-X3
      A3=X1-X4
      A4=X2-X3
      A5=X2-X4
      A6=X3-X4
      B1=X-X1
      B2=X-X2
      B3=X-X3
      B4=X-X4
      Y=B2/A1*B3/A2*B4/A3*Y1-B1/A1*B3/A4*B4/A5*Y2+
     A  B1/A2*B2/A4*B4/A6*Y3-B1/A3*B2/A5*B3/A6*Y4
      RETURN
      END
C
C     INTERPOLATION ROUTINE
C     LAGRANGE INTERPOLATION IS USED WHENEVER PERMITTED
C     LINEAR INTERPOLATION AT EITHER END OF THE DATA SET
C
        SUBROUTINE TABSEQ(X,TABX,TABY,NTOTAL,Y)
        IMPLICIT REAL*8(A-H,O-Z)
        DIMENSION TABX(0:NTOTAL),TABY(0:NTOTAL)
        I=0
381     IF(X.GT.TABX(I)) THEN
           I=I+1
           GOTO 381
        ELSE
           IF(X.EQ.TABX(I)) THEN
              Y=TABY(I)
           ELSE
              IF((I-1).EQ.0.OR.I.EQ.NTOTAL) THEN
                 Y=TABY(I-1)+(X-TABX(I-1))/(TABX(I)-TABX(I-1))
     A              *(TABY(I)-TABY(I-1))
              ELSE
                 CALL XLGR4(X,TABX(I-2),TABX(I-1),TABX(I),
     A            TABX(I+1),Y,TABY(I-2),TABY(I-1),TABY(I),
     B            TABY(I+1))
              ENDIF
           ENDIF
        ENDIF
        RETURN
        END
C
```

```
C     NATURAL GAS VISCOISTY ESTIMATION
C     REQUIRES SUBROUTINE XLGR4
C
      SUBROUTINE VISCY(TEMPRD,PRSPRD,SPG,TEM,CNCH2S,CNCCO2,
     A                 CNCN2,VISGR,VISG,IERR)
C
C     ALL INPUTS AND OUTPUTS ARE IN FIELD UNITS :
C     TEMPRD,PRSPRD : PSEUDO REDUCED TEMPERATURE AND PRESSURE
C     SPG : GAS SPECIFIC GRAVITY
C     TEM : TEMPERATURE
C     CNCH2S,CNCCO2,CNCN2 : MOLE PERCENT OF H2S,CO2 AND N2
C     VISGR : (VISCOSITY)/(VISCOSITY AT 1 ATM.)
C     VISG : NATURAL GAS VISCOSITY
C     IERR :ERROR FLAG INDICATING BOUND ERROR
C
      IMPLICIT REAL*8 (A-H,O-Z)
      DIMENSION TEMTBL(13),PRSTBL(22),VISTBL(22,13),VISTB1(22,
     A          7),VISTB2(22,6)
      EQUIVALENCE (VISTB1(1,1),VISTBL(1,1)),
     A            (VISTB2(1,1),VISTBL(1,8))
      DATA TEMTBL /
     A1.05,1.10,1.15,1.20,1.30,1.40,1.50,1.60,1.75,2.00,2.25,
     B2.50,3.00 /
      DATA PRSTBL /
     A0.1,0.2,0.3,0.4,0.5,0.6,0.7,0.8,0.9,1.0,1.2,
     B1.4,1.6,1.8,2.0,3.0,4.0,6.0,8.0,10.0,15.0,20.0 /
      DATA VISTB1 /
     A1.0,1.012,1.025,1.05,1.075,1.1,1.145,1.195,1.285,1.415,1.76,
     B2.285,2.865,3.29,3.65,4.76,5.5,6.46,7.15,7.68,8.65,9.37,

     D1.0,1.011,1.023,1.043,1.065,1.086,1.12,1.15,1.195,1.255,1.435,
     E1.7,2.07,2.465,2.8,3.85,4.655,5.72,6.5,7.06,8.1,8.8,

     G1.0,1.01,1.021,1.036,1.055,1.073,1.095,1.12,1.145,1.175,1.28,
     H1.42,1.59,1.85,2.16,3.225,3.975,5.03,5.82,6.385,7.41,8.18,

     J1.000,1.009,1.019,1.030,1.045,1.060,1.070,1.085,1.110,1.135,
     K1.195,1.285,1.425,1.570,1.750,2.600,3.350,4.380,5.125,5.740,
     L6.750,7.500,
     M1.000,1.008,1.017,1.027,1.040,1.054,1.063,1.075,1.100,1.120,
     N1.155,1.215,1.285,1.360,1.460,2.020,2.560,3.500,4.185,4.755,
     O5.790,6.500,
     P1.000,1.007,1.015,1.024,1.035,1.048,1.056,1.067,1.089,1.100,
     Q1.135,1.185,1.235,1.280,1.335,1.690,2.110,2.790,3.380,3.860,
     R4.790,5.410,
     S1.000,1.006,1.013,1.021,1.030,1.042,1.049,1.059,1.078,1.100,
     T1.120,1.150,1.185,1.220,1.260,1.500,1.785,2.325,2.820,3.230,
     U4.060,4.610 /
C
      DATA VISTB2 /
     A1.000,1.005,1.011,1.018,1.025,1.036,1.042,1.051,1.067,1.070,
     B1.095,1.120,1.150,1.180,1.215,1.385,1.595,2.030,2.425,2.770,
     C3.490,4.025,
     D1.000,1.004,1.009,1.015,1.021,1.030,1.035,1.043,1.056,1.065,
     E1.090,1.110,1.125,1.145,1.165,1.280,1.435,1.770,2.095,2.375,
     F2.990,3.500,
     G1.000,1.003,1.007,1.012,1.017,1.024,1.028,1.035,1.045,1.055,
     H1.060,1.070,1.080,1.095,1.110,1.205,1.290,1.500,1.725,1.955,
     I2.480,2.925,
     J1.000,1.002,1.005,1.009,1.013,1.018,1.021,1.027,1.034,1.040,
     K1.045,1.055,1.065,1.075,1.085,1.145,1.210,1.340,1.485,1.665,
     L2.085,2.460,
     M1.000,1.001,1.003,1.006,1.009,1.012,1.015,1.019,1.023,1.025,
     N1.030,1.040,1.050,1.060,1.065,1.105,1.155,1.245,1.360,1.485,
```

```
     O1.830,2.150,
     P1.000,1.000,1.001,1.003,1.005,1.007,1.009,1.011,1.013,1.015,
     Q1.020,1.025,1.030,1.035,1.040,1.060,1.085,1.140,1.205,1.265,
     R1.495,1.750 /
      LOPRS=2
      IHIPRS=21
      LOTEM=3
      IHITEM=11
      IERR=0
      IF (TEMPRD.LT.1.05.OR.TEMPRD.GT.3.00) GO TO 340
      IF (PRSPRD.LT.0.01.OR.PRSPRD.GT.20.00) GO TO 340
      IF (SPG   .LT.0.55.OR.SPG   .GT.1.50) GO TO 340
      IF (TEM   .LT.40.0.OR.TEM   .GT.400.00) GOTO 340
      DO 100 J=LOTEM,IHITEM
         IF (TEMTBL(J).GE.TEMPRD) GO TO 120
100   CONTINUE
      J=IHITEM+1
120   IF (PRSTBL(LOPRS-1).LT.PRSPRD) GO TO 160
      I=1
      ICALL=1
      GO TO 320
140   VISGR=1.00+(PRSPRD*(VISI-1.0))
      GO TO 300
160   IF (PRSTBL(IHIPRS+1).GT.PRSPRD) GO TO 200
      I=IHIPRS+1
      ICALL=2
      GO TO 320
180   VISGR=VISI
      GO TO 300
200   DO 220 I=LOPRS,IHIPRS
         IF (PRSTBL(I).GE.PRSPRD) GO TO 240
220   CONTINUE
      I=IHIPRS+1
240   ICALL=3
      GO TO 320
260   VISJ=VISI
      I=I-1
      ICALL=4
      GO TO 320
280   I=I+1
      VISGR=VISI+(((PRSPRD-PRSTBL(I-1))/(PRSTBL(I)-PRSTBL(I-1)))
     A      *(VISJ-VISI))
300   VISGU=(0.126585E-01)-(0.611823E-02)*SPG+(0.164574E-02)*SPG
     A      *SPG+(0.164574E-04)*TEM-(0.719221E-06)*SPG*TEM
     B      -(0.609046E-06)*SPG*SPG*TEM
      CORH2S=(0.000113*CNCH2S*SPG-0.000038*CNCH2S+0.000001)
     A       *(1.0/(1.0+SPG))+0.000001
      CORCO2=(0.000134*CNCCO2*SPG-0.000004*CNCCO2+0.000004*SPG)
     A       *(1.0/(1.0+SPG))-0.000003
      CORN2 =(0.000170*CNCN2*SPG+0.000021*CNCN2+0.000010*SPG)
     A       *(1.0/(1.0+SPG))-0.000006
      VISGA=VISGU+CORH2S+CORCO2+CORN2
      VISG=VISGR*VISGA
      GO TO 360
320   CALL XLGR4(TEMPRD,TEMTBL(J-2),TEMTBL(J-1),TEMTBL(J),
     A           TEMTBL(J+1),VISI,VISTBL(I,J-2),VISTBL(I,J-1),
     B           VISTBL(I,J),VISTBL(I,J+1))
      GO TO (140,180,260,280)ICALL
340   IERR=1
      VISGR=0.
      VISG=0.
360   RETURN
      END
C
```

```
C     SUBROUTINE TO CALCULATE NATURAL GAS COMPRESSIBILITY FACTOR (Z)
C     AND COMPRESSIBILITY (CG)
C
      SUBROUTINE ZANDC(TEM,TEMPC,PRS,PRSPC,CNCH2S,CNCCO2,ZED,
     A                 CMPG,IERR)
      IMPLICIT REAL*8 (A-H,O-Z)
C
C     ALL INPUT AND OUTPUTS ARE IN FILED UNITS :
C     TEM :TEMPERATURE
C     TEMPC : CRITICAL TEMPERATURE
C     PRS : PRESSURE
C     PRSPC : CRITICAL PRESSURE
C     CNCH2S,CNCCO2 : MOLE PERCENT OF H2S AND CO2
C     ZED : GAS COMPRESSIBILITY FACTOR
C     CMPG : GAS COMPRESSIBILITY FACTOR
C
      DIMENSION A(8)
      DATA A /
     A  0.31506237, -1.04670990, -0.57832729, 0.53530771,
     B -0.61232032, -0.10488813,  0.68157001, 0.68446549 /
       FRCA=(CNCH2S+CNCCO2)/100.
       FRCB=CNCH2S/100.
       EPS=120.*(FRCA**0.9-FRCA**1.6)+15.*(FRCB**0.5-FRCB**4.0)
       TEMPCA=TEMPC-EPS
       PRSPCA=PRSPC*TEMPCA/(TEMPC+FRCB*(1.-FRCB)*EPS)
       TEMPRD=(TEM+460.)/TEMPCA
       PRSPRD=PRS/PRSPCA
       IERR=0
       IF (TEMPRD.LT.1.05.OR.TEMPRD.GT.3.00) GO TO 140
       IF (PRSPRD.LT.0.00.OR.PRSPRD.GT.15.00) GO TO 140
       IF (FRCA.LT.0.00.OR.FRCA.GT.0.85) GO TO 140
       ITER=0
       T1=A(1)*TEMPRD+A(2)+A(3)/(TEMPRD*TEMPRD)
       T2=A(4)*TEMPRD+A(5)
       T3=A(5)*A(6)
       T4=A(7)/(TEMPRD*TEMPRD)
       T5=A(8)
       DENRD=1.0
       DO 120 ITER=1,10
       DENRD2=DENRD*DENRD
       DENRD3=DENRD2*DENRD
       DENRD4=DENRD2*DENRD2
       DENRD5=DENRD3*DENRD2
       P=(TEMPRD+T1*DENRD+T2*DENRD2+T3*DENRD5)*
     A   DENRD+T4*DENRD3*(1.0+T5*DENRD2)*EXP(-T5*DENRD2)
       DP=TEMPRD+2.0*T1*DENRD+3.0*T2*DENRD2+6.0*T3*DENRD5+
     A    T4*DENRD2*EXP(-T5*DENRD2)*(3.0+3.0*T5*DENRD2-
     B    2.0*T5*T5*DENRD4)
       DENRD1=DENRD-(P-0.270*PRSPRD)/DP
       IF (DENRD1.GT.0.0) GO TO 100
       DENRD1=0.5*DENRD
100    IF (DENRD1.LT.2.2) GO TO 110
       DENRD1=DENRD+0.9*(2.2-DENRD)
110    IF (ABS(DENRD-DENRD1).LT.0.00001) GO TO 130
120    DENRD=DENRD1
130    ZED=0.270*PRSPRD/(DENRD1*TEMPRD)
       DENRD=DENRD1
       DENRD2=DENRD*DENRD
       DENRD4=DENRD2*DENRD2
       DZED=T1/TEMPRD+2.0*T2/TEMPRD*DENRD+5.0*T3*DENRD4/TEMPRD+
     A     (1.0+T5*DENRD2-T5*T5*DENRD4)*2.0*T4/TEMPRD*DENRD*
     B     EXP(-T5*DENRD2)
       CMPPRD=1.0/PRSPRD-0.270*DZED/(ZED*ZED*TEMPRD*(1.0+DENRD/
     A       ZED*DZED))
```

```
      CMPG=CMPPRD/PRSPCA
      GO TO 150
140   IERR=1
      ZED=0.0
      CMPG=0.0
150   RETURN
      END
C
C     SUBROUTINE TO CALCULATE THE NATURAL GAS PSEUDO-PRESSURE
C     REQUIRES VISCY AND XLGR4
C
      SUBROUTINE PSUDOP(PRSMAX,PRSDEL,TEM,SPG,TEMPC,PRSPC,CNCH2S,
     A                  CNCCO2,CNCN2,PSI,PPSI,NSTEP)
C
C     ALL INPUTS AND OUTPUTS ARE IN FILED UNITS :
C     PRSMAX : MAXIMUM PRESSURE FOR M(P) TO BE CALCULATED
C     PRESDEL : PRESSURE INCREMENT USED IN M(P) NUMERICAL INTEGRATION
C     TEM : TEMPERATURE
C     SPG : GAS SPECIFIC GRAVITY
C     TEMPC : CRITICAL TEMPERATURE
C     PRSPC : CRITICAL PRESSURE
C     CNCH2S,CNCCO2,CNCN2 : MOLE PERCENT OF H2S,CO2 AND N2
C     PSI : PRESSURE ARRAY
C     PPSI : PSEUSO-PRESSURE ARRAY
C     NSTEP : NUMBER OF THE INCREMENTS
C
      IMPLICIT REAL*8 (A-H,O-Z)
      PARAMETER (NMAX=200)
      DIMENSION PSI(0:NMAX),PPSI(0:NMAX)
      PRSSI1=0.0
      PSI(0)=0.0
      PPSI(0)=0.0
      TEMPRD=(TEM+460.)/TEMPC
      DO 100 I=1,NMAX
         PSI(I)=PRSDEL*I

         PRSPRD=PSI(I)/PRSPC
         CALL ZANDC(TEM,TEMPC,PSI(I),PRSPC,CNCH2S,CNCCO2,ZED,
     A              CMPG,IERR)
         CALL VISCY(TEMPRD,PRSPRD,SPG,TEM,CNCH2S,CNCCO2,CNCN2,
     A              VISGR,VISG,IERR)
         PRSSI2=2.*PSI(I)/(ZED*VISG)
         PPSI(I)=(PRSSI1+PRSSI2)/2.*PRSDEL+PPSI(I-1)
         PRSSI1=PRSSI2
         IF (PSI(I).GE.PRSMAX) THEN
            NSTEP=I
            GOTO 110
         ENDIF
100   CONTINUE
110   RETURN
      END
```

```
      PROGRAM RH_DERV
C
C     CAUTION : RH(I) IS ALWAYS BIGGER THAN HR(I=1)
C               THIS PROGRAM IS WRITTEN SPECIFICALLY
C               FOR THE CORRECT INTERPOLATION
C               OF THE INDEPENDENT VARIABLES RUNNING
C               FROM BIG TO SMALL
C
C     INPUT ARRAYS :
C     TIME  :     SHUT-IN TIME
C     P     :     DIMENSIONLESS PSEUDO-PRESSURE
C     HR    :     HORNER TIME RATIOS
C
C     VARIABLES :
C     IMAX  :     SIZE OF THE ARRAY
C     NMAX  :     NUMBER OF ARRAYS
C     SLD   :     SEMI-LOG DERIVATIVES
C
      PARAMETER (IMAX=100,NMAX=5)
      DIMENSION TIME(IMAX),P(IMAX),HR(NMAX,IMAX),
     A          ARRAY(IMAX),SLD(NMAX,IMAX)
      CHARACTER*11 INPUT,OUTPUT
      WRITE(6,*)'ENTER INPUT FILE NAME : '
      READ(5,*)INPUT
      WRITE(6,*)'ENTER THE NUMBER OF HORNER TIME RATIO : '
      READ(5,*)NHR
      WRITE(6,*)'ENTER TIME INCREMENT PARAMETER..'
      WRITE(6,*)'BETWEEN 0 AND 0.5 (0.2 RECOMMENDED) : '
      READ(5,*)D
      OPEN (UNIT=7,FILE=INPUT,STATUS='OLD')
      I=1
10       READ(7,*,END=20) TIME(I),P(I),(HR(J,I),J=1,NHR)

C        WRITE(6,*)TIME(I),P(I),(HR(J,I),J=1,NHR)
         I=I+1
      GOTO 10
20    CLOSE(UNIT=7)
      NDATA=I-1
      DO 30 I=1,NDATA
         DO 40 J=1,NHR
            TA=10.**(LOG10(HR(J,I))+D)
            TB=10.**(LOG10(HR(J,I))-D)
C           WRITE(6,*) 'TA,TB',TA,TB
            IF(TA.GT.HR(J,1))THEN
               SLD(J,I)=0.
               GOTO 30
            ENDIF
            IF(TB.LT.HR(J,NDATA))THEN
                SLD(J,I)=0.
                GOTO 30
            ENDIF
            DO 50 II=1,NDATA
                ARRAY(II)=HR(J,II)
50          CONTINUE
            CALL TABSEQ(ARRAY,P,NDATA,TA,PPA)
            CALL TABSEQ(ARRAY,P,NDATA,TB,PPB)
C           WRITE(6,*)'TA,TB,HR',TA,TB,HR(J,I)
            S1=(PPA-P(I))/(TA-HR(J,I))
            S2=(P(I)-PPB)/(HR(J,I)-TB)
            SLOPE=0.5*(ABS(S1)+ABS(S2))
            SLD(J,I)=SLOPE*HR(J,I)
40       CONTINUE
30    CONTINUE
      OUTPUT='H.'//INPUT
```

```
      OPEN(UNIT=7,FILE=OUTPUT,STATUS='NEW')
      DO 60 I=1,NDATA
         WRITE(7,*)TIME(I),(SLD(J,I),J=1,NHR)
60    CONTINUE
      CLOSE(UNIT=7)
      STOP
      END
C
      SUBROUTINE TABSEQ(X,Y,N,XX,YY)
C
C     THIS SUBROUTINE IS WRITTEN SPECIFICALLY
C     FOR X ARRAY WHOSE ELEMENT GETS SMALLER
C     AS THE INDEX IS INCREASED {X(I)>X(I+1)}
C
      DIMENSION X(N),Y(N)
      I=1
100   IF(XX.LT.X(I))THEN
         I=I+1
         GOTO 100
      ENDIF
      YY=Y(I-1)+(Y(I)-Y(I-1))*(XX-X(I-1))/(X(I)-X(I-1))
      RETURN
      END
```

```
      PROGRAM MDH_DERV
C
C     THIS PROGRAM COMPUTES THE SEMI-LOG DERVIVATIVES
C     OF THE DATA ARRAY WITH THE METHOD SUGGESTED BY
C     BOURDET ET AL. (1989)
C
C     INPUT ARRAY:
C
C     T     :     SHUT-IN TIME
C     T1,T2,T3 :  MDH TIMES (DEFINED IN EQUATIONS 3.42 TO 3.44)
C     P     :     DIMENSIONLESS SHUT-IN PRESSURE
C
C     VARIABLES :
C
C     D     :     TIME PARAMETER SPECIFYING THE INTERPOLATED TIME USED
C                 IN DERIVATIVE COMPUTATION
C     SLOPE1,SLOPE2,SLOPE3 :
C                 CARTESIAN SLOPES FOR T1,T2, AND T3
C
      DIMENSION T(200),T1(200),T2(200),T3(200),P(200)
      CHARACTER*11 INPUT,OUTPUT
      WRITE(6,*)'INPUT FILE NAME'
      READ(5,*) INPUT
      WRITE(6,*)'TIME PARAMTER (0-0.5,0.2 OPM)'
      READ(5,*)D
      OPEN(UNIT=7,FILE=INPUT,STATUS='OLD')
      OUTPUT='D.'//INPUT
      OPEN(UNIT=8,FILE=OUTPUT,STATUS='NEW')
      I=1
10       READ(7,*,END=20) T(I),P(I),T1(I),T2(I),T3(I)
         I=I+1
      GOTO 10
20    CLOSE(7)
      NDATA=I-1
      DO 4 I=1,NDATA
         TA=10.**(LOG10(T1(I))+D)
         TB=10.**(LOG10(T1(I))-D)
         IF (TA.LT.T1(1))THEN
            GOTO 2
         ENDIF
         IF (TB.GT.T1(NDATA))THEN
            GOTO 2
         ELSE
            CALL TABSEQ(T1,P,NDATA,TA,PA)
            CALL TABSEQ(T1,P,NDATA,TB,PB)
            S1=(PA-P(I))/(TA-T1(I))
            S2=(P(I)-PB)/(T1(I)-TB)
            SLOPE1=0.5*(ABS(S1)+ABS(S2))
         ENDIF
2        CONTINUE
         TA=10.**(LOG10(T2(I))+D)
         TB=10.**(LOG10(T2(I))-D)
         IF (TA.LT.T2(1))THEN
            GOTO 3
         ENDIF
         IF (TB.GT.T2(NDATA))THEN
            GOTO 3
         ELSE
            CALL TABSEQ(T2,P,NDATA,TA,PA)
            CALL TABSEQ(T2,P,NDATA,TB,PB)
            S1=(PA-P(I))/(TA-T2(I))
            S2=(P(I)-PB)/(T2(I)-TB)
            SLOPE2=0.5*(ABS(S1)+ABS(S2))
         ENDIF
```

```
3         CONTINUE
          TA=10.**(LOG10(T3(I))+D)
          TB=10.**(LOG10(T3(I))-D)
          IF (TA.LT.T3(1))THEN
             GOTO 4
          ENDIF
          IF (TB.GT.T3(NDATA))THEN
             GOTO 4
          ELSE
             CALL TABSEQ(T3,P,NDATA,TA,PA)
             CALL TABSEQ(T3,P,NDATA,TB,PB)
             S1=(PA-P(I))/(TA-T3(I))
             S2=(P(I)-PB)/(T3(I)-TB)
             SLOPE3=0.5*(ABS(S1)+ABS(S2))
          ENDIF
C         WRITE(6,*)PA,PB
          WRITE(8,*)T(I),SLOPE1*T1(I),SLOPE2*T2(I),SLOPE3*T3(I)
4         CONTINUE
      STOP
      END
C
C
      SUBROUTINE TABSEQ(X,Y,N,XX,YY)
      DIMENSION X(N),Y(N)
      IF(XX.LT.X(1))GOTO 99
          I=1
100       I=I+1
          IF(I.GT.N)GOTO 98
          IF(XX.GT.X(I))GOTO 100
          YY=Y(I-1)+(Y(I)-Y(I-1))*(XX-X(I-1))/(X(I)-X(I-1))
          RETURN
99        YY=Y(1)
          RETURN
98        YY=Y(N)
          RETURN
          END
```

APPENDIX B

Sample input and output data

The input file for a gas well in the center of a 200 ft square, with a producing time corresponding to t_{pDA} of 10, and a producing rate corresponding to q_D of 0.1 :

```
CASE NAME : 1b10
BUILDUP ANALYSIS
Tfdd Tflog Tcons Tsi,.1000000000000000E-03,10.,10.,452.51,
Tfbup Tslb,.1000000000000000E-02,1000.,
Dp in p vs M(p),50.,
Q (MSCFD),34.85,
SG %H2S CO2 N2,.6,0.,0.,0.,
k (md),1.,
Pi,9000.,
Tres (F),150.,
Por (frac),.2,
Rw ,.1,
xl (Ft),200.,
yl (Ft),200.,
Xwell,100.,
Ywell,100.,
Grid Area I,1.,
Area I Grid Fraction,.5000000000000000E-01,
Grid Area II,2.,
Space Multiplier,3.,
Blocks x y,41,41,
Well Block #,21,21,
```

The following is a selected portion of an output file for the sample input data presented earlier. The information provided is as follows:

TCUM	:	producing time, hr
PB	:	block-averaged reservoir pressure, psia
PMB	:	average reservoir pressure estimated from the material balance, psisa
(P/Z)B	:	$(p/z)_{avg}$, psia
PB/ZB	:	p_{avg}/z_{avg}, psia
MBG	:	global material balance error, fraction (from the initial condition up to the current time step)
MBL	:	local material balance error, frcation (computed at the current time step)

TCUM	PB	PMB	(P/Z)B	PB/ZB	MBG	MGL
0	9000	9000	6734.343	6734.343	0	0
1.00E-04	8999.999	8999.023	6734.343	6734.343	1.37E-06	1.37E-06
1.10E-04	8999.999	8999.023	6734.343	6734.343	1.37E-06	1.37E-06
2.10E-04	8999.998	8999.021	6734.343	6734.343	1.35E-06	1.32E-06
3.10E-04	8999.997	8999.02	6734.343	6734.343	1.32E-06	1.28E-06
4.10E-04	8999.996	8999.019	6734.342	6734.342	1.31E-06	1.25E-06
5.10E-04	8999.995	8999.018	6734.342	6734.342	1.29E-06	1.24E-06
1.00001	8989.279	8988.112	6731.262	6731.271	1.43E-06	1.43E-06
2.00001	8978.482	8977.218	6728.158	6728.172	1.43E-06	1.44E-06
3.00001	8967.646	8966.342	6725.04	6725.057	1.44E-06	1.44E-06
4.00001	8956.794	8955.483	6721.914	6721.932	1.44E-06	1.45E-06
5.00001	8945.942	8944.641	6718.783	6718.803	1.44E-06	1.45E-06
100	7988.578	7989.055	6420.87	6420.896	1.45E-06	1.45E-06
110	7895.94	7896.657	6389.51	6389.537	1.45E-06	1.45E-06
120	7804.742	7805.685	6358.151	6358.177	1.45E-06	1.45E-06
130	7714.957	7716.111	6326.791	6326.818	1.45E-06	1.45E-06
140	7626.557	7627.562	6295.431	6295.459	1.45E-06	1.45E-06
150	7539.516	7540.748	6264.072	6264.1	1.45E-06	1.45E-06
400	5736.512	5740.097	5480.075	5480.126	1.45E-06	1.45E-06
410	5676.889	5680.608	5448.715	5448.766	1.45E-06	1.45E-06
420	5618.063	5621.904	5417.355	5417.407	1.45E-06	1.45E-06
430	5560.02	5563.971	5385.994	5386.048	1.45E-06	1.45E-06
440	5502.744	5506.795	5354.634	5354.688	1.45E-06	1.45E-06
450	5446.218	5450.172	5323.273	5323.329	1.45E-06	1.45E-06
452.51	5432.146	5436.134	5315.402	5315.458	1.45E-06	1.45E-06

The following is a selected portion of the buildup data used to perform the analysis. The data are from the sample input provided earlier.

t	p	m(p)	vis	z	cg	tn	tA	MD	RH1	RH2	RH3
1.0E-3	5101.7	1.5E+9	2.5E-2	1.00	1.2E-4	3.3E+2	3.3E+2	51.09	4.5E+5	9.1E+5	9.2E+5
1.1E-3	5109.1	1.5E+9	2.5E-2	1.00	1.2E-4	3.7E+2	3.6E+2	50.99	4.1E+5	8.3E+5	8.4E+5
2.1E-3	5144.8	1.5E+9	2.6E-2	1.00	1.2E-4	7.1E+2	7.0E+2	50.51	2.2E+5	4.3E+5	4.3E+5
3.1E-3	5165.1	1.5E+9	2.6E-2	1.00	1.2E-4	1.0E+3	1.0E+3	50.24	1.5E+5	2.9E+5	2.9E+5
4.1E-3	5178.4	1.5E+9	2.6E-2	1.00	1.2E-4	1.4E+3	1.4E+3	50.06	1.1E+5	2.2E+5	2.2E+5
7.0E-2	5290.4	1.6E+9	2.6E-2	1.01	1.1E-4	2.4E+4	2.4E+4	48.57	6.5E+3	1.2E+4	1.3E+4
8.0E-2	5295.7	1.6E+9	2.6E-2	1.01	1.1E-4	2.8E+4	2.8E+4	48.50	5.7E+3	1.1E+4	1.1E+4
9.0E-2	5300.4	1.6E+9	2.6E-2	1.01	1.1E-4	3.1E+4	3.1E+4	48.44	5.0E+3	9.7E+3	9.7E+3
1.0E-1	5304.5	1.6E+9	2.6E-2	1.01	1.1E-4	3.5E+4	3.5E+4	48.38	4.5E+3	8.7E+3	8.8E+3
7.0E+2	5431.6	1.6E+9	2.6E-2	1.02	1.1E-4	2.5E+8	2.5E+8	46.69	1.6E+0	3.1E+0	3.1E+0
8.0E+2	5431.6	1.6E+9	2.6E-2	1.02	1.1E-4	2.9E+8	2.9E+8	46.69	1.6E+0	2.9E+0	2.9E+0
9.0E+2	5431.6	1.6E+9	2.6E-2	1.02	1.1E-4	3.2E+8	3.2E+8	46.69	1.5E+0	2.8E+0	2.8E+0
1.0E+3	5431.6	1.6E+9	2.6E-2	1.02	1.1E-4	3.6E+8	3.6E+8	46.69	1.5E+0	2.7E+0	2.7E+0

APPENDIX C

An Investigation on The Average Pressure Determination for a Gas Well

A comparison of Figures 5.3 and 6.1 reveals that the buildup responses for different gas and reservoir properties plotted in the dimensionless graph do not overlie each other after a certain producing time. The dimensionless producing time, t_{pDA} is defined by :

$$t_{pDA} = \frac{0.0002637kt_p}{\phi\mu_i c_{ti} A} . \qquad (C.1)$$

For liquid flow, the buildup response plotted in a dimensionless graph is uniquely characterized by t_{pDA}. For different oil and reservoir properties, the buildup responses on the dimensionless graph trace each other, if the producing time t_{pDA} for every case is the same. For different t_{pDA}, however, the responses are parallel but displaced so that the $\bar{p}_{sD}$ corresponding to the average reservoir pressure are different. The $\bar{p}_{sD}$ can be determined from the material balance relationship, which, in dimensionless form, can be written as :

$$\bar{p}_{sD} = \frac{kh}{141.3qB\mu}(p_i - \bar{p}) = 2\pi t_{pDA} . \qquad (C.2)$$

In Figure 6.1, different displacements of the m_{sD} for each case indicates that the depletion is different for each case, although the dimensionless producing time t_{pDA} for each case is the same.

The results in Chapter 7 show that an accurate estimate of the average reservoir pressure for a gas well can be obtained from an analysis of a buildup test, regardless of the gas and reservoir properties. The MBH (1954) and Dietz's (1965) methods are used in Chapter 7. For both methods, accurate

estimates of the average reservoir pressure can be determined if the modified Horner time ratios, or the modified MDH times, are used in conjunction with the dimensionless producing time as defined by Equation C.1 for the Horner or MDH graph, respectively. The MBH function for a long producing time is given by :

$$p_{DMBH} = \frac{kh}{70.6qB\mu}(p^* - \bar{p}) = \ln(C_A t_{pDA}) \ , \qquad (C.3)$$

for liquid flow, and :

$$m_{DMBH} = \frac{kh}{712qT}\{m(p^*) - m(\bar{p})\} = \ln(C_A t_{pDA}) \ , \qquad (C.4)$$

for gas flow.

The different displacements of the buildup response for different gas and reservoir properties with the same t_{pDA} on the dimensionless graph suggest that the depletion level is different. However, the same t_{pDA} is used for each case for accurate estimation of the average reservoir pressure. This rather confusing observation has never been discussed in the literature.

The following investigation is conducted to gain some insight into the mechanism of the average reservoir pressure estimation from buildup test of gas wells. No theoretical explanation has been attempted.

Figure C.1 is a dimensionless graph of the buildup responses of a gas well and an oil well in the center of a square. The base case's gas and reservoir properties are used in Figure C.1, but the initial pressure and gas specific gravity are changed to 5,000 psia and 1.0, respectively. The modified

Horner time ratio R_{H2} is used to graph the buildup response of the gas well. The conventional Horner time ratio R_{H1} is used for the buildup response of the oil well. The producing time t_{pDA} for the gas well is 10. In Figure C.1, the dimensionless pseudo-pressure for the gas well stabilizes at 44.6. Using Equation C.2, the t_{pDA} for an oil well to reach the dimensionless pressure of 44.3 is 7.1. This dimensionless producing time is used to generate the buildup response for the oil well in Figure C.1.

From Figure C.1, the extrapolation of the portion of data corresponding to the infinite-acting radial flow period for the buildup response of the gas well and the oil well leads to a dimensionless pseudo-pressure m^*_{sD} and a dimensionless pressure p^*_{sD} of 41.79 and 41.95, respectively. To estimate the average reservoir pressure for the oil well, the MBH function is computed from Equation C.3, using t_{pDA} of 7.1. Similarly, the pseudo-pressure corresponding to the average reservoir pressure can be obtained by estimating the MBH function using Equation C.4 for the gas well, using a t_{pDA} of 10. The MBH function for the oil well is 5.39 and the MBH function for the gas well is 5.73.

For the average reservoir pressure of the gas well to be accurately determined from Figure C.1, the difference between the MBH functions of the gas and the oil well must satisfy the following relationship :

$$\frac{1}{2}(m_{DMBH} - p_{DMBH}) = p^*_{sD} - m^*_{sD} \quad . \qquad \text{(C.5)}$$

For Figure C.1, the difference between the MBH functions is 0.34, and the difference between p^*_{sD} and m^*_{sD} is 0.16. This approximately satisfies the relationship in Equation C.5.

To investigate a different well/reservoir geometry, buildup response for a gas well producing from a corner of a 4:1 reservoir for a producing time corresponding to t_{pDA} of 30 is graphed with R_{H2} in

Figure C.2. The gas and reservoir properties used are the same as Figure C.1. In Figure C.2, the dimensionless pseudo-pressure stabilizes at 77.99. The producing time for the buildup response of an oil well with similar well/reservoir geometry is 12.41, using Equation C.2. In Figure C.2, m^*_{sD} and p^*_{sD} are 77.18 and 77.64, respectively. Using the producing time t_{pDA} of 30 and 12.41, the MBH for functions are 1.24 and 0.36 for the gas and oil well, respectively. The difference between p^*_{sD} and m^*_{sD} is about half the difference in the MBH functions, which approximately satisfies Equation C.5.

Similarly, Figures C.3 and C.4 present the Horner plots of the dimensionless pressures and pseudo-pressures of buildup tests for a well in the center of a square and a well in a corner of a 4:1 reservoir, respectively. The gas and reservoir properties used are taken from the base case, except that the reservoir temperature is 250° F in Figures C.3 and C.4.

In Figure C.3, the difference between p^*_{sD} and m^*_{sD} is 0.11. The MBH function for the gas well is 5.73, and the MBH function for the oil well is 5.48. In Figure C.4, the difference between p^*_{sD} and m^*_{sD} is 0.37. The MBH function for the gas well is 1.24 and the MBH function for the oil well is 0.53. Thus, the relationship given by Equation C.5 is approximately satisfied in Figures C.3 and C.4.

The observation from Figures C.1 to C.4 suggests that the accuracy of the average reservoir pressure estimation using the MBH method is accomplished due to a combined effect of the use of R_{H2} and the t_{pDA} as given by Equation C.1. The buildup data of a gas well graphed with R_{H2} will be displaced from the data of an oil well whose dimensionless pressure stabilizes to the same numerical value of the dimensionless pseudo-pressure corresponding to the average reservoir pressure for the gas well. For the dimensionless pseudo-pressure and dimensionless pressure corresponding to the average reservoir pressure to be equal numerically, different MBH functions are required for the gas and oil well. This difference in the MBH functions is accomplished by the use of different t_{pDA}'s. Using different t_{pDA}'s corrects the m^*_{sD} and p^*_{sD} to the same numerical value of dimensionless

pseudo-pressure and dimensionless pressure corresponding to the correct average reservoir pressures, respectively.

It has been shown that t_{pDA} as given by Equation C.1 does not adequately reflect the depletion level of a gas reservoir and the buildup response graphed with dimensionless pseudo-pressure and Horner time ratios for a given t_{pDA} is different for each gas and reservoir property used. Since pseudo-pressure is used in the analysis, the dimensionless graph might be general, if the initial condition is defined by the same initial pseudo-pressure.

Figure C.5 is a dimensionless graph of the buildup responses for two cases. The initial pseudo-pressure for both cases is $3.10*10^8$ psi^2/cp, and the producing time used for both cases corresponds to t_{pDA} of 30 (defined by Equation C.1). Since the responses graphed in Figure C.5 do not overlay each other, starting the production from the same initial pseudo-pressure condition does not generalize the dimensionless graphs for the buildup responses for gas flow.

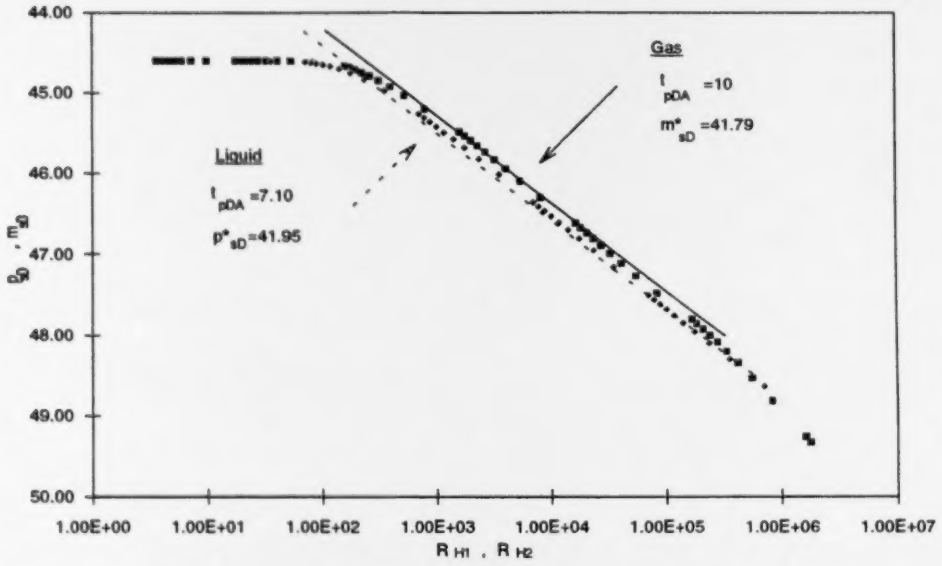

Figure C.1 Dimensionless graph of buildup responses of a gas and an oil well at the center of a square
(base case properties except p_i=5,000 psia and γ_g=1.0)

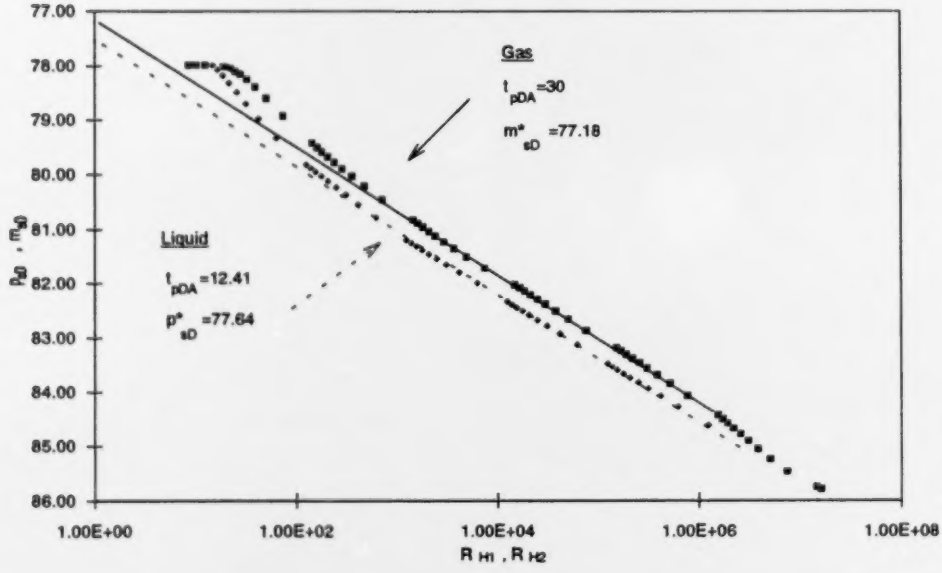

Figure C.2 Dimensionless graph of buildup responses of a gas and an oil well in a corner of a 4:1 reservoir
(base case properties except p_i=5,000 psia and γ_g=1.0)

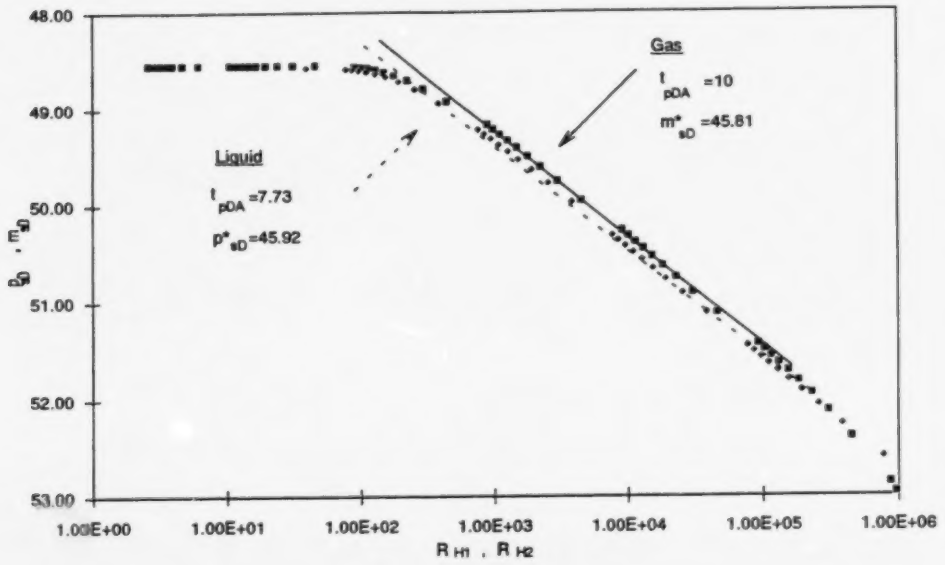

Figure C.3 Dimensionless graph of buildup responses of a gas and an oil well at the center of a square
(base case properties, except T=250° F)

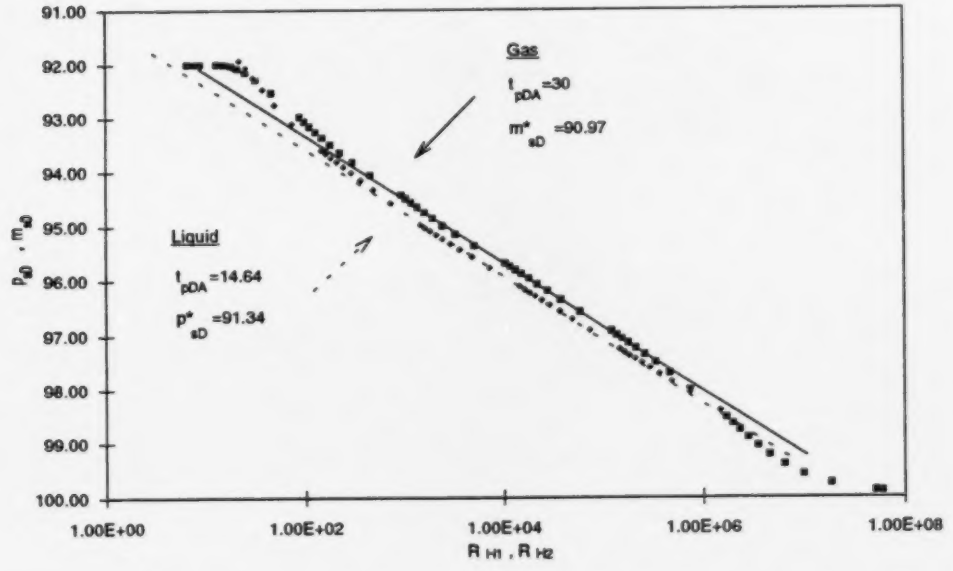

Figure C.4 Dimensionless graph of buildup responses of a gas and an oil well in a corner of a 4:1 reservoir
(base case properties except T=250° F)

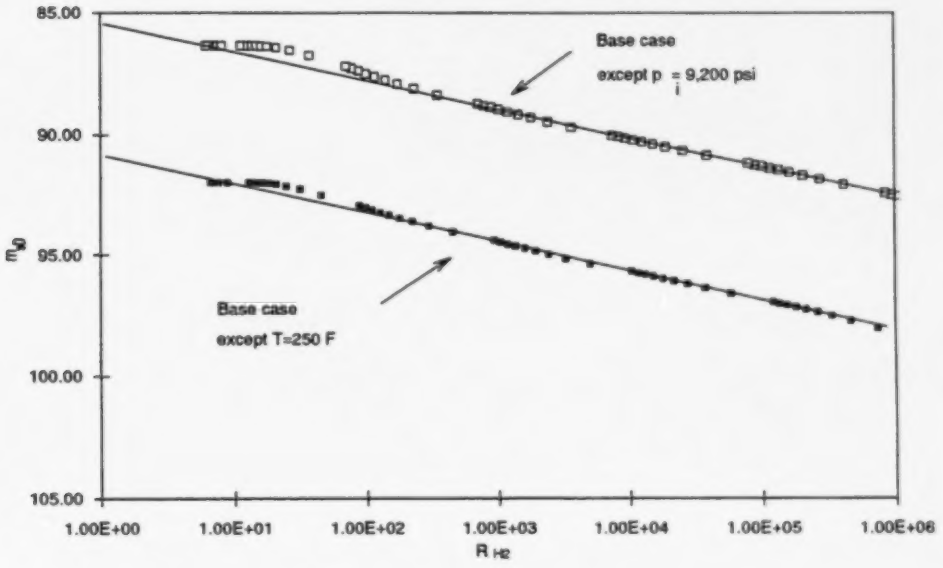

Figure C.5 Dimensionless graph of buildup responses for a gas well in a corner of a 4:1 reservoir, m(pi)=3.10*10^8 psi^2/cp and t_{pDA}=30

APPENDIX D

Gas Properties for Selected Compositions and Reservoir Temperatures

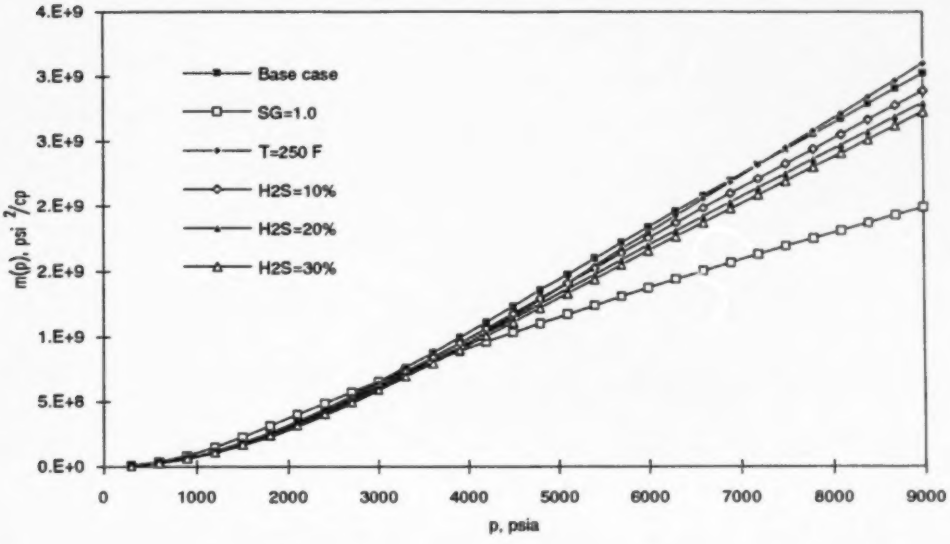

Figure D.1 Pseudo-pressure for selected compositions and reservoir temperatures

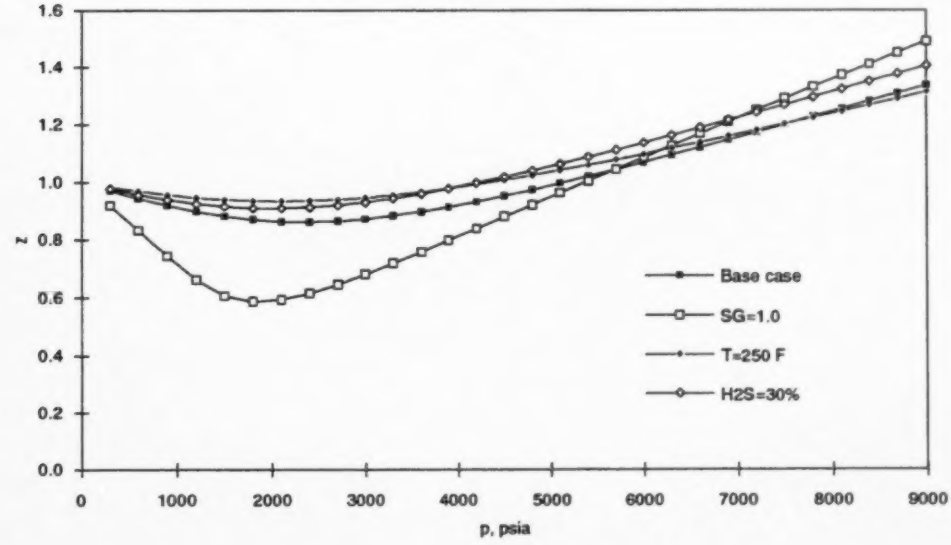

Figure D.2 Gas compressibility factor for selected compositions and reservoir temperatures

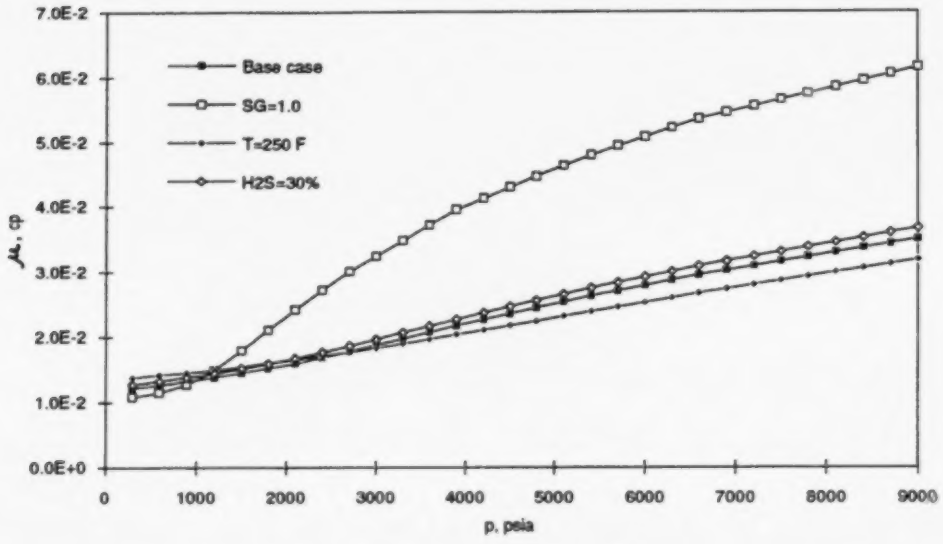

Figure D.3 Gas viscosity for selected gas compositions and reservoir temperatures

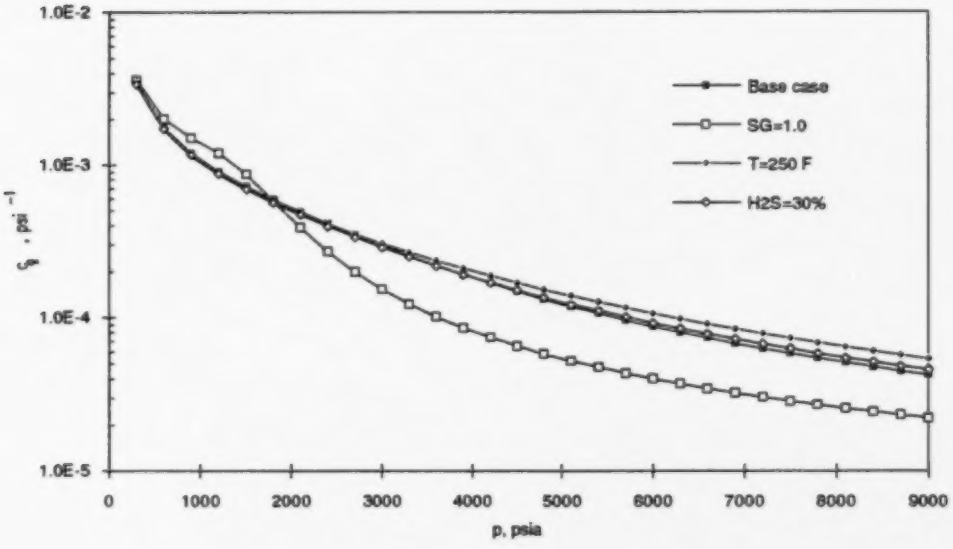

Figure D.4 Gas compressibility for selected gas compositions and reservoir temperatures